博士論文番号：**118022**
(Doctoral student number)

Nitric oxide (NO) signaling and its importance in oxidative stress response in the fission yeast *Schizosaccharomyces pombe*

RIKA INDRI ASTUTI

Laboratory of Applied Stress Microbiology
Graduate School of Biological Sciences
Nara Institute of Science and Technology

(Prof. Hiroshi Takagi)

Submitted on 2015/11/23

Lab name (Supervisor)	Laboratory of Applied Stress Microbiology Prof. Hiroshi Takagi		
Name (surname) (given name)	Astuti Rika Indri	Date	**(2015/11/23)**
Title	**Nitric oxide (NO) signaling and its importance in oxidative stress response in the fission yeast *Schizosaccharomyces pombe***		

Abstract

As a ubiquitous signaling molecule, nitric oxide (NO) plays fundamental roles in physiological as well as pathological events in mammalian cells. Increasing evidence suggests that this gaseous molecule functions as a signaling messenger in unicellular eukaryotes, including yeast. Indeed, our laboratory demonstrated that NO is involved in cellular responses to environmental stresses in the budding yeast *Saccharomyces cerevisiae* (Sasano *et al.,* 2012, Nishimura *et al.,* 2013, Nasuno *et al.,* 2014). Despite the pertinent contribution of NO signaling in sporulation and cell cycle processes, however, little is known about the physiological importance of NO upon stress responses in the fission yeast *Schizosaccharomyces pombe*. Since *S. pombe* cells share the similar systems to those of higher eukaryotes at the molecular and metabolic levels, better understanding of the NO physiology of fission yeast may give a conceptual perspective about the NO-related events in higher eukaryote systems. Hence, the aim of this study is to investigate the presence and the potential roles in the stress responses of NO signaling in *S. pombe*.

The determination of intracellular NO indicated a fluctuation of free NO and NO-derivative *S*-nitrosothiols (RSNO) throughout the growth of fission yeast in rich medium. Consistently, NO-detoxification systems represented by NO dioxygenase (encoded by *SPAC869.02c*) and *S*-nitrosoglutathione reductase (encoded by *fmd2$^+$*), both of which were identified in this study, showed distinct behavior in respect to the growth phase. The *SPAC869.02c* gene, later defined as *yhb1$^+$* and its product were constitutively expressed and likely contributed to maintain NO homeostasis throughout growth phases. In contrast, *fmd2$^+$* was induced once cells entered the stationary phase, while absent during the log phase. This might be correlated with the high RSNO level observed in the stationary phase.

Previous findings claimed that L-arginine-dependent NO synthetic activity via NO synthase (NOS) was detected in cell lysates of *S. pombe*. Supporting this, the inhibition of NOS activity markedly abolished NO signaling during the log phase indicated by the reduction of Yhb1 protein levels. In contrast, the expression of Fmd2 in the late stationary phase was not fully diminished with the treatment of NOS inhibitor, demonstrating the existence of a novel unknown source of NO in this stage. The stresses related to physiological state in the stationary phase (i.e., oxidative stress, low-glucose stress, and rapamycin treatment) were also found to increase the expression of Fmd2 in the log-phased cells. This suggests the potential linkage of NO and reactive oxygen species (ROS) either from exogenous sources or mitochondria. Subsequently, it was shown that the cytochrome *bc$_1$* (complex III) in the mitochondrial respiratory chain (MRC) is responsible as the NO source during the stationary phase. In consistent with this, subcellular localization of NO was

observed as punctate structures co-localizing with the mitochondria in the stationary phase. By contrast, NO was mainly detected in the vacuole during the log phase.

Further experiments were designed to reveal the physiological importance of NO signaling in cell survival rates upon H_2O_2-induced oxidative stress. Remarkably, pretreatment of *S. pombe* cells with an NO donor (0.5 mM DETA NONOate) for 2 hours prior to exposure to a high concentration of H_2O_2 (2 mM) led to a marked increase in cell viability. The generation of ROS by H_2O_2 was also clearly suppressed by the pretreatment with DETA NONOate. The DNA microarray analysis revealed that the genes involved in gene ontology term cellular respiration were significantly down-regulated by the DETA NONOate treatment. This suggests that NO production has a negative role on further progression of mitochondrial respiration and its associated ROS generation at the transcriptional level. Interestingly, the genes related to iron assimilation were up-regulated after exposure to DETA NONOate, potentially due to low levels of soluble iron (Fe^{2+}) observed in DETA NONOate pre-treated cells under oxidative stress conditions. It is thus suggested that NO causes iron starvation, leading to the induction of the iron uptake genes. The observed low levels of Fe^{2+} by DETA NONOate treatment might be associated with the impaired induction of the thioredoxin gene $trx1^+$, which contributes to the reduction of Fe^{3+} to Fe^{2+}. This mechanism might prevent Fe^{2+} from reacting with H_2O_2 to further generate more toxic radical OH^- via Fenton reactions.

Given that NO essentially inhibits Fenton reactions during the exposure to H_2O_2, it is likely that a large amount of H_2O_2 remains within the cells pretreated with DETA NONOate. Hence, NO positively regulated peroxidases activity of sulfiredoxin (Srx1) and glutathione-S-transferase (Gst3). Indeed, cell viability after exposure to H_2O_2 was not rescued by the DETA NONOate pretreatment in the $\Delta srx1$ or $\Delta gst3$ strains. Consistently, under oxidative stress conditions, the activities of sulfiredoxin and glutathione peroxidase (attributed to Gst3) were enhanced in the DETA NONOate-pretreated cells. Additionally, the deletion of $spc1^+$, an effector kinase gene of stress-responsive mitogen activated protein kinase (MAPK) cascade that up-regulates both $srx1^+$ and $gst2^+$, caused a severe damage on the cell viability regardless of the DetaNONOate pretreatment, suggesting that NO-dependent stress tolerance mechanism is partly mediated by Spc1.

This study provides the evidence that the fine-tuned NO signaling is present in the fission yeast *S. pombe*. The switching of the NO synthetic mechanisms and its designated NO-detoxification enzymes at distinct growth phases implies dynamic physiological changes underlying the NO signaling and metabolic shift, which potentially determine specific cellular responses. Furthermore, I found that NO protects *S. pombe* cells against H_2O_2-induced oxidative stress by concomitantly regulating distinct antioxidant mechanisms at the transcriptional level: (i) repression of the cellular respiration-induced ROS generations, (ii) inhibition of the thioredoxin activity leading to impairment of Fe^{2+}-mediated Fenton reactions, and (iii) activation of the potent H_2O_2 scavengers, sulfiredoxin and glutathione peroxidase. Thus, it is worth noting that this study gives a new insight of diverse stress responses mediated by the multifunctional signaling molecule, NO.

List of Contents

List of Tables

List of Figures

Abbreviations

APF : aminophenyl fluorescein;

Cco : cytochrome-c-oxidase

DAF-FM DA : 4-amino-5-methylamino-2',7'-difluorofluorescein diacetate;

DCF DA : 2',7'-dichlorofluorescein diacetate;

DETA : diethylenetriamine;

DETA NONOate : (*Z*)-1-[2-(2-aminoethyl)-*N*-(2-ammonioethyl)amino]diazen-1-ium-1,2-diolate

DPTA : dipropylenetriamine;

DTT : dithiothreitol;

DTPA : diethylene triamine pentaacetic acid;

EDTA : ethylene diamine tetraacetate;

EMM : Edinburgh minimum medium;

eNOS : endothelial NOS

FAD : flavin adenine dinucleotide;

GO : gene ontology;

GS-FDH : glutathione-dependent formaldehyde dehydrogenase;

GSH : glutathione

GSNO : *S*-nitrosoglutahione;

GSNOR : *S*-nitrosoglutahione reductase;

GSSG : glutathione disulfide;

HA : hemagglutinin;

H_2O_2 : hydrogen peroxide

iNOS : inducible NOS;

KCN : potassium cyanide;

L-NAME : L-N^G-nitroarginine methyl ester;

LC/MS : liquid chromatography/tandem mass spectrometry;

MAPK : mitogen-activated protein kinase;

MRC : mitochondrial respiratory chain;

NADPH : Nicotinamide adenine dinucleotide phosphate

NIR : nitrite reductase;

NOD : nitric oxide dioxygenase;

nNOS   : neuronal NOS;

NOS   : nitric oxide synthase;

NP-40   : 4-Nonylphenyl-polyethylene glycol;

ONOO$^-$: peroxynitrite;

PMSF   : phenylmethylsulfonyl fluoride;

PVDF   : polyvynylidene difluoride;

qRT-PCR   : quantitative realtime PCR;

ROS   : reactive oxygen species;

RSNO   : *S*-nitrosothiols

SNAP   : *S*-nitroso-*N*-acetylpenicillamine;

SNP   : sodium nitropusside;

SDS PAGE   : sodium dodecyl sulphate polyacrylamide gel electrophoresis;

TBST   : Tris-buffered saline with Tween-20;

TCA   : thrichloroacetic acid;

TOR   : target of rapamycin;

YES   : yeast extract with supplements.

1. Introduction

1.1 Nitric oxide (NO) as a reactive molecule

Although the systematic name for NO is nitrogen monoxide, "nitric oxide" is commonly used for this compound. NO is a radical gas molecule equipped with one unpaired electron, leading to its high reactivity with other radicals and the formation of derivatives with higher reactivity and toxicity (Hughes *et al.*, 2008). NO is chemically reactive, but it is unlikely that NO forms dimer either in the gas phase or in solution. Instead, NO modifies cellular compounds via three distinct mechanisms: *S*-nitrosation, *S*-nitrosylation, and *S*-nitration. Most strikingly, the NO-based protein modifications mediate cellular responses involving the complex regulatory network underlying the NO signaling.

Three modes of actions of NO by different NO species are reported; namely, NO radical (NO•), nitrosonium cation (NO^+), and nitrosyl anion (NO^-) (Arnelle & Stamler, 1995) (Figure 1). It is worth noting that the direct binding of free NO radical to its corresponding target molecule is highly unfavourable. It is due to the reduction potential for the NO/H-NO couple is extremely low (-0.55 V), even lower than oxygen molecule (-0.33 V). Moreover, the H-NO bond dissociation energy is only 47 kcal/mol indicating that NO will be very poor at abstracting H-atoms from biological substrates (Fukuto *et al*., 2012). Accordingly, it requires oxidation or reduction of NO• species to its reactive species prior to modify the target biomolecules (Figure 1).
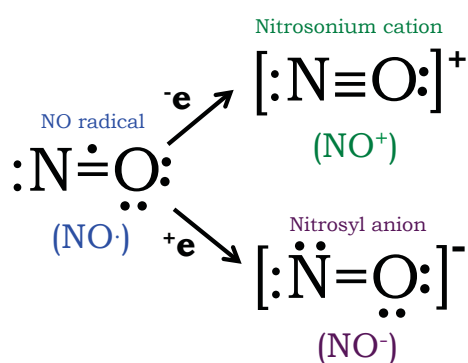
Figure 1. Three different forms of NO reacting with biomolecules.
NO radical (NO•) is rapidly reduced by one electron to form nitrosyl anion (NO^-) or oxidized by one electron to form nitrosonium cation (NO^+).

The NO^+ species directly modifies nucleophilic center, often to a sulfur of thiol group of a target molecule, generating *S*-nitrosothiols (RSNO) (Heinrich *et al.,* 2013). Such modifications refer to *S*-nitrosation reaction. *S*-Nitrosation can also be conducted by the other two NO species, NO• and NO^-. However, due to their negative electromagnetic charge, NO•

and NO$^-$ cannot be directly transferred to the nucleophilic sulfur residue of a biomolecule. Yet, these two NO species can react with oxygen, metal or even reactive oxygen species (ROS), mostly superoxide anion (O$_2$-), yielding various NO derivatives such as N$_2$O$_3$, NO$_x$, ONOO- as well as metal-NO, that potentially modify thiol moiety of a biomolecule to further form RSNOs (Martinez-Ruiz & Lamas 2004) (Figure 2).

Distinctively, addition of NO$^-$ to a reactant, for example the metal moiety of biological target molecules, is a common definition of nitrosylation (Ford *et al.*, 2005). As decribed earlier, this metal nitrosyl complex (metal-NO) may undergo sequential *S*-nitrosation reactions upon nucleophilic thiolate, thus resulting RSNOs. Such additional reactions are commonly described as transnitrosation. It is worth mentioning that both *S*-nitrosation and nitrosylation prominently hallmark the development of intracellular RSNOs. Additionally, nitration mediates the addition of NO$_2^+$ to negative nucleophilic group at position 3 of the phenolic ring of tyrosine residues to form nitrotyrosine (nTyr) (Abello *et al.*, 1999). Since it has been reported that peroxynitrite (ONOO$^-$) contributes to protein tyrosine nitration, hence, NO• should first react with O$_2^-$ to form ONOO$^-$ prior to nitration (Turko & Murad, 2002). The NO-based modifications of biomolecules are summarized in Figure 2.
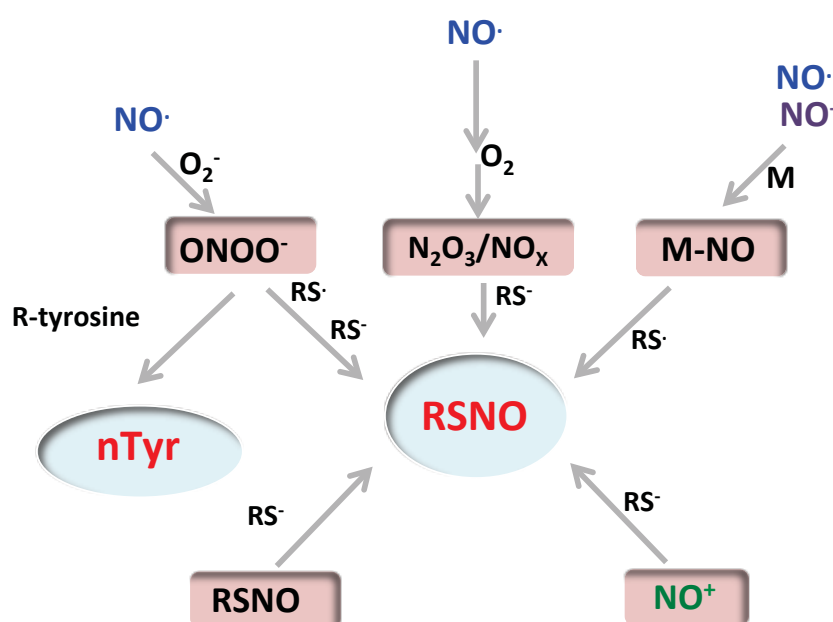
Figure 2. Summary of the pathways contributing to the formation of *S*-nitrosothiols (RSNOs) and nitrotyrosine (nTyr).
Free radical (NO•) may first react with superoxide (O$_2^-$), oxygen (O$_2$), or metal ions (M), yielding NO-based modification agents, such as peroxynitrite (ONOO$^-$), NO oxides (N$_2$O$_3$/NO$_x$), or metal-NO complexes (M-NO). Subsequently, those intermediates further react with nucleophilic thiolate (RS$^-$) or radical thiolate (RS•), generating *S*-nitrosothiols (RSNOs). Nitrosyl anion (NO$^-$) also forms M-NO and subsequent RSNOs in a similar way. Importantly, nitrosonium cation (NO$^+$) directly modifies RS$^-$ to form RSNOs. ONOO$^-$ also contributes in nitrating tyrosine residue of phenolic compounds, yielding nitrotyrosine (nTyr).

In spite of an increase in number of the studies of NO-based modifications upon biomolecules, it remains elusive how NO attacks at specific residue(s) of a targeted molecule. Consensus motifs denoted as acid-base motifs provide the reactive thiol cysteine sites favorable for *S*-nitrosation. This particular motif comprises a cysteine residue flanking acidic (aspartate and glutamate) and basic (arginine, histidine, and lysine) residues, namely [KRHDE]-C-[DE] motif, which ensures the formation of nucleophilic RS^- through electrostatic interactions (Kovacs & Lindermayr, 2013). In respect to nitrosylation reactions, NO^- has been reported to highly react with oxidized metals, such as Fe^{3+} (Heinrich *et al.*, 2013) or Cu^{2+} (Wright *et al.*, 2010). The binding of nitrosyl to metal ion, for example Fe^{3+}, will further result Fe^{2+}-NO^+ moiety, which can mediate trans-nitrosation reactions toward nucleophilic thiolate (Wade & Castro, 1990). Consensus motifs of nitration-based modifications are unknown, except for the selective tyrosine residues (Radi 2004).

1.2 Biosynthesis of NO in yeast

To date, little is known about the NO synthetic mechanism in yeast. In contrast, a family of enzymes denoted as NO synthases (NOSs) (EC 1.14.13.39) are well studied in mammalian cells. NOSs catalyze the conversion of L-arginine (Arg) to L-citrulline (Cit) in the presence of molecular oxygen (O_2) and NADPH (Bredt & Snyder, 1990). NOSs are active in homodimer forms, and each of the subunit comprises two distinctive catalytic domains, namely the C-terminal reductase and N-terminal oxygenase domains (Stuehr, 1999) (Figure 3). There are three main isoforms of NOSs, namely inducible NOS (iNOS), endothelial NOS (eNOS), and neuronal NOS (nNOS), and each of them possesses unique features regarding structures, functions, and regulations. iNOS generates a high level of NO once its expression is induced by inflammatory mediators, such as macrophages (Zamora *et al.*, 2000). It is thus likely that iNOS-derived NO is correlated with the critical role of NO in the responsive immune system against antigens. In contrast, eNOS and nNOS are constitutively expressed as NOSs with low NO-releasing activity and function in a Ca^{2+}-dependent manner (Mc Murry *et al.*, 2011). These features are associated with the homeostatic functions of NO in the cardiovascular and nervous systems, respectively.
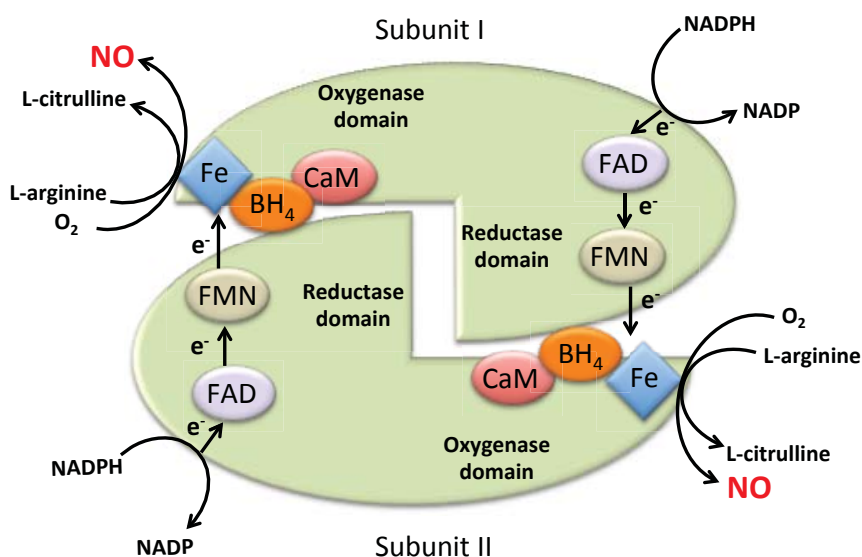
Figure 3. The scheme of NOS dimer with oxygenase and reductase domains that mediates the synthesis of NO from L–arginine (Arg).
The reductase domain is responsible for electron transfer from NADPH to the final acceptor, Fe^{3+} center of heme, of the oxygenase domain of the binding partner via flavin adenine nucleotide (FAD) and flavin mononucleotide (FMN). Electron is further used in the two steps of molecular oxygen (O_2)-mediated oxidation of the substrate L-arginine (Arg). Calmodulin (CaM) accelerates this process, whereas tetrahydrobiopterin (BH_4) is critical for coupling the reduction of O_2 at the heme group to the multistep oxidation of Arg yielding NO and L-citrulline (Cit).

In addition to Arg, O_2, and NADPH, redox cofactor tetrahydrobiopterin (HB_4), flavins (flavin adenine dinucleotide (FAD) and flavin mononucleotide (FMD)), calmodulin (CaM), and heme are required for NOSs-mediated NO synthetic reactions (Bredt & Snyder, 1990). The reductase domain provides the binding site for one molecule each of NADPH, FAD, and FMN essential for electron transfer, whereas the oxidase domain is important for binding of Arg, HB_4, and heme and contributes to O_2-mediated oxidation of Arg to Cit and NO. Electron from NADPH will be transferred sequentially via flavin compounds to the final acceptor, heme, thus providing the oxidizing power for Arg oxidation. In addition, heme is substantial for dimerization of two NOS subunits, thus allowing the binding of BH_4 to the oxygenase domains. BH_4 is crucial in dimer stabilization as well as electron coupling, since lack of BH_4 leads to the uncoupled reduction of O_2, which therefore induces the production of O_2^-. In addition, the binding site of CaM that resides in between these two domains is essential for maintaining protein structure as well as enzymatic function (Figure 3) (Andrew & Mayer, 1999). Figure 4 shows the detailed stoichiometry of the two-step oxidation reaction from Arg to Cit and NO. The NOS-catalyzed reaction consumes 2 moles O_2 and 1.5 moles NADPH per mole Cit yielded.
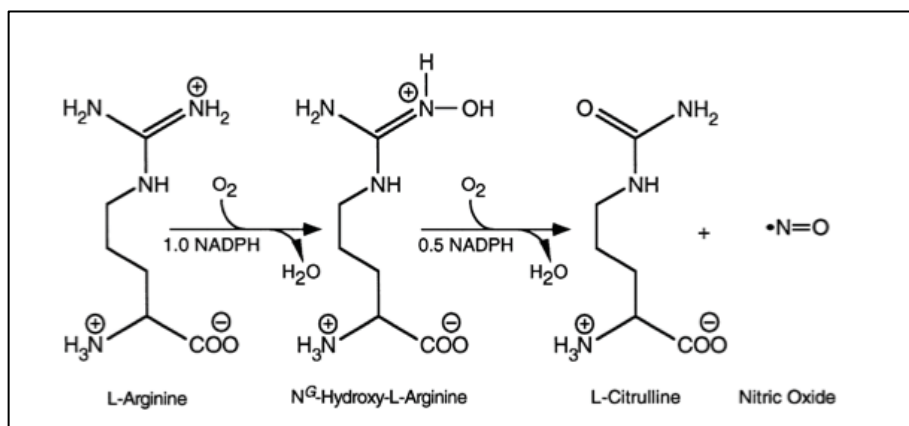
Figure 4. The two-step oxidation of Arg to Cit and NO.
In this reaction, Arg is converted into the intermediate compound, N^G-hydroxy-Arg (OH-Arg), prior to yielding Cit and NO. NADPH, an electron donor, as well as O_2, is required for each step.

Moreover, nitrite reductase (NIR) has been determined to be the major NO producer under hypoxic conditions that commonly occur in hypoxic vasodilation of cardiovascular systems (Totzeck *et al*., 2012), muscle tissue during extensive exercises (Larsen *et al*., 2007), and ischemic tissues (Webb *et al*., 2004). Unlike NOS, NIR produces NO in an O_2-independent manner, emerging the potential contribution of NO in mediating the hypoxic signaling-dependent cellular responses (Dijkers & O'Farrell, 2009). The heme-binding proteins, such as hemoglobin (Gladwin & Kim-Saphiro, 2008) and myoglobin (Totzeck *et al*., 2012; Hendgen-Cotta *et al*., 2012), and cytochrome *c* (Basu *et al.*, 2008), cytochrome *bc1* (Nohl *et al.,* 2000) and cytochrome *c* oxidase (Cco) (Castello *et al*., 2006) of the mitochondrial electron transport chain have been reported to possess the catalytic function of NIR-dependent NO generation.

Finding NO-biosynthetic mechanisms in the unicellular eukaryote yeast is challenging because yeast genome is believed to not have mammalian NOS orthologues. It was reported, however, that crude extracts of the budding yeast *Saccharomyces cerevisiae* show positive immunoreactivity against an anti-nNOS antibody (Kanadia *et al*., 1998). In fission yeast *Schizosaccharomyces pombe*, the generation of NO via NOS-like activity has been confirmed by *in vitro* analysis (Kig & Temizkan, 2009), yet the corresponding NOS-encoding gene has not been identified so far. More recently, our laboratory demonstrated the generation of NO via Arg-dependent Tah18 activity in *S. cerevisiae* (Nishimura *et al*., 2013). Nonetheless, the full display of Tah18-associated NOS activity has not been clearly elucidated, because Tah18 does not contain an intact oxygenase domain of NOS.

Previous findings have also exhibited the ability of Cco of *S. cerevisiae* to produce NO from NO_2^- through the NIR function, particularly under low oxygen conditions (Castello *et*

15

al., 2008; Li *et al.*, 2011). It has been postulated that the conversion mechanism of NO_2^- to NO via Cco in yeast cells mimics the NIR-mediated NO generation by hemoglobin (Huang *et al.*, 2005; Castello *et al.*, 2008) (Figure 5). NO is mainly produced through the function of Vb subunits of Cco, which is highly expressed during hypoxic conditions (Castello *et al.*, 2008).

$$(1) \quad NO_2^- + HbFe^{2+} + H^+ \rightarrow NO + HbFe^{3+} + OH^-$$

$$(2) \quad NO + HbFe^{2+} \rightarrow HbFe^{2+}\text{-}NO$$
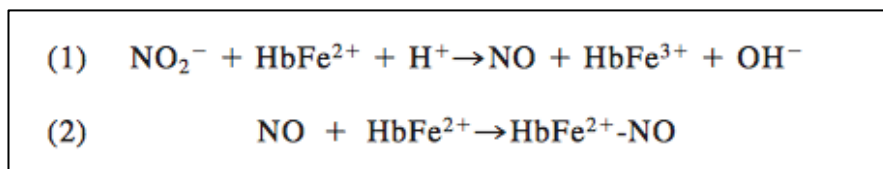
Figure 5. Nitrite reductase (NIR)-dependent NO synthesis via hemoglobin.
Nitrite (NO_2^-) is rapidly reduced to NO at lower pH simultaneously with the oxidation of ferrous deoxyhemoglobin ($HbFe^{2+}$) to methemoglobin ($HbFe^{3+}$) (reaction 1). The NO resulted from reaction 1 will subsequently bind to vacant $HbFe^{2+}$ molecule resulting iron nitrosyl species ($HbFe^{2+}$-NO).

1.3 NO as a signaling molecule in yeast

In 1980, NO was first discovered as a unique cellular signaling molecule by Dr. Furchgott from State University of New York Downstate Medical Center. At that time, the pharmacological effects on contraction of blood vessels was investigated. Subsequently, it turned out that endothelial cells generate an unknown signal molecule for vascular smooth muscle cells relaxation, and thus, this was termed an endothelium-derived relaxing factor (EDRF) (Furchgott & Zawadski, 1980). Independently, Dr. Murad from the University of Virginia found that NO is released from NO_3^- and relaxes smooth muscle tissue, thereby initiating vasodilation (Murad *et al.*, 1978). Around the year of 1986, Dr. Ignarro from the University of California, Los Angeles settled the fact that EDRF was actually NO (Ignarro *et al.*, 1987). For such fundamental and important findings, a Nobel Prize was awarded to those three scientists for NO discoveries in 1998. Studies of NO have been widely conducted at greatly various aspects ever since, especially to uncover the biological significance of this gaseous signaling molecule. In fact, the importance of NO signaling has been investigated not only in mammals, but other organisms, including plants, yeasts and bacteria. However, the physiological significance of NO in yeast cells has not been well studied yet.

1.3.1 Regulation of intracellular NO levels

The regulation of intracellular NO level accounts for the primary NO signaling in the cells. This regulation is required to ensure that NO with the radical and reactive properties elicits its protective functions instead of cytotoxic actions in the cells. NO dioxygenases

(NODs) and denitrosylation enzymes (*S*-nitrosoglutahione reductases (GSNORs)) have been demonstrated to play significant roles in controlling intracellular NO levels and thus preventing the damaging effects of redox status perturbations (Gardner *et al*., 1998; Liu *et al*., 2001). These enzymes constitute the major mechanism of NO detoxification, suggesting that their respective catalytic activities combat the excessive intracellular NO levels and maintain NO at its physiological levels to concomitantly prevent from nitrosative stress.

NODs, also known as flavohemoglobins (flavoHbs), catalyze NO dioxygenation rapidly with high fidelity by utilizing NAD(P)H to incorporate two-atoms from O_2 into the susbtrate NO to form NO_3^- (Gardner, 2005). In the yeast *Candida albicans* and *S. cerevisiae*, the *YHB1* gene encoding flavoHb is substantially enhanced by exposure of the cells to NO donors (Ulmann *et al*., 2004; Hromatka *et al*., 2005). Deletion of *YHB1* in *S. cerevisiae* abolishes NO-consuming activity and increases the levels of RSNOs for more than 10 folds, compared to wild-type cells (Lewinska *et al*., 2000). Interestingly, the induction of *YHB1* of *C. albicans* and *S. cerevisiae* depends on non-homologous transcriptional factors, namely, a $Zn(II)_2$-Cys_6 transcriptional factor Cta4 and a zinc-finger transcription factor Fzf1, respectively (Sarver & DeRisi, 2005; Chirandand *et al*., 2008). To date, little is known about the regulation of flavoHb in fission yeast *S. pombe*.

Groundbreaking studies of the denitrosylation activity of GSNORs have revealed the importance of a fine-tuned NO signaling represented by the intracellular NO and RSNO levels. Although the generated RSNOs are essential for NO signaling-dependent cellular responses, its excessive amount may develop severe nitrosative stress. Since the reduced form of glutathione (GSH) is the most abundant thiol-containing compound in the cytosol, NO easily binds to its nucleophilic thiolate residues to further form *S*-nitrosoglutathione (GSNO) (Singh *et al*., 1996), which is thus a representative RSNO. Due to important roles of GSH in maintaining cellular redox homeostasis, the ratio of GSH to its oxidized forms glutathione disulfide (GSSG) or GSNO should be strictly regulated. GSNOR converts GSNO into GSSG and ammonia (NH_3) (Liu *et al*., 2001). Oxidized GSSG is further converted into reduced GSH via glutathione reductase (GR) activity (Lopez-Miraba & Winter, 2008). GSNOR regulates not only GSNO levels but also other RSNOs (Liu *et al*., 2001), and thus, emerges the critical function of GSNOR in maintaining the intracellular RSNO levels. In addition to GSNOR, a potential function of thioredoxin in catalyzing the denitrosylation of RSNOs other than GSNO is also reported (Wu *et al*., 2011; Sengupta & Holmgren, 2013). Interestingly, the activity of known GSNOR is attributed to GSH-dependent formaldehyde dehydrogenase (GS-FDH) (Liu *et al*., 2001). In *S. cerevisiae*, the *SFA1* gene has been reported to encode GS-FDH

with the GSNOR activity (Li *et al*., 2011). Although GSNOR activity, which is impaired by high levels of GSNO, has also been confirmed in the crude extract of *S. pombe* cells (Sahoo *et al*., 2006), the functional GSNOR-encoding gene has not been identified yet.

1.3.2 NO-dependent cellular responses

Studies of the functions of NO as a signaling molecule in yeast system are quite limited. In mammalian cells, NO modulates cellular responses mostly via soluble guanylate cyclase (sGC) and cyclic guanidine monophosphate (cGMP). This NO-sGC-cGMP pathway appears to play an essential role in smooth muscle relaxation (Lincoln *et al*., 2006), platelet inhibition (Walter & Gambaryan, 2009), anti-apoptotic effect (Noguchi *et al*., 2008), and anti-inflammatory effect (Ahluwalia *et al*., 2004). Despite the reports of the sGC activity that converts guanidine triphosphate (GTP) to cGMP and of the detection of cGMP in *S. cerevisiae* (Eckstein & Schlobohm, 1997; Kuo *et al*., 1998), to date, little is known about the NO-sGC-cGMP signaling in unicelullar eukaryotes. In *S. pombe*, a study using potential sGC inhibitors suggested that NO regulates ascus and spore formation partly via the cGMP pathway (Kig & Temizkan, 2008).

Better understanding of NO signaling in yeast is mainly obtained by various cellular effects caused by exogenous NO donor treatment. A genome-wide expression profile of the pathogenic yeast *C. albicans* in response to an NO donor dipropylenetriamine (DPTA) NONOate revealed a significant induction of the *YHB1* gene by NO and its pivotal role in virulence (Hromatka *et al*., 2005). A more recent study has confirmed the regulatory activity of transcription factor Cta4 upon the Yhb1 activity (Chiranand *et al.,* 2008). These results indicate the potential contribution of NO signaling in pathogenicity of *C. albicans*.

In *S. cerevisiae*, NO has been reported to show cytoprotective actions under variety of environmental stresses including high temperature (Nishimura *et al*., 2013) and freeze-thaw stresses (Sasano *et al*., 2012). Regarding the NO-mediated antioxidative mechanism, both exogenous NO-donor treatment using *S*-nitroso-*N*-acetylpenicillamine (SNAP; NO^- generator) and high-temperature stress have been found to activate the transcription factor Mac1 involved in cupper metabolism, leading to the induction of copper transporters as well as the increase of intracellular copper levels, which eventually activates copper-dependent superoxide dismutase Sod1 (Nasuno *et al*., 2014). Related to this, a previous study observed that exposure of *S. cerevisiae* cells to high concentrations of an NO donor 2-(N,N-diethylamino)-diazenolate-2-oxide (DEA/NO; NO^- generator) results in a dramatic and rapid

inhibition of the activity of the metal-responsive transcription factor Ace1 (Shinyashiki *et al*., 2000). Also, it is worth noting that, regardless to NO species released from NO donor, the concentrations of NO donors determine the cellular responses. For instance, treatment of *S. cerevisiae* cells with an NO^+ donor, 1 mM sodium nitropusside (SNP) shows a cytoprotective effect upon heat shock treatment, whereas 2 mM SNP severely damages cells growth (Domitrovic *et al*., 2003). The cytotoxic effects caused by excessive levels of NO occur through various mechanisms, such as increasing metal toxicity (Chiang *et al*., 2000) and promoting glyceraldehyde-3-phosphate dehydrogenase (GAPDH)-targeted proteolysis by metacaspase through *S*-nitrosation (Almeida *et al*., 2007; Silva *et al*., 2011).

In *S. pombe*, NO donors, $ONOO^-$ and SNP, were reported to decrease the ratio of GSH to GSSG, suggesting that the treated cells are suffered from oxidative stress (Sahoo *et al*., 2006). Consistently, lack of the activity of Pap1, an oxidative stress response regulator, leads to the increased sensitivity to nitrosative stress (Sahoo *et al*., 2006; Kang *et al*., 2011; Majumdar *et al*., 2012). It was also revealed that NO is indeed involved in the activation of Pap1 (Kim *et al*., 2008), as well as of a nutrient-sensing transcription factor Rst2 (Kato *et al*., 2012). Therefore, it is likely that the defensive mechanisms against nitrosative and oxidative stresses are partly overlapped in *S. pombe*. Moreover, treatment with high concentrations of an NO donors (*Z*)-1-[2-(2-aminoethyl)-*N*-(2-ammonioethyl)amino]diazen-1-ium-1,2-diolate (DETA NONOate) results in mitotic delay of *S. pombe* cells through G2/M checkpoint activation. This phenotype is highly correlated with an inactivation of Cdc25, a Cdc2-activated protein kinase, through its *S*-nitrosylation (Majumdar *et al*., 2012).

1.4 *Schizosaccharomyces pombe*, a model organism for studies of eukaryotic cells

S. pombe is a unicellular free-living ascomycete fungus with a genome size of 13.8 Mb. In 2002, Wood and his colleagues presented a remarkable works of the completion of the fully annotated genome sequence of *S. pombe*. The genome consists of chromosomes I (5.7 Mb), II (4.6 Mb), and III (3.5 Mb), as well as 20 kb of mitochondrial genome, with 4,824 protein-coding genes (Wood *et al*., 2002). This compact genome size allows us to perform genome-wide studies, such as transcriptomic and proteomic profiling (Hwang *et al*., 2006; Schmidt *et al*., 2007; Sun *et al*., 2013; Biswas & Gosh, 2014), and systems biology-based approaches. *S. pombe* is also widely known as a useful model organism for molecular biological researches of higher eukaryotes due to the fact that *S. pombe* relatively shares common features in terms of molecular and metabolic properties with higher eukaryotic cells.

19

Hence, various studies of critical biological processes, such as cell cycle (Shiozaki *et al.*, 1997; Ikeda *et al.*, 2008), DNA replication (Bartlett & Nurse, 1990; Novak & Tyson, 1997), stress- (Shiozaki & Russel, 1996; Shiozaki *et al.*, 1998; Morigasaki *et al.*, 2013) or nutrient-mediated signal transduction (Nakase *et al.*, 2013; Becker *et al.*, 2012), and aging (Coelho *et al.*, 2013), have been intensively conducted using *S. pombe* cells. In addition, pathological studies of human genetic diseases have been carried out with *S. pombe*. For example, *S. pombe* has been applied to study lysosomal storage disorders of metabolic Batten disease (Haines *et al.*, 2009), target specificity of chemotherapeutic agents for cancer (Mojardin *et al.*, 2013), and molecular mechanisms of a viral protein of human immunodeficiency virus (Elder *et al.*, 2001). To support the use of *S. pombe* as a model organism, useful genetic tools, such as for epitope tagging (Tamm *et al.*, 2012), for conditional expression (Moreno *et al.*, 2000; Bellemare *et al.*, 2001; Fujita *et al.*, 2006), and for selective protein degradation (Kanke *et al.*, 2012), have been developed. In addition to the use as a model of eukaryotic systems, *S. pombe* has also become one of the attractive hosts for synthesis of heterologous proteins with eukaryote-type post-translational modifications (Kumar & Singh, 2004; Mukaiyama *et al.*, 2010) attributed with advanced strategy to enhance the product yield (Giga-Hama, 2007, Idiris *et al.*, 2010, Lyngso *et al.*, 2010).

1.5 H_2O_2-induced oxidative stress responses in *S. pombe*

As a major causal factor of various pathological events, aging, and cell death, oxidative stress in yeast has gained wide attentions and studied in many different aspects. Oxidative stress is commonly defined as a disturbance in the balance between production of ROS and antioxidant defenses (Betteridge, 2000). ROS are originated by exogenous oxidative environments or endogenously via mitochondrial respiratory chain (Murphy, 2009), uncoupled NOS (Sullivan & Pollock, 2006), or NADPH oxidase (NOX) (Rinnerthaler e*t al.*, 2012), although the presence of NOX as well as NOS in yeast cells is still debatable. The free radicals causing oxidative stress, such as O_2^- and hydroxyl radicals (OH$^-$), are oxygen-containing molecules that have one or more unpaired electrons and easily react with other molecules. Other ROS, such as H_2O_2 and ONOO$^-$, are also powerful oxidants, though they are not free radicals (Hyberston *et al.*, 2011). Among them, OH$^-$ is a very dangerous compound because it highly reacts with all biomolecules. For example, OH$^-$ straightforwardly oxidizes polyunsaturated fatty acid into labile lipid hydroperoxides that act as reactive derivatives themselves, thus intensifying the oxidative damage (Niki *et al.*, 2005). Also, DNA damage is

20

predominantly caused by OH$^-$. Oxidative stress is monitored by an imbalance in redox couples, such as reduced to oxidized glutathione (GSH/GSSG) (Schafer & Buettner, 2001), NADPH/NADP$^+$ (Ogasawara *et al*., 2009) or L-cysteine/cystine (Cys/CySS) (Go & Jones, 2011).

In *S. pombe*, the cellular responses upon H_2O_2-induced oxidative stress are well studied. Two independent but cross-talking pathways, the mitogen-activated protein (MAP) kinase Spc1 and the downstream transcription factor Atf1 pathway (Spc/Atf1 pathway) and the stress-responsive transcription factor Pap1 pathway, are responsible in combating oxidants. The former mainly responds to high levels of oxidants to maintain cell viability, whereas the latter is activated by mild or moderate oxidants levels (*i.e.* less than 0.2 mM H_2O_2) and important in adaptive responses (Quinn *et al*., 2002; Vivancos *et al*., 2005; Chen *et al*., 2008).

Once *S. pombe* cells are exposed to low level of H_2O_2, peroxiredoxin Tpx1 is directly oxidized to its active form. Subsequently, Pap1 is activated by active Tpx1 through disulfide bond formation between Cys278 and Cys285 and further transported to the nucleus to induce the expression of antioxidant genes, such as *trx2$^+$* encoding thioredoxin, *trr1$^+$* encoding thioredoxin reductase, *pgr1$^+$* encoding glutathione reductase, and *ctt1$^+$* encoding catalase (Calvo *et al*., 2013). In contrast, the crosstalk between the Spc1/Atf1 and Pap1 pathways occurs during exposure to high concentrations of H_2O_2. H_2O_2-mediated hyperoxidation of Tpx1 transiently inhibits the Tpx1 activity. Simultaneously, Spc1 is phosphorylated at Thr171 and Tyr173 residues by the MAP kinase kinase Wis1 and accumulated into the nucleus (Shiozaki & Russel, 1995; Gaits *et al*., 1995). Phosphorylated Spc1 subsequently phopsphorylates and stabilizes Atf1 (Wilkinson *et al*., 1996) to promote the expression of Atf1-dependent stress-responsive genes, including H_2O_2 scavengers catalase (*ctt1$^+$*), glutathione peroxidase (*gpx1$^+$*), and also a redox regulatory protein namely sulfiredoxin (*srx1$^+$*) (Shieh *et al*., 1998; Lawrence *et al*., 2007). Sulfiredoxin reduces hyperoxidized Tpx1 to the active form, leading to the reactivation of the Pap1 pathway (Vivancos *et al*., 2005) (Figure 6).
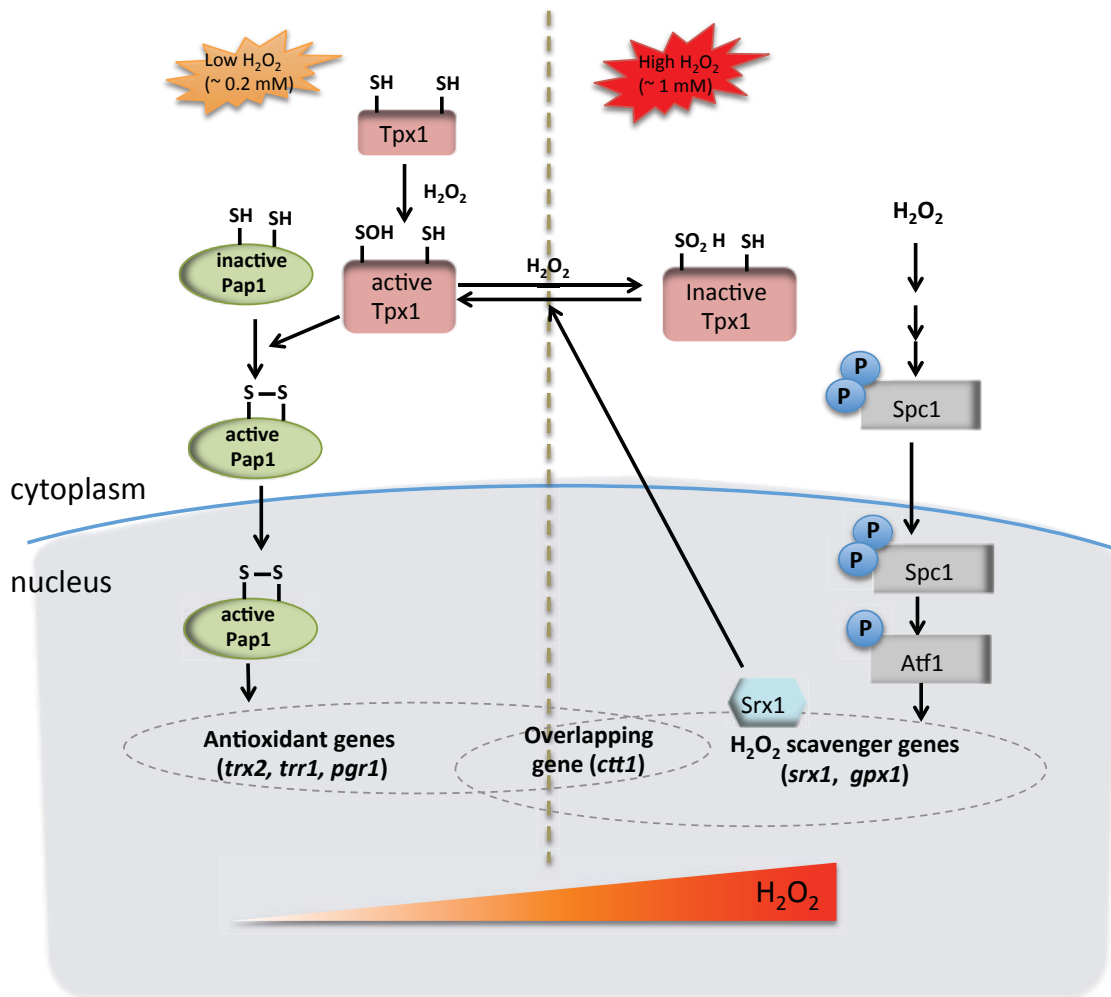
Figure 6. Oxidative stress response pathways in *S. pombe*.
H_2O_2 levels determine which of the Spc1/Atf1 or Pap1 pathway to be activated. The Pap1 pathway is responsible in dealing with low levels of H_2O_2 and induces antioxidant responses in a peroxiredoxin Tpx1-dependent manner. High levels of H_2O_2, on the other hand, activate the Spc1-MAP kinase cascade to further induce stress-responsive genes, as well as to reactivate the Pap1 pathway, through phosphorylation-induced Spc1/Atf1 activity.

1.6 Objectives of my research

As mentioned above, independent lines of studies have revealed the potential contribution of NO in diverse cellular responses in yeasts so far. However, the key questions are still remaining: Does NO signaling indeed occur under the physiological conditions of yeast cell growth? If yes, what are the pivotal roles of the NO signaling in yeast? To address these issues, first I focused on the fluctuations of the NO and RSNO levels throughout the growth phases to identify the functional NOD and GSNOR genes, the presence of which may provide strong evidence of the regulatory mechanisms of NO signaling in yeast. Detailed analysis of the NO signaling profile may also help revealing important clues to the growth

22

phase-specific NO biosynthetic mechanisms. Next, to gain better understanding about the significance of NO signaling, I performed a DNA microarray analysis of yeast cells treated with an NO donor. The roles of candidate genes under the control of NO signaling were further investigated particularly under oxidative stress conditions. This study using a promising model organism *S. pombe* will contribute to the finding of a novel type of NO signaling and its physiological role that may be conserved in higher eukaryotes.

2. Materials and Methods

2.1 Strains, culture media, and plasmids

The strains of *S. pombe* used in this study are listed in Table 1. Yeast cells were cultured in either rich medium (yeast extract with supplements, YES) or Edinburgh minimum medium (EMM) supplemented with amino acids in correspondence to the auxotrophic character of each strain used. Genetic manipulations including gene deletions and epitope tagging were conducted through chromosomal integration of PCR-amplified cassettes of the targeted DNA-flanking regions as described (Janke *et al*., 2004). The PCR-cassettes for gene deletions were constructed by using several types of template plasmids harboring different selection markers, including pUG6 (geneticin-resistant), pFA6a-natNT2 (nourseothricin-resistant) and pFA6a-hphNT1 (hygromycin-resistant). In addition, pFA6a-3HA-kanMX6 was used as plasmid template for the generation of C-terminal 3HA-tagged proteins cassettes, accordingly, the kanMX6 module allowed selection of G418-resistant cells in yeast. A simple yeast transformation procedure was then performed to introduce the corresponding PCR cassettes into fission yeast cells (Morita & Takegawa, 2004). For selective growth of the respective transformants, antibiotics were added in the following concentration to YES medium: 100 μg/ml geneticin (Santa Cruz Biotech), 100 μg/ml nourseothricin (Jena Bioscience), and 100 μg/ml hygromycin (Wako Pure Chemicals).

To test the mitochondrial physiology under the conditions related to the stationary phase, yeast cells were cultured at initial $OD_{600} = 0.05$ to mid-log phase in EMM medium containing rapamycin (200 and 500 nM) or with modified glucose concentrations (0.5, 1, and 2%). Alleviation of mitochondria activity was carried out by cultivating yeast cells to stationary phase in rich medium containing a cytochrome bc_1 inhibitor, antimycin A (1.5 μM), or cytochrome *c* oxidase inhibitor, potassium cyanide (125 μM; Wako Pure Chemicals).

To inhibit the intrinsic NOS-like activity, treatment of Arg analogue, L-N^G-nitroarginine nitroarginine methyl ester (L-NAME; Bachem AG), was conducted. For this purpose, yeast cells were grown to the mid-log phase in rich medium containing different concentrations of L-NAME (0, 50, 75, and 100 mM). Inhibition of NOS-like activity in stationary phased cells was conducted with 75 mM L-NAME to the late-log phased culture and then continuing the incubation until stationary phase (3 days after inoculation).

To assay the effect of exogenous NO under oxidative stress conditions, cells were grown to the mid-log phase in rich medium and then treated with 0.5 mM DETA NONOate (Cayman Chemical) for two hours, followed by 2 mM hydrogen peroxide (H_2O_2)-induced

oxidative stress treatment for next two hours. Cell cultures without 0.5 mM DETA NONOate treatment and/or without 2 mM H_2O_2 treatment were also prepared as controls.

Table 1. List of yeast strains used in this study

Strain	Genotype	Background and/or source
WT (ARC039)	*h-leu1-32 ura4-294*	derived from strain L972
Fmd1-3HA	*h-leu1-32 ura4-294 Fmd1-3HA::kanMX6*	this study
Fmd2-3HA	*h-leu1-32 ura4-294 Fmd2-3HA::kanMX6*	this study
Fmd3-3HA	*h-leu1-32 ura4-294 Fmd3-3HA::kanMX6*	this study
SPAC869.02c-3HA or Yhb1-3HA	*h-leu1-32 ura4-294 SPAC869.02c-3HA::kanMX6*	this study
Δ*SPAC869.02c* or Δ*yhb1*	*h-leu1-32 ura4-294 SPAC869.02c::kanMX6*	this study
Δ*fmd1*	*h-leu1-32 ura4-294 fmd1::natNT2*	this study
Δ*fmd2*	*h-leu1-32 ura4-294 fmd2::kanMX6*	this study
Δ*fmd3*	*h-leu1-32 ura4-294 fmd3::hphNT1*	this study
Δ*fmd1* Δ*fmd2*	*h-leu1-32 ura4-294 fmd1::natNT2 fmd2::kanMX6*	this study
Δ*fmd1* Δ*fmd3*	*h-leu1-32 ura4-294 fmd1::natNT2 fmd3::hphNT1*	this study
Δ*fmd2* Δ*fmd3*	*h-leu1-32 ura4-294 fmd2::kanMX6 fmd3::hphNT1*	this study
Δ*fmd1* Δ*fmd2* Δ*fmd3*	*h-leu1-32 ura4-294 fmd1::natNT2 fmd2::kanMX6 fmd3::hphNT1*	this study
Δ*SPAC869.02c* Δ*fmd1*	*h-leu1-32 ura4-294 SPAC869.02c::hphNT1 fmd1::natNT2*	this study
Δ*SPAC869.02c* Δ*fmd2*	*h-leu1-32 ura4-294 SPAC869.02c::hphNT1 fmd2::kanMX6*	this study
Δ*SPAC869.02c* Δ*fmd3*	*h-leu1-32 ura4-294 SPAC869.02c::kanMX6 fmd3::hphNT1*	this study
Δ*srx1*	*h-leu1-32 ura4-294 srx1::kanMX6*	this study
Δ*spc1*	*h-leu1-32 ura4-294 spc1::kanMX6*	this study
Δ*gst2*	*h-leu1-32 ura4-294 gst2::hphNT1*	this study
Δ*gst3*	*h-leu1-32 ura4-294 gst3::hphNT1*	this study
Δ*trx1*	*h-leu1-32 ura4-294 trx1::kanMX6*	this study

2.2 Quantitation of intracellular nitrosothiols (RSNO)

Intracellular RSNO levels were quantified by using a colorimetric-based method, the Saville assay (Engelman *et al.*, 2013). Wild-type yeast cells were grown to either log or stationary phase in rich medium. Cells were then harvested and lysed by using Multi Beads Shocker (Yasui Kikai) in the lysis buffer, which is phosphate-buffered saline containing 20mM diethylene triamine pentaacetic acid (DTPA), 0.5mM ethylene diamine tetraacetate (EDTA), 0.1% 4-Nonylphenyl-polyethylene glycol (NP-40), and 1mM phenylmethylsulfonyl fluoride (PMSF). Two solutions for the Saville assay, solution A (containing 3.4% (w/v) sulfanilamide and 0.1% (w/v) *N*-(1-naphthyl) ethylenediamine in 0.4 M hydrochloric acid) and solution B (containing the same substances as solution A, except for the addition of 1% (w/v) mercury(II) chloride), were prepared. *S*-Nitrosoglutathione (GSNO; Oxonon) was used as a standard for RSNO. In separate vials, crude extracts or standards were mixed with either solution A or B. Each sample was then subjected into spectrophotometer (540 nm) to monitor nitrite (NO_2^-) concentrations. RSNO levels were calculated from the difference in the absorbance values between the solution B and solution A assays. Finally, total RSNO levels were standardized by the concentrations of proteins of corresponding samples.

2.3 Transcription level analyses

Total RNA was isolated by using RNeasy Mini Kit (Qiagen) and used as a template for the generation of cDNA via reverse transcription reaction. Transcript levels of the targeted open reading frames (ORFs) were assessed with quantitative real-time PCR (qRT-PCR) using SYBR Green as a fluorescent reporter. The oligonucleotide primers are listed in supplementary information (Table S1). Appropriate dilutions of cDNA solutions were prepared to optimize the amplification efficiencies of approximately 60-70 nucleotides of DNA fragments of the target ORFs using corresponding specific pairs of primers. The differences in threshold cycles (ΔC_t) between the target ORFs and a housekeeping gene, *act1*[+], were considered as relative expression levels. Further, the fold changes in respect of the mRNA transcription levels were estimated from the exponential values of the differences between relative ΔC_t values of the sample and control treatments ($\Delta \Delta C_t$).

Transcriptomic analysis for the effects of DETA NONOate treatment was also conducted by a comprehensive GeneChip expression array. Total RNA was extracted as described above. Affymetrix GeneChip Command Console Software was used for the control and processing of the GeneChip array, and Affymetrix Expression Console Software was applied for data management and processing. Changes in the transcript levels were defined as

the ratios of 0.5 mM DETA NONOate-treated cells to mock-treated cells and calculated as logarithmic values. Genes that were found to have significant differences in expression were classified into the gene ontology (GO) categories of biological process, molecular function, and cellular component by using the AmiGO GO term enrichment tool (Carbon *et al.*, 2009).

2.4 Observation of active mitochondria

Mitochondrial activity was monitored with a fluorescent dye rhodamine 123, which is particularly used to assess mitochondrial membrane potential. Yeast cells were cultured in YES or EMM medium containing different glucose concentration (0.5, 1, and 2%) or with rapamycin (200 and 500 nM) until OD_{600} of 1. Cells were then harvested by centrifugation and further suspended in 50 mM sodium citrate buffer (pH 5) containing 2% glucose. The Rhodamine 123 solution was added at a final concentration of 50 μM to the cell suspensions, and the stained cells were observed with a fluorescent microscope (Axiovert 200M, Carl Zeiss).

2.5 Intracellular NO, ROS, and Fe^{2+} measurement using flow cytometry

The NO levels were monitored with flow cytometry based on previous studies (Strijdom *et al.*, 2004; Lampiao *et al.*, 2006) with certain modifications. After growing yeast cells on designated conditions, the cells were harvested, washed, and suspended in 1 ml of 50 mM potassium phosphate buffer (pH 7.4) containing 10 μM final concentration of a cell-permeable NO probe, 4-amino-5-methylamino-2,7 difluorofluorescein diacetate (DAF-FM DA; Sekisui Medical) at a density of approximately 10^7 cells/ml ($OD_{600} = 1$). The cell suspensions were then incubated with gently shaking for 1 h at 30°C in the dark. Light exposure was avoided as far as possible throughout experimentation. The samples were then washed with 50 mM potassium phosphate buffer (pH 7.4), and the cell pellets were suspended in 1 ml of the same buffer solutions. About 10 times cell dilutions were prepared prior to the flow cytometry analysis.

To assess intracellular ROS levels, samples were prepared as described above, except for staining with 10 μM final concentration of 2',7'-dichlorofluorescin diacetate (DCFDA; AnaSpec Inc) instead of DAF-FM DA. DCFDA treatment was conducted for 30 min prior to the flow cytometry analysis.

The detection of intracellular Fe^{2+} contents was conducted by using the Fe^{2+}-specific probe RhoNox-1 (kindly provided by Prof. Nagasawa of Gifu Pharmaceutical University). Each sample was suspended in 50 mM potassium phosphate buffer (pH 7.4), treated with final about 5 μM of RhoNox-1, incubated for 1 h, and further subjected to flow cytometry analysis.

For all experiments, the fluorescence intensity was quantified by using the BD Accuri C6 instrument (BD Biosciences) with the FL1-H channel using 488 nm for excitation and 530 nm for emission. Data are expressed as mean fluorescence intensities.

2.6 Observation of intracellular NO

Samples were prepared as those for the flow cytometry-based quantitative analysis of NO (described above). Double staining of NO and organelle was carried out by staining the cells first with the NO-fluorescence probe DAF-FM DA for 45 min at 30°C and further with organelle staining. Mitochondria and vacuoles were properly stained with 400 nM MitoTracker Red CMXRos (Life technologies) and 40 μM FM 4-64 dye (Life technologies), respectively. The stained cells were visualized with a fluorescent microscope (Axiovert 200M, Carl Zeiss) immediately without fixation.

2.7 Western blotting

Whole cell extracts were prepared as described elsewhere (Matsuo *et al*., 2006). For sodium dodecyl sulfate-polyacrylamide gel electrophoresis (SDS-PAGE), 5 μg of total protein were subjected to 10% of polyacrylamide gel. The proteins were then transferred to polyvynylidene difluoride (PVDF) membranes (Immobilon, Millipore) and then probed with a mouse monoclonal anti-HA antibody (12CA5, Roche Life Science) followed by a mouse IgG secondary antibody. After proper extensive washing with Tris-buffered saline with Tween-20 (TBST), western blot signals were then detected by a chemiluminescence-based approach using the ImageQuant LAS 4000 (GE Healthcare Life Sciences).

For in vivo analysis of hyperoxidized-peroxiredoxin Tpx1, crude extract of *S. pombe* was prepared by using trichloroacetic acid (TCA) method (Jara *et al*., 2007). *S. pombe* cells were pelleted and washed with 20% TCA. Cells were then disrupted by glass beads in 12.5% TCA solutions through vortexing in Multi Beads Shocker. Cell lysates were collected, washed in acetone and dried. Alkylation of free thiols was performed by resuspension of the pellets in 50 μl of a solution containing 75 mM iodoacetamide (Wako Pure Chemicals), 1% SDS, 100 mM Tris-HCl, pH 8.0, and 1 mM EDTA, and incubation at 25°C for 15 min. Lysates were then dissolved in 2x Laemli sample buffer prior boiling at 98°C for 3 minutes. Samples were then subjected to non-reducing SDS PAGE and followed with Western blotting as described above. Hyperoxidized Tpx1 was detected using anti- mammalian peroxiredoxin-$SO_{2/3}$ antibody (10A1, LabFrontier).

2.8 Quantitation of intracellular glutathione (GSH) and L-cysteine (Cys)

In order to estimate the intracellular levels of the reduced or oxidized form of glutathione (GSH) and L-cysteine (Cys) in yeast cells, a thiol-specific fluorescent dye monobromobimane (mBBr) was used. Yeast cells were grown to the mid-log phase in rich medium, and treated with 0.5 mM DETA NONOate and/or 2 mM H_2O_2. The cultures were separated into two tubes for with and without DTT treatment (10 mM for 10 min). The cells were subsequently harvested at the density of approximately $OD_{600} = 2$ and washed twice with cold water. Then, 100 µl of the solution containing 1 mM mBBr and 200 nM D-camphor-10-sulfonic acid sodium salt (CSA; as an internal standard) in methanol was added to the cell pellets and mixed thoroughly by vortex for 10 min at the room temperature. The cell suspensions were centrifuged (15,000 rpm, 4°C for 1 min), and about 60 µl of the supernatants, which mostly contained cellular thiol derivatives, were then withdrew. Equal amount of water was added to these supernatant solutions, centrifugation (15,000 rpm, 4°C for 1 min) was carried out, and 100 µl of the resulted supernatant was subjected to liquid chromatography/tandem mass spectrometry (LC/MS; LC-MSMS 8030, Shimadzu) with specific conditions as described (Kawano *et al*., 2014). The mass spectrophotometer was operated in the selective ion mode using ions at *m/z* 498 and *m/z* 435 for GSH-bimane, and *m/z* 312 and *m/z* 225 for Cys-bimane derivatives. The peak areas of the appropriate retention times were measured by the integration routine included in the data system. The areas of GSH-bimane and Cys-bimane were normalized to the areas of the internal standards CSA, which further considered as concentration. Oxidized GSH (GSSG) and Cys (Cystine) concentrations were calculated by subtracting the GSH and Cys levels, respectively, of the samples with DTT treatment from those without DTT treatment.

3. Results

3.1 A fine-tuned NO signaling in the fission yeast *S. pombe*

3.1.1 The dynamic state of the intracellular levels of NO and RSNOs during growth

To determine the presence of NO signaling in the fission yeast *S. pombe*, I first monitored intracellular levels of NO and its derivatives RSNOs with DAF FM-DA and Saville assay, respectively, during cell growth (Figure 7). NO was detected at a relatively high level during the log phase, and then decreased by almost 80% as cells entered the stationary phase. In contrast, RSNO levels displayed an opposite pattern, in which a relatively low level during the log phase and a significant increase in the stationary phase was observed. Although the physiological importance of these dynamic changes in NO and RSNO levels during growth period is still unclear, these data suggest the existence of NO and potentially the corresponding signal transduction throughout the growth period of *S. pombe* cells. Moreover, it is likely that such fluctuations on the NO and RSNO levels are attributed to distinct physiological and metabolic state occurred in the log and stationary phases.
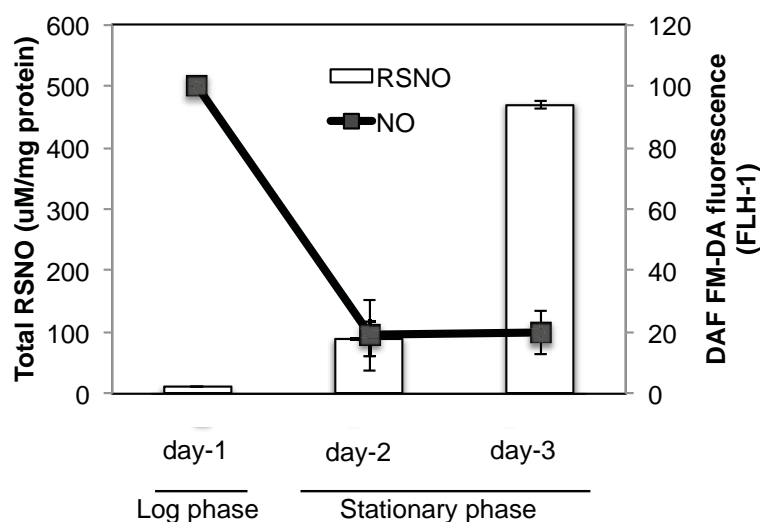
Figure 7. The intracellular levels of NO and RSNOs throughout the growth phase of fission yeast.
Cells were grown to the log and stationary phases in rich medium and then collected for NO staining and RSNOs measurement. Intracellular NO was detected by using a specific fluorescence probe for NO, DAF FM-DA, with subsequent flow cytometry analysis, whereas RSNOs were measured by Saville assay. The data shown are means ± SD of three independent experiments.

3.1.2 Identification of NO detoxification enzymes in *S. pombe*

In order to confirm the existence of NO signaling throughout the growth of *S. pombe*, I investigated the potential occurrence of NO detoxification system mediated by NOD and

GSNOR. NO detoxification is an important regulatory property of the cells with indigenous NO signaling to modulate intracellular NO homeostasis. Notably, the accumulation of NO as well as its derivative molecules in a greater extent levels than the physiological concentration is potentially toxic to the cells. For this purpose, I focused on the expression of putative NOD and GSNOR mRNAs and proteins and also their function in NO detoxification. *S. pombe* cells have a single known NOD ortholog, the predicted *SPAC869.02c⁺* gene. It is well established that the GSNOR activity is attributed to the GS-FDH proteins (Jensen *et al.*, 1998; Liu *et al.*, 2001). According to *S. pombe* genome database (www.pombase.org), there are three isoforms of GS-FDH encoded by the *fmd1⁺*, *fmd2⁺*, and *fmd3⁺* genes.

3.1.2.1. Multiple sequence alignment of the potential NO detoxification proteins

3.1.2.1.1 NOD

NOD catalyzes NO• dioxygenation to NO_3^- in a manner dependent on O_2, NADPH, and FAD. NOD consists of three distinguished functional domains, namely the N-terminal globin, FAD-binding, and C-terminal NADPH-binding domains (Bonamore & Boffie, 2008). The predicted gene product of *SPAC869.02c⁺* also harbors these three conserved domains (Figure 8).

Figure 8. The predicted NOD, SPAC869.02c, of *S. pombe*.
NOD comprises three conserved domains: the N-terminal globin domain that fused with FAD- and C-terminal NADPH-binding domains.

Multiple amino acid sequence alignment of predicted SPAC869.02c protein with the *Escherichia coli* Hmp1, the *S. cerevisiae* Yhb1, and the *C. albicans* CaYhb1 indicated conservation of the amino acid residues regarded as the hallmarks of globin structure as well as substrate- and cofactor-binding sites (Figure 9). The heme pocket region of the globin domain is essential for the NOD catalytic function. The Fe^{3+}-heme prosthetic group is the final electron acceptor from the electron donor NADPH. The Fe^{2+}-heme pocket resulted from electron reduction binds O_2 with high affinity to yield heme-Fe^{3+}-O_2^- intermediate that reacts rapidly with NO• to produce NO_3^- (Gardner *et al.*, 1998). Two amino acid residues, Tyr58 and Gln77, of SPAC869.02c, resided within the heme pocket of the globin domain, which are

proposed to contribute to iron-ligand distal stabilization during O_2 fixation, were conserved amongst the NODs of the other organisms examined. Also, His114, Tyr124, and Glu167, which are responsible for structural architecture of the heme pocket in the proximal region, were conserved. Regarding the FAD-binding site, the binding motifs for the pyrophosphate and isoalloxazine moieties within an FAD molecule (GQY and RXYS, respectively) (Dym & Eisenberg, 2001) were conserved in the *SPAC869.02c⁺* gene product. For the NADPH-binding domain, the responsible GXGXXP motif (Roma *et al*., 2005) was conserved in all sequences tested (Figure 9).

Figure 9. Multiple sequence alignment of NODs.
Multiple sequence alignment of the deduced amino acid sequence of designated NODs including SPAC869.02c from *S. pombe* (accession number NP_595017.1); Hmp1 from *E. coli* (accession number WP_016242403); Yhb1 from *S. cerevisiae* (accession number CAA97262) and CaYhb1 from *C. albicans* (accession number Q59MV9). Alignment analysis was performed with ClustalW. Important conserved residues for structural architecture of the globin domain are shaded in yellow, and the binding motifs of FAD and NADPH are shown in blue boxes. The identical amino acids are shown with asterisks. Dashes represent gaps introduced for optimal sequence alignment.

3.1.2.1.2 GSNOR

Regarding the enzymes with GSNOR activity, fission yeast harbors three genes that encode GS-FDH proteins, namely *fmd1$^+$*, *fmd2$^+$*, and *fmd3$^+$*. GSNOR catalyzes the conversion of GSNO, a representative RSNO, to GSSG and NH_3, and therefore, mainly contributes to the regulation of intracellular RSNOs. GSNOR is a zinc-containing enzyme and functions as a dimeric form. A GSNOR monomer consists of the catalytic and coenzyme domains and comprises two zinc atoms. One zinc atom (catalytic zinc) may activate the substrate GSNO during catalysis, since this zinc ion coordinates the hydroxyl and carbonyl groups of the substrate to activate the hydride transfer reaction. The second zinc atom (structural zinc) is considered to have a structural function only. In addition, five residues, namely Thr49, Asp58, Glu60, Arg117, and Lys287 of the *Solanum lycopersium* GSNOR, are involved in the binding activity to *S*-(hydroxymethyl) glutathione (HMGSH), a GSH adduct (Kubienova *et al.*, 2013).

Multiple sequence alignment of these three isoforms of *S. pombe* GS-FDHs (Fmd1, Fmd2, and Fmd3) with the *Mus musculus* GSNOR and the *S. cerevisiae* Sfa1 revealed many conserved amino acid residues important for the structural and catalytic functions (Figure 10). Except for Fmd2, Fmd1 and Fmd3 shared high identity with mammalian and budding yeast GSNORs, ranging from 60 to 66%. In contrast, Fmd2 was relatively different from the other GS-FDHs and GSNORs (17% and 13% identity with Fmd1 and Fmd3, respectively). Although most of amino acid residues responsible for binding of the catalytic zinc atom were conserved amongst the three Fmd isoforms and the other GSNOR sequences, Cys179 in Fmd3 engaged in the binding of the catalytic zinc atom was replaced by Asp in Fmd2 only. Four residues that bind with the structural zinc atom were fully conserved in all sequences examined. Whereas, all five residues reported to bind HMGSH, were not conserved in Fmd2.

```
Fmd3    ------------------------MQQSPTAGKIINCKAAVAWQPAAPLSIENVQVFPP-R  36
Sfa1    -----------------------MSAATVGKPIKCIAAVAYDAKKPLSVEEITVDAP-K  35
Fmd1    ------------------------MSFEGKTITCKAAVAWGAKEPLSIEDIQVAPP-K  33
GSNOR   -----------------------MANQVIRCKAAVAWEAGKPLSIEEIEVAPP-K  31
Fmd2    MEYLTNLKTNIMDKQLGHREVSEGSTQPKPDPSGATMKACVWDGPLNVKIAEVPKPTITH  60
                          .      * .:    :.: ::   . :

Fmd3    VHEVRIKIVNSGVCH-TDAYTLSGKDPECLFPVILGHEGAGIVESVGPQVTTVQVGDPVI  95
Sfa1    AHEVRIKIEYTAVCH-TDAYTLSGSDPECLFPCVLGHEGAGIVESVGDDVITVKPGDHVI  94
Fmd1    AHEVRVKVDWSAVCH-TDAYTLSGVDPECAFPIVLGHEGAGIVESIGEGVINVRPGDHVI  92
GSNOR   AHEVRIKILATAVCH-TDAYTLSGADPECCFPVILGHEGAGIVESVGEGVTKLKAGDTVI  90
Fmd2    PKDVIVKTTACTICSGSDSHIFSGEMPGIEKGAILGHESCGIVAEKGDEVNNLEIGDRVV  120
        ::* :*    :*   :*:: :** *      :****..*** . *  * .:. ** *:

Fmd3    ALYTPECKTCKFCKSGKTNLCCRIRTTQGKGLMPDGTSRFS-CNGNTLLHFMGCSTFSEY  154
Sfa1    ALYTAECCKCKFCTSGKTNLCCAVRATQGKGVMPDGTTRFHNAKGEDIYHFMGCSTFSEY  154
Fmd1    LLYTPECKECKFCRSGKTNLCSKIRETQGRGLMPDGTSRFS-CRDKTLLHYMGCSSFSQY  151
GSNOR   PLYIPQCCECKFCLNPKTNLCQKIRVTQGKGLMPDGTSRFT-CKGKSVFHFMGTSTFSEY  149
Fmd2    IAFDLACCQCSFCKRHEYAACDTTNDSKLMDVNYGSHHSAIFGYTKLLGDVPGCQAEYIR  180
         :   * *.**   :   *    .::  .:  ..     : : . * .:

Fmd3    TVVADISVVAIERLAPLDSVCLLGCGITTGYGAATITADIKEGDSVAVFGLGSVGLAVIQ  214
Sfa1    TVVADVSVVAIDPKAPLDAACLLGCGVTTGFGAALKTANVQKGDTVAVFGCGTVGLSVIQ  214
Fmd1    TVVADISLVAISHSAPLRSICLLGCGVTTGFGAVTHSAKVESGSTVAVVGCGCVGLAAMQ  211
GSNOR   TVVADISVAKIDPSAPLDKVCLLGCGISTGYGAAVNTAKVEPGSTCAVFGLGGVGLAVIM  209
Fmd2    VPFAEINCCKLPDDIPDSEGLFMSDVLCTSLHACTLG-EVKKGDTVAIWGMGPIGLYAGR  239
        . .*::.  :    *     ::. : *. *    .:: *.: *: * * :** .

Fmd3    GAVKKRAGRIFGIDVNPEKKNWAMSFGATDFINPND---LQSPIQDVLIHETDGGLDWTF  271
Sfa1    GAKLRGASKIIAIDINNKKKQYCSGATDFVNPKEDLAKDQTIVEKLIEMTDGGLDFTF  274
Fmd1    GAVAAGASRIIAIDINADKEVYAKKFGATDFIDSSK----VKDLVQYVIDVTDGGVDYAF  267
GSNOR   GCKVAGASRIIGIDINKDKFAKAKEFGASECISPQD---FSKSIQEVLVEMTDGGVDYSF  266
Fmd2    WAQILGASKVIGIEVVPERIELARQKFGFTVIDRNE----VSDVPKKIMELVSNGVDCAI  295
         .    *.::::.*::  .:   .   .   :.  ..    . : . ::. ...*:* ::

Fmd3    DCTGN-------------VHVMRSALEACHKGWGQSIVIGVAAAGQEISTRPFQLVTGRV  318
Sfa1    DCTGN-------------TKIMRDALEACHKGWGQSIIIGVAAAGEEISTRPFQLVTGRV  321
Fmd1    DCTGN-------------VTVMQQELQFCHKGWGKLCVIGVAAAGKTLDFRPFLVVTGRQ  314
GSNOR   ECIGN-------------VKVMRSALEAAHKGWGVSVVVGVAASGEEISTRPFQLVTGRT  313
Fmd2    EASGFRFSTSILHKVERAVGLETDSPDMITECLNAVRKYGHVSIIADYVGTSNQFPIGHV  355
        :. *                . : . :  *   .:       * .:    . . *:

Fmd3    WRG---CAFGGVKGRSQLPDLVKEYLDHKLEIDKYITHRRPLKEINEAFTDMHNGN--CI  373
Sfa1    WKG---SAFGGIKGRSEMGGLIKDYQKGALKVEEFITHRRPFKEINQAFEDLHNGD--CL  376
Fmd1    VLG---SAFGGVKGRSELPNFVDEYMQGHFKVDEYITNEEPLKNINKAFDHMHEGK--CI  369
GSNOR   WKG---TAFGGWKSVESVPKLVSEYMSKKIKVDEFVTGNLSFDQINQAFDLMHSGD--SI  368
Fmd2    VMKHLTIRSGQCPCQNYFGYVIDNIRSGKIDPRWMVTNKIKFDDLPDAYNKLFYKEDGYV  415
           *         .  . .:::  .  :.    :* . :.:: .*: :.  .   :

Fmd3    KTVLSIP--- 380
Sfa1    RTVLKSDEIK 386
Fmd1    RCVVDMNKP- 378
GSNOR   RTVLKM---- 374
Fmd2    KVYCDMTE-- 423
        :   .
```

Figure 10. Multiple sequence alignment of GSNORs

Multiple sequence alignment of the deduced amino acid sequence of designated GSNORs including: GSNOR from *Mus muculus* (accession number NP_031436.2); Fmd1 (accession number NP_596821.1), Fmd2 (accession number NP_595070.1), and Fmd3 (accession number NP_588247.1) from *S. pombe*; and Sfa1 from *S. cerevisiae* (accession number CAA98742.1). Alignment analysis was performed with ClustalW. Conserved residues engaged in the binding of the catalytic and structural zinc atoms are shaded in yellow and grey, respectively. The residues involved in substrate (*S*-(hydroxymethyl) glutathione, HMGSH) binding are shaded in red color. For the residues different from conserved GSNOR sequences are colored red. The identical amino acids are shown with asterisks. Dashes represent gaps introduced for optimal sequence alignment.

3.1.2.2. Effects of putative NOD and GSNORs on intracellular NO levels

In order to clarify the essential function of these two kinds of NO-detoxification enzymes in regulating intracellular NO signaling, I assessed the capacity of the mutant strains

lacking the particular genes encoding the respective NO-detoxification enzymes, either singly or in combination, to cause alteration upon the intracellular NO level (Figure 11). Single deletion of each of the genes or double or triple disruption of the *fmd* genes did not significantly alter the intracellular NO level either at the log or the stationary phase. Only when both the *SPAC869.02c*[+] and *fmd2*[+] genes were deleted, however, the NO levels significantly increased both in the log and stationary phases. Although the NO level decreased in the stationary phase in wild-type and most mutant cells, it was further elevated after the Δ*SPAC869.072c* Δ*fmd2* cells entered the stationary phase. This result indicates the essential role of these two genes in cooperatively controlling the physiological levels of NO to ensure homeostasis. This finding is interesting particularly because Fmd2 showed a low sequence similarity to the other GSNOR family proteins (Figure 10).
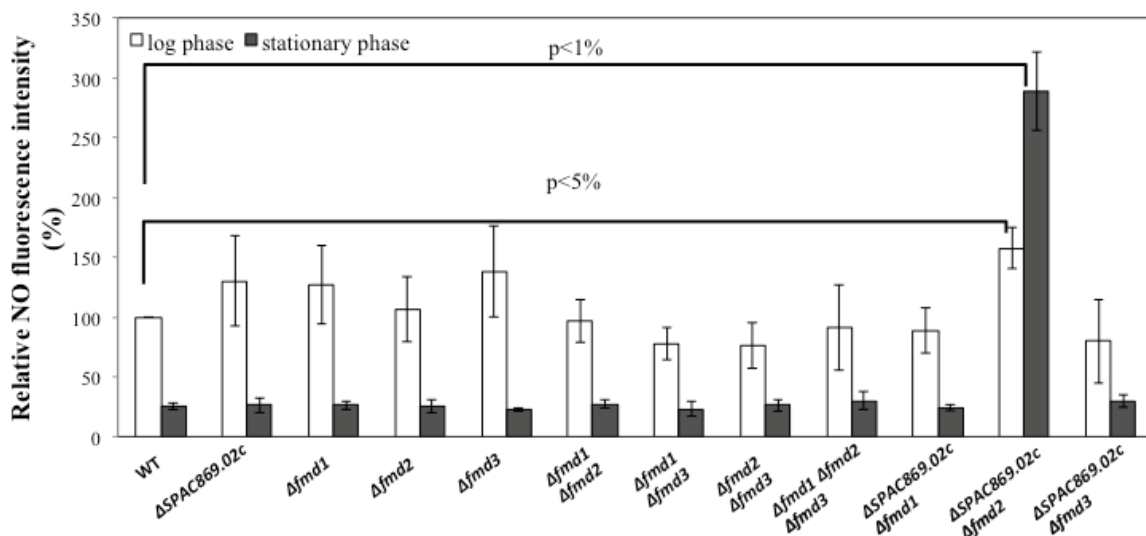

Figure 11. NO levels of SPAC869.02c and Fmd isoforms mutants in the log and stationary phases
Intracellular NO levels of wild-type (WT) and mutant strains lacking the genes involved in NO detoxification, *SPAC869.02c*[+] and/or *fmd*[+](s). NO was assessed by staining with an NO-specific fluorescence probe DAF FM-DA and subsequent fluorescence intensity measurement with flow cytometry in both the log and stationary phased cells (3 days of incubation). Data are means of three independent experiments.

3.1.2.3. Expression of putative NOD and GSNOR genes

Next, I measured the expression levels of the genes potentially engaged in the NO-detoxification activity at the mRNA and protein levels in two distinct growth phases (Figure 12). Although the transcription level of *fmd1*[+] remained stable throughout growth phases, its protein was highly expressed only during the log phase. However, the contribution of Fmd1 in

modulating NO levels during the log phase was debatable since deletion of *fmd1+* did not significantly alter the intracellular NO level in the log phase (Figure 11). Notably, the *fmd2+* mRNA and its corresponding protein were essentially induced once cells entered the stationary phase, while absent during the log phase. Although a weak upregulation of the *fmd3+* gene was observed, Fmd3 protein was not clearly detected through the growth phases. *SPAC869.02c+* mRNA and protein were constitutively expressed (Figure 12B). Taken together with Figure 11, the function of NO detoxification likely occurred throughout the growth phases, mainly involving a constitutive NOD SPAC869.02c and an inducible GSNOR Fmd2. Hereafter, the *SPAC869.02c+* gene was renamed *yhb1+*, according to the *S. cerevisiae* and *C. albicans* NOD-encoding *YHB1* (yeast flavohemoglobin 1) genes (Liu *et al*., 2000; Ullman *et al*., 2004). The intense induction of the *fmd2+* gene might be correlated with high levels of RSNO observed in the stationary phase (Figure 7).
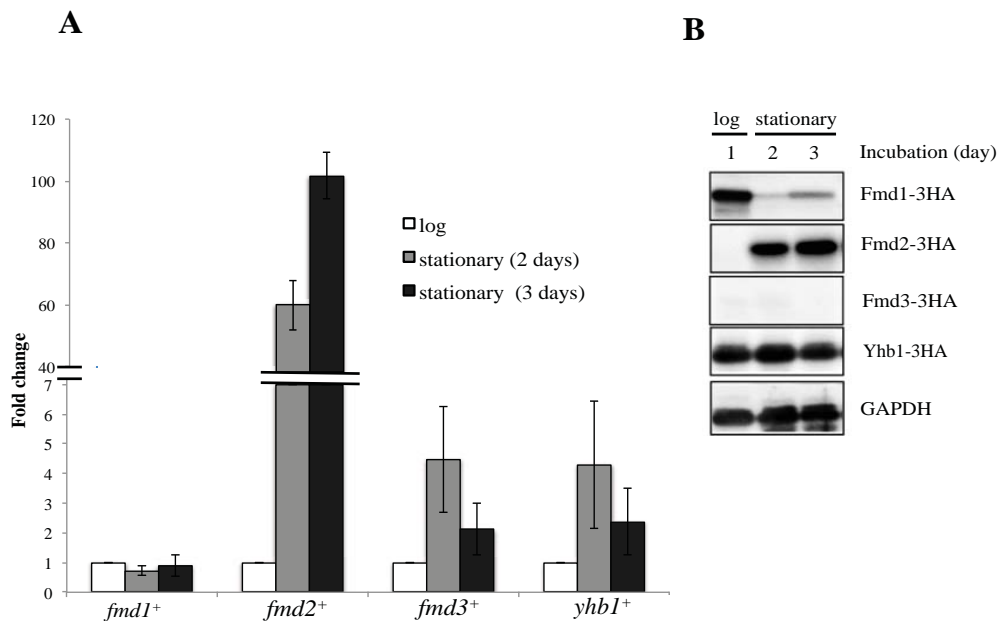

Figure 12. The mRNA and protein levels of the putative NO detoxification enzymes throughout the growth phases.
(A) The mRNA levels of the NO detoxification-related genes throughout growth phases. Transcript levels were assessed with quantitative real-time PCR analysis using cDNA prepared from yeast cells grown in rich medium at each growth phase. The fold changes were normalized with the *act1+* transcript levels. Data are means of three independent experiments. (B) Expression of the NO detoxification-related proteins throughout growth phases. Cell lysates were extracted from yeast cells grown in rich medium at either log or stationary phase. Each of 3HA-tagged protein was detected by Western blotting using anti-HA antibody (12CA5), and GAPDH was used as a loading control. Blots are representatives from three independent experiments.

3.1.3 NO-synthetic mechanisms specific to growth phases

3.1.3.1 NOS as a major NO producer during the log phase

Previous study by Kig and Temizkan (2009) demonstrated the *in vitro* NOS catalytic activity in *S. pombe*. Supporting this result, I also observed that the treatment of log-phase cells with L-NAME, a NOS inhibitor, significantly reduced the intracellular NO level in a dose-dependent manner (Figure 13A). This suggests a potential role of NOS as a main NO generator during the log phase of *S. pombe*. Furthermore, L-NAME treatment decreased the expression of the discovered NOD, Yhb1, in a similar dose-dependent manner (Figure 13B). Thus, the protein level of SPAC869.02c is highly correlated with the intracellular levels of NO. It is also noted that no significant alterations in the cells viability by L-NAME treatment were observed (Figure 13C). Taken together, specifically in the log phase, it is likely that NO is predominantly produced via the unidentified NOS activity, and the consequent intracellular NO level controls the expression of Yhb1 protein to maintain NO homeostasis.
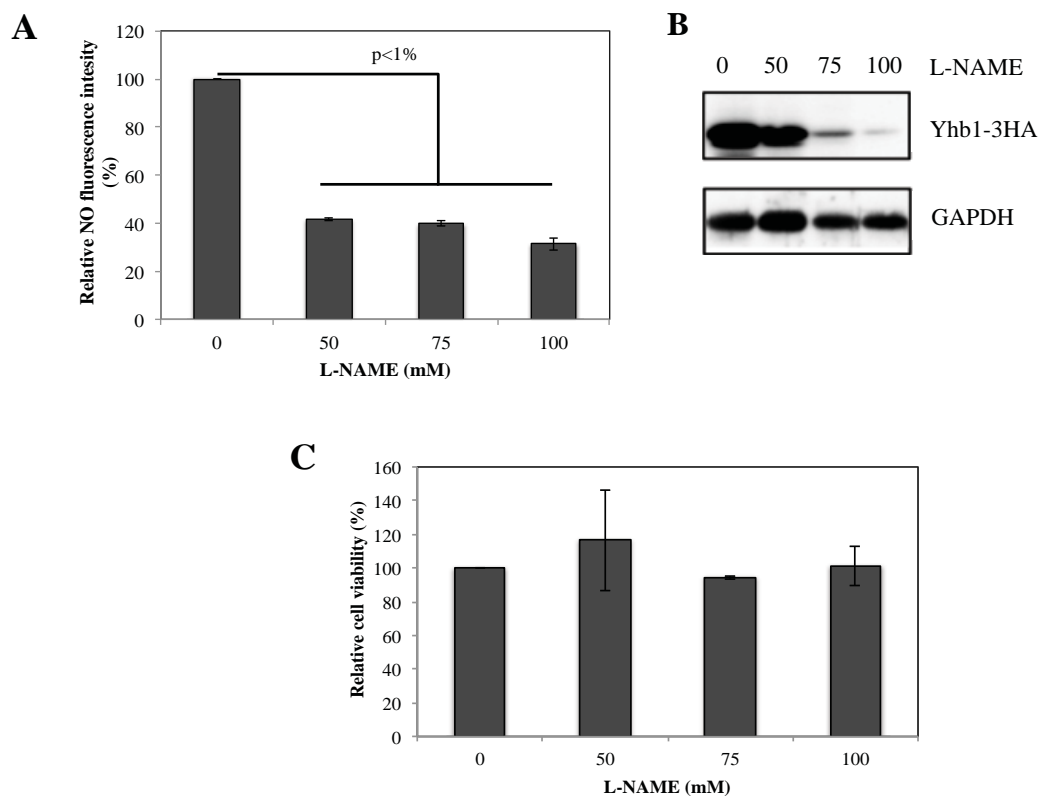

Figure 13. Effects of a NOS inhibitor, L-NAME, on the intracellular NO level the Yhb1 protein level, and the cell viability in the log phase.
(A) NO level. Cells were grown in YES medium supplemented with L-NAME (0, 50, 75, or 100 mM). DAF FM-DA was used for NO staining, and the cells were further subjected to flow cytometry analysis to quantify the NO levels. Data are means from three independent experiments. (B) Yhb1 protein level. Cell extracts were prepared from the cells with or without L-NAME treatment and analysed by Western blotting. Western blot data is the representative from three independent experiments. Yhb1-3HA was detected with an anti-HA antibody (12CA5), and GAPDH was used as a loading control. (C) Cell viability. For cells viability assay, cells were grown in YES medium until log phase, L-NAME was then added and incubated again for the next two hours. Cells were then appropriately harvested and spread on to YES agar plates for colony counting after 3 days of incubation.

3.1.3.2 Association of mitochondrial activity with the NO production during the stationary phase

Next, I focused on the effects of L-NAME on the expression of Yhb1 and the other NO-detoxyfication enzyme, GSNOR, encoded by *fmd2*$^+$, in the stationary phase (Figure 14). While L-NAME treatment significantly decreased the Yhb1 protein level in the stationary phase as well as in the log phase, most of the Fmd2 signal remained after L-NAME treatment in the late stationary phase (day 3; Figure 14). These data suggests the existence of the NOS-independent NO signaling that induces the Fmd2 expression specifically in the stationary phase.
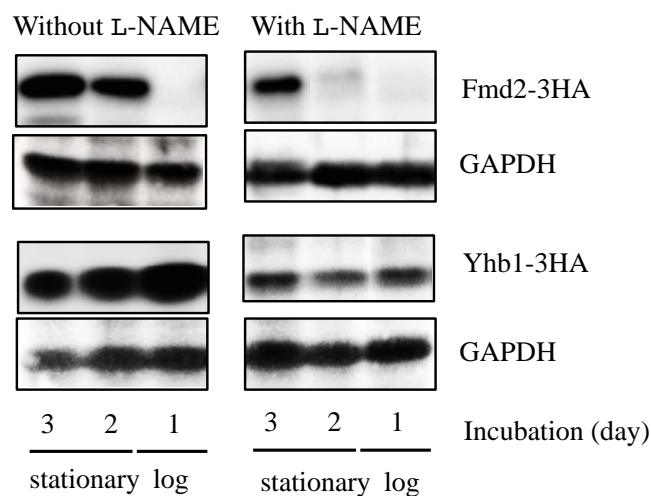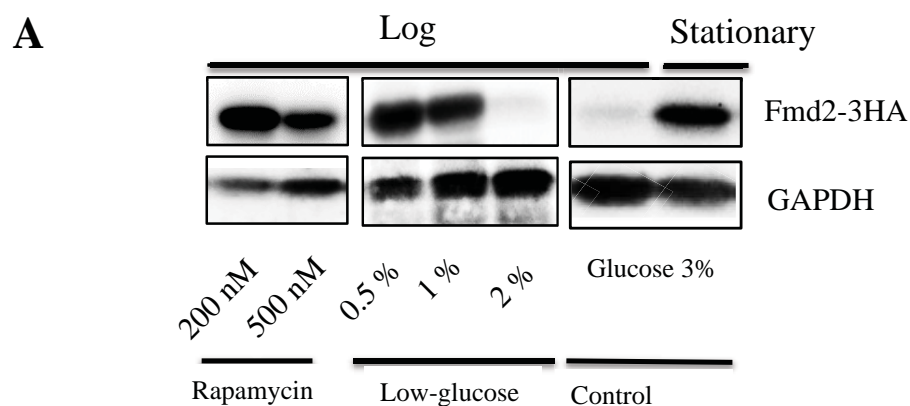

Figure 14. Effects of a NOS inhibitor, L-NAME, on the expression levels of Yhb1 and Fmd2 proteins throughout growth phases.
Cells were grown to either log or stationary phase in rich medium containing 75 mM L-NAME. Cell lysates were used for Western blot analysis to determine the protein level of both Fmd2-3HA and Yhb1-3HA. Fmd2-3HA and Yhb1-3HA were detected by anti-HA antibody (12CA5), and GAPDH was used as a loading control. Data are representatives of three independent experiments.

The stationary phase is at least partly characterized by nutrient depletion and subsequent inhibition of the target-of-rapamycin (TOR) pathway. Fmd2, which was absent in log-phase cells, was expressed during the growth under the presence of rapamycin or low-glucose conditions (e.g. 0.5 or 1%), as highly as the entry into the stationary phase (Figure 15A). In addition, during the transition from the log phase to the stationary phase, the rate of fermentation decreases, and simultaneously, the rate of oxygen uptake for mitochondrial respiratory chain (MRC) increases (Gray *et al*., 2004). Consistently, the log-phase cells grown in the low-glucose conditions or with rapamycin, as well as stationary-phase cells, commonly increased the MRC activity assayed by Rhodamine 123 staining (Figure 15B). To address

whether mitochondrial electron transport is related to NO signaling, I further examined the specific involvement of the MRC complexes in the induction of Fmd2. Under low-oxygen conditions, cytochrome *bc1* (complex III) or Cco (complex IV) of MRC is responsible for the NIR activity that converts NO_2^- to NO (Nohl *et al.,* 2000; Castello *et al.,* 2008). Therefore, the cells treated with antimycin A and potassium cyanide (KCN) that inhibit the electron transfer in complexes III and IV, respectively (Rosenfeld *et al*. 2002), were analyzed (Figure 15C). As a result, suppression of the Fmd2 expression was observed in antimycin-A treated cells partly in day 2 and almost completely in day 3 while no obvious alteration was observed by the KCN treatment. Taken together, these data suggest that specifically in the stationary phase, NO signaling occurs via the NIR activity caused by the activation of complex III of MRC. In fact, previous studies revealed the mitochondria-dependent NO synthesis mechanism in mammalian (Castello *et al.,* 2006) and yeast cells (Li *et al.,* 2011).

In accordance to mitochondrial respiration, it is well established that MRC enhances ROS generation, such as O_2^- or H_2O_2, as a result of the sequential reduction of O_2. Thus, I also assessed the effect of either menadione, which is an O_2^- generator, or H_2O_2 upon the Fmd2 expression of the log-phase cells (Figure 15D). Interestingly, Fmd2 was indeed induced by these treatments. In addition, treatment of H_2O_2 significantly increased the intracellular NO levels (Figure 15E). Taken together, it is indicated that NO may act as signaling molecule in regulating oxidative tress response in *S. pombe*.
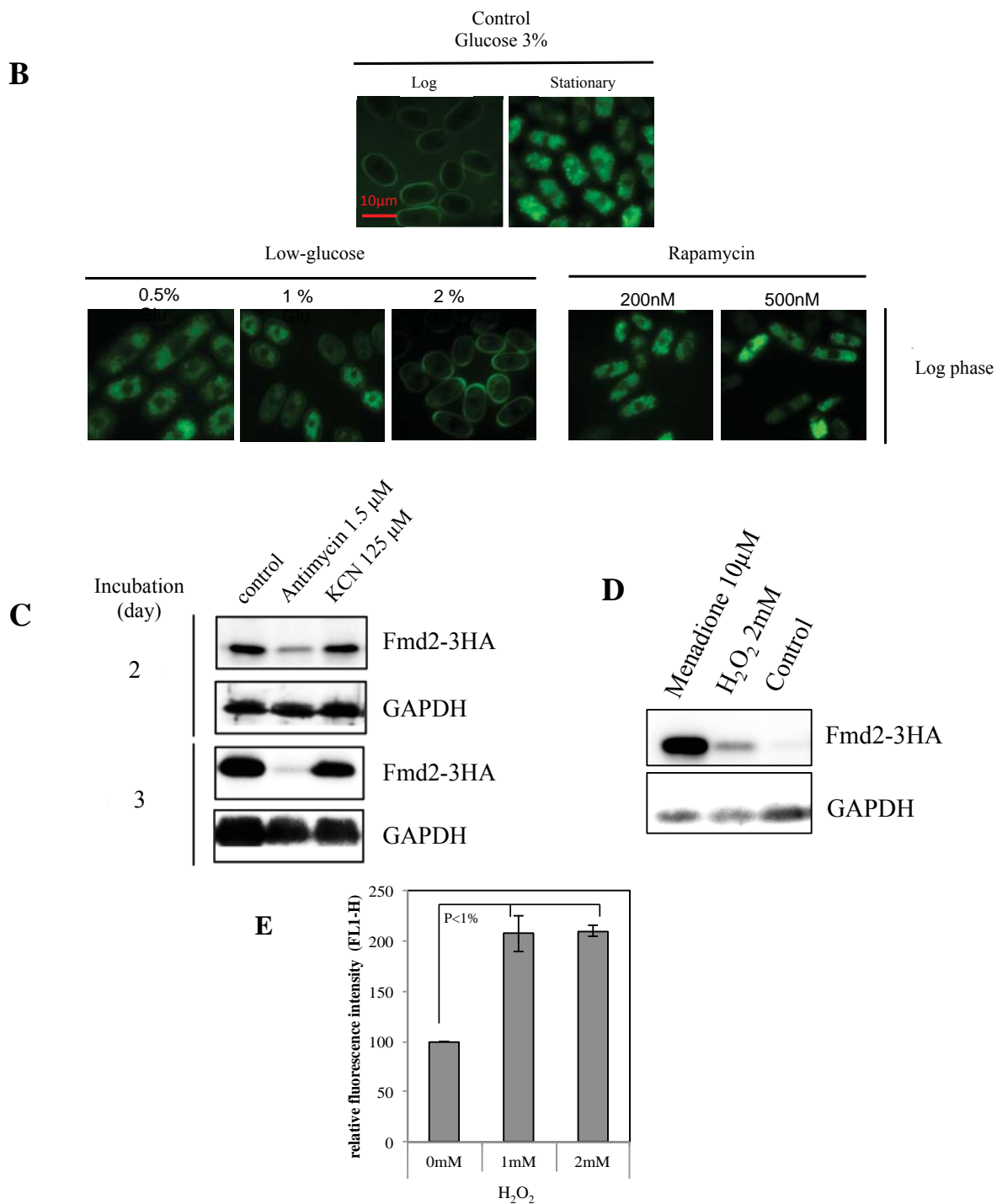
B

Control
Glucose 3%

Log   Stationary

10μm

Low-glucose   Rapamycin

0.5%   1 %   2 %   200nM   500nM

Log phase

C

Incubation (day)

control / Antimycin 1.5 μM / KCN 125 μM

2   Fmd2-3HA

GAPDH

3   Fmd2-3HA

GAPDH

D

Menadione 10μM / H_2O_2 2mM / Control

Fmd2-3HA

GAPDH

E

relative fluorescence intensity (FL1-H)

250
200
150
100
50
0

P<1%

0mM   1mM   2mM

H_2O_2

Figure 15. Association of the induction of Fmd2 with the mitochondrial respiratory chain (MRC) activity and oxidative stress.

(A) Expression of Fmd2 under the growth conditions related to the stationary phase. Cells were grown to the log phase in minimum medium (EMM) containing 200 nM or 500 nM rapamycin or with different glucose concentrations (0.5, 1, or 2%). The cells grown to the log and stationary phases in EMM supplemented with 3% glucose were used as controls. Cell lysates were then subjected to Western blot analysis to determine the protein level of Fmd2-3HA. The protein level of Fmd2-3HA was detected with an anti-HA antibody (12CA5), and GAPDH was used as a loading control. Western blot data are representatives from three independent experiments. (B) Effects of low glucose and rapamycin on the mitochondria respiratory activity based on Rhodamine 123 staining. Bright green fluorescent signals indicate active mitochondria respiratory systems. Images are representatives of three independent experiments. (C) Effects of mitochondria respiratory inhibitors on the Fmd2 protein

levels. Cells were grown to the stationary phase (2 or 3 days) in rich medium (YES) with or without either 1.5 µM antimycin A or 125 µM potassium cyanide (KCN) that inhibits complex III or complex IV, respectively. Cell lysates were then subjected to Western blot analysis to determine the protein level of Fmd2-3HA. The protein level of Fmd2-3HA was detected with an anti-HA antibody (12CA5), and GAPDH was used as loading control. Western blot data are representatives from three independent experiments. (D) Effects of oxidative stresses on the Fmd2 protein level. Cells were grown to the log phase in rich medium (YES) and treated with 10 µM menadione or 2 mM H_2O_2 for 30 min. Cell lysates were then subjected to Western blot analysis to determine the protein level of Fmd2-3HA. The protein level of Fmd2-3HA was detected with an anti-HA antibody (12CA5), and GAPDH was used as a loading control. Western blot data are representatives from three independent experiments. (E) Effects of H_2O_2 on the intracellular levels of NO. Cells were grown in YES medium supplemented with H2O2 (0, 1 and 2mM). DAF FM-DA was used for NO staining, which further subjected to flow cytometry analysis for quantitative measurement. Data are means from three independent experiments

3.1.4 Intracellular NO localization

As mitochondria have a predominant regulatory role in NO signaling, I further speculated the mitochondrial localization of NO of the stationary-phase cells. Indeed, NO was observed as punctate structures co-localizing with mitochondria in the stationary phase (Figure 16A). On the other hand, during the log phase, NO was accumulated at distinct compartments apart from mitochondria. Notably, a vacuolar localization of NO was observed in mid-log phase cells (Figure 16B). Taken together, NO is likely localized at specific organelle in correspond to its respective major NO-synthesis mechanisms.
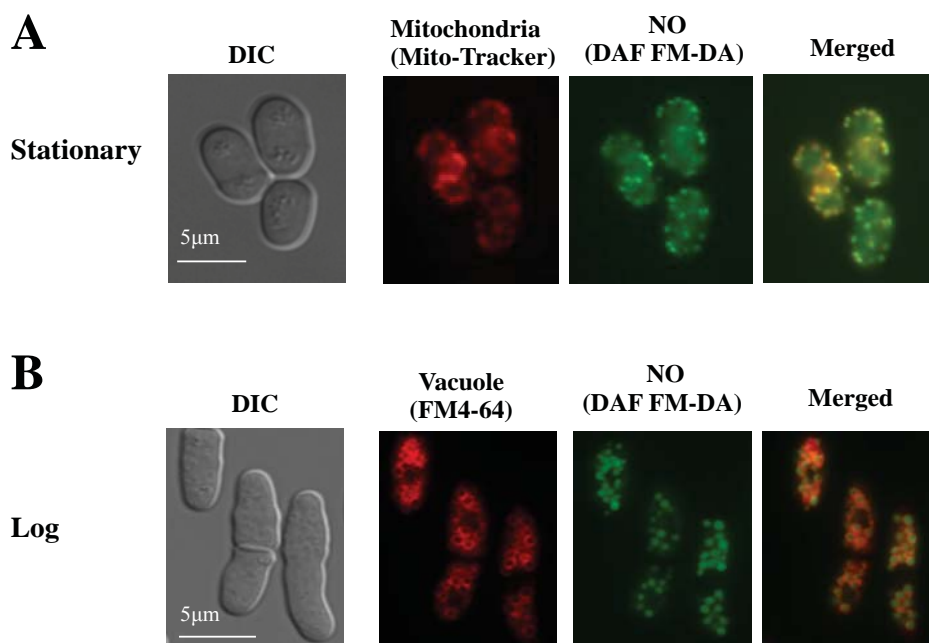

Figure 16. Intracellular NO localization during the log and stationary phases.
Cells were grown to the stationary (A) or the log (B) phase in rich medium. NO was stained in advance by 10 µM DAF FM-DA prior to mitochondria or vacuole staining using 400 nM Mito-tracker or 8 µM FM4-64, respectively. Fluorescence signals were then observed by fluorescence microscopy. Bars, 10 µm.

3.2 NO protects *S. pombe* cells against H_2O_2-induced oxidative stress

3.2.1 DETA NONOate treatment elicits a protective effect against H_2O_2-induced oxidative stress

As I mentioned above, oxidative stresses, such as H_2O_2 and menadione treatments, significantly induced NO signaling (Figure 15D and 15E). These data indicate the potential involvement of NO signaling in response to oxidative stress. To gain better understanding upon this issue, I investigated the effects of NO signaling in fission yeast cells toward H_2O_2-induced oxidative stress by administrating an exogenous NO donor, DETA NONOate with sophisticated chemical properties. DETA NONOate is a non-enzymatic nitrosyl ion donor and highly stable due to its relatively long half-life time (approximately 20 h). One mole parent compound may liberate 2 moles of NO at pH 7.4 solutions. It is reported that low concentrations of DETA NONOate (0.5 and 1 mM) are not microbicidal to *S. pombe* (Majumdar *et al*., 2012).

Remarkably, pretreatment with this exogenous NO donor (0.5 mM DETA NONOate) for 2 h prior to high H_2O_2 stress (2 mM) rescued the cell viability comparable to that without H_2O_2 treatment (Figure 17A). Subsequent to that finding, under oxidative stress, the intracellular ROS level was markedly lower in NO-donor pretreated cells than that in the cells without NO-donor pretreatment (Figure 17B). These data indicated the damaging effect of H_2O_2 is limited by NO-donor pretreatment.
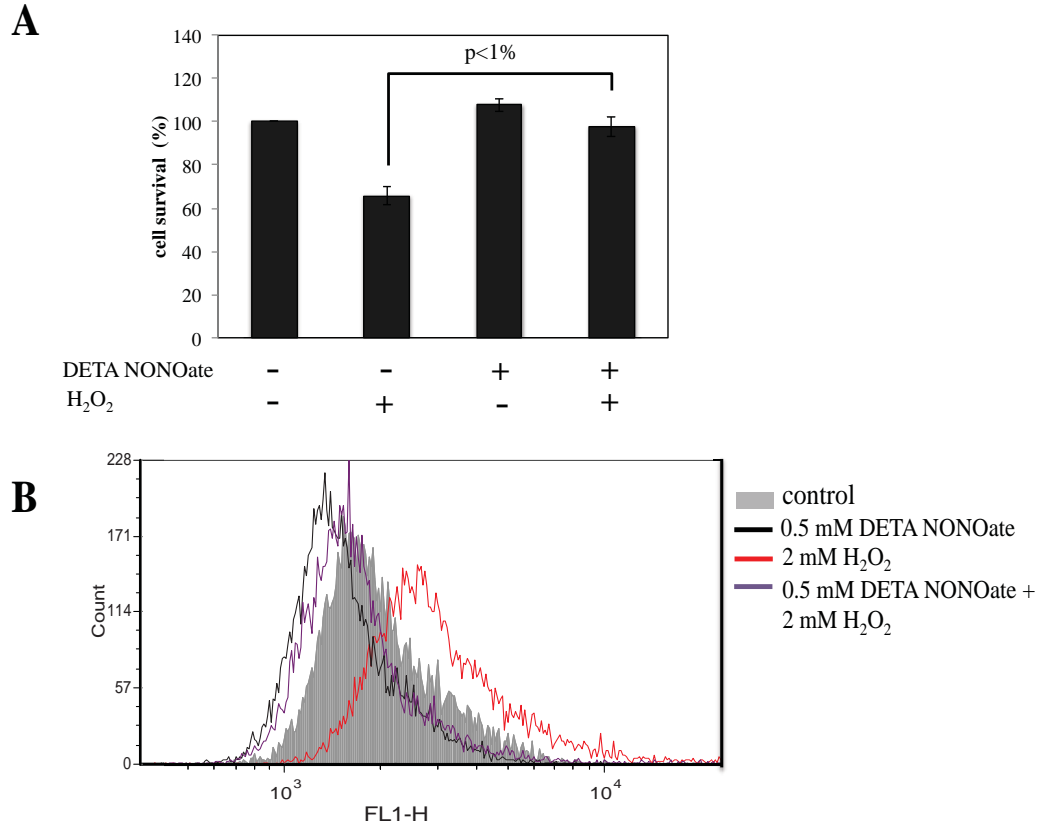
A

B

control
0.5 mM DETA NONOate
2 mM H$_2$O$_2$
0.5 mM DETA NONOate +
2 mM H$_2$O$_2$

Figure 17. Protective effect of DETA NONOate from H$_2$O$_2$-derived oxidative stress.
(A) Effects of DETA NONOate treatment prior to H$_2$O$_2$-derived oxidative stress exposure on the cell viability. Cells were grown to the mid-log phase in rich medium, and 0.5mM DETA NONOate was then applied to the cell cultures for 2 h, followed by 2 mM H$_2$O$_2$ treatment for the next 2 h. Single treatment with 0.5 mM DETA NONOate or 2 mM H$_2$O$_2$ and mock treatment were also performed as controls. Cultures were subjected to spread-plating in YES agar plates to enumerate viable yeast colonies. (B) Intracellular ROS levels under DETA NONOate and H$_2$O$_2$ treatments. Cells were grown in similar conditions as mentioned in (A). Cells were then collected for ROS measurement by using DCFH-DA, a specific fluorescent probe. Fluorescence intensity was quantified by flow cytometry analysis at FL1-H scatter light detector. Data shown in (A) and (B) are means and representatives, respectively, from three independent experiments.

3.2.2 Transcriptional responses of *S. pombe* to DETA NONOate

To gain better understanding of the cellular responses upon the DETA NONOate pretreatment, a transcriptomic analysis through DNA microarray was conducted. Consequently, 155 and 126 genes showed enhanced (2 to 500-fold increase) and weakened (2 to 32-fold decrease) expression, respectively, 2 h after the addition of DETA NONOate. A statistical analysis for the purpose of gene annotation study was conducted for the dataset pf these up-regulated and down-regulated genes by using AmiGO (http://amigo.geneontology.org/amigo), a gene ontology (GO) term enrichment tool (Table 2).

The GO term iron assimilation-belonging 7 genes were significantly up-regulated by the NO donor treatment, in respect to GO biological process categories. The included genes were relevant to both reductive (*fio1$^+$*, *fip1$^+$*, and *frp1$^+$*) and non-reductive (*str1$^+$*, *str2$^+$*, and

43

str3⁺) iron-transport systems. Additionally, 31 genes included in the GO term oxidoreductase activity were transcriptionally enhanced by the NO donor treatment in terms of GO molecular function categories. In association with GO cellular component categories, NO donor markedly increased the transcription levels of 13 genes that encode plasma membrane proteins. Notably, not only a subset of genes encoding plasma membrane proteins designated for iron transport, but the genes involved in copper, oligopeptide, and also hexose transport were found to be induced by the NO donor treatment. Lists of the genes of its respective significant GO term are summarized in Supplementary data (Tables S2-S4).

DETA NONOate, on the other hand, down-regulated the transcription of the genes belonging to the GO biological process of cellular respiration, the GO molecular function of metal binding, and the GO cellular component of mitochondrial respiratory chain, which mostly encode the MRC complexes (Table S5-S7). Regarding the metal binding category, most of the MRC complex components have the iron-sulfur (Fe-S) cluster-binding activity. It is thus likely that mitochondria, especially MRC, is one of the direct targets of NO signaling Since the MRC activity positively regulates NO signaling, as well as ROS generation, as I mentioned above (Figure 15), the inhibition of MRC by NO at the transcriptional level might be one of the plausible negative feedback mechanisms of NO-mediated oxidative stress responses.

Table 2. Gene ontology (GO) categories of biological process, molecular function, and cellular component of the genes significantly up-regulated and down-regulated in response to 0.5 mM DETA NONOate.

Ontology	Up-regulated genes		Down-regulated genes	
	GO term	p-value	GO term	p-value
Biological process	iron assimilation (GO:0033212)	1.95E-09	cellular respiration (GO:0045333)	8.20E-22
	cellular iron ion homeostasis (GO:0006879)	1.51E-08	oxidative phosphorylation (GO:0006119)	8.37E-20
	cellular transition metal ion homeostasis (GO:0046916)	4.83E-08	oxidation-reduction process (GO:0055114)	2.29E-19
	metal ion transport (GO:0030001)	1.96E-06	generation of precursor metabolites and energy (GO:0006091)	2.85E-17
	cellular cation homeostasis (GO:0030003)	3.31E-05	ATP metabolic process (GO:0046034)	6.59E-17
	GO term	p-value	GO term	p-value
Molecular function	oxidoreductase activity (GO:0016491)	3.99E-15	metal cluster binding (GO:0051540)	2.79E-15
	transition metal ion transmembrane transporter activity (GO:0046915)	1.16E-04	ubiquinol-cytochrome-c reductase activity (GO:0008121)	1.14E-09
	oxidoreductase activity, acting on the CH-OH group of donors, NAD or NADP as acceptor (GO:0016616)	1.65E-04	monovalent inorganic cation transmembrane transporter activity (GO:0015077)	2.34E-09
	iron ion transmembrane transporter activity (GO:0005381)	1.78E-04	hydrogen ion transmembrane transporter activity (GO:0015078)	7.93E-09
	oxidoreductase activity, oxidizing metal ions (GO:0016722)	4.99E-04	electron carrier activity (GO:0009055)	3.67E-06
	GO term	p-value	GO term	p-value
Cellular component	plasma membrane (GO:0005886)	1.37E-03	mitochondrial respiratory chain (GO:0005746)	5.23E-20
	intrinsic component of membrane (GO:0031224)	8.05E-03	mitochondrion (GO:0005739)	2.92E-16
	anchored component of membrane (GO:0031225)	3.16E-02	mitochondrial inner membrane (GO:0005743)	7.39E-15
	endoplasmic reticulum (GO:0005783)	4.71E-02	mitochondrial envelope (GO:0005740)	2.72E-14
	cell surface (GO:0009986)	5.87E-02	oxidoreductase complex (GO:1990204)	1.21E-13

3.2.3 DETA NONOate impairs Trx1-cysteine system to limit iron-mediated Fenton reactions.

3.2.3.1 DETA NONOate limits the bioavailability of Fe^{2+} under oxidative stress.

Next, I focused on iron transport as a candidate target of NO signaling in the oxidative stress response. It is highly expected that iron is involved in the H_2O_2-induced oxidative stress response because of the soluble ferrous form of iron (Fe^{2+})-dependent H_2O_2 reduction, widely known as Fenton reactions, which bears the oxidized ferric form (Fe^{3+}) and more toxic radical OH^- (Luo *et al.*, 1994, Nakamura *et al.*, 2003). Thus, I investigated the transcriptional levels of the reductive iron-transport system composed of three membrane-bound proteins namely Fio1, Fip1, and Frp1 under both DETA NONOate and H_2O_2 treatments by qRT-PCR experiments (Figure 18A). In line with the microarray data described above, the DETA NONOate treatment increased the transcriptional levels of these iron uptake genes. Although I also found that the H_2O_2 treatment alone up-regulated these genes, the transcript levels of the iron uptake genes were further dramatically increased in the cells pretreated with DETA NONOate prior to an exposure to H_2O_2. This suggests that the DETA NONOate-pretreated cells experience severe iron starvation under the H_2O_2-induced oxidative stress.

To gain insight into possible involvement of NO-dependent iron transport in mediating oxidative stress responses, I further checked the intracellular Fe^{2+} level determined by a specific fluorescent probe RhoNox (Mukaide *et al.*, 2014) under both DETA NONOate and H_2O_2 treatments (Figure 18B). The DETA NONOate treatment alone did not alter the Fe^{2+} level in spite of the observed induction of *fio1*$^+$, *fip1*$^+$, and *frp1*$^+$, suggesting a robust Fe^{2+}-homeostatic regulation without oxidative stress. In contrast, under the H_2O_2 treatment, the intracellular level of Fe^{2+} was significantly increased. Considering the induction of the iron uptake genes, Fe^{2+} is likely highly consumed by exogenous H_2O_2, leading to the decreased availability of intracellular iron and subsequent enhancement of iron uptake. The DETA NONOate-pretreated cells, however, clearly suppressed the increase of Fe^{2+} under the H_2O_2 treatment, irrespective of the synergistically higher expression level of the iron uptake genes. It is worth noting that iron is transported to the cells from the environment in the Fe^{3+}, instead of Fe^{2+}, form. Thus, the bioavailable Fe^{2+} ion is primarily originated from the intracellular reduction of Fe^{3+} (Labbe *et al.*, 2007). Taken together, it is likely that the severe iron starvation experienced in the DETA NONOate-pretreated cells under the oxidative environment occurred due to the defective reduction of Fe^{3+}. This suppressed Fe^{2+} level might help preventing cells from further Fenton reactions that generate toxic radical OH- from
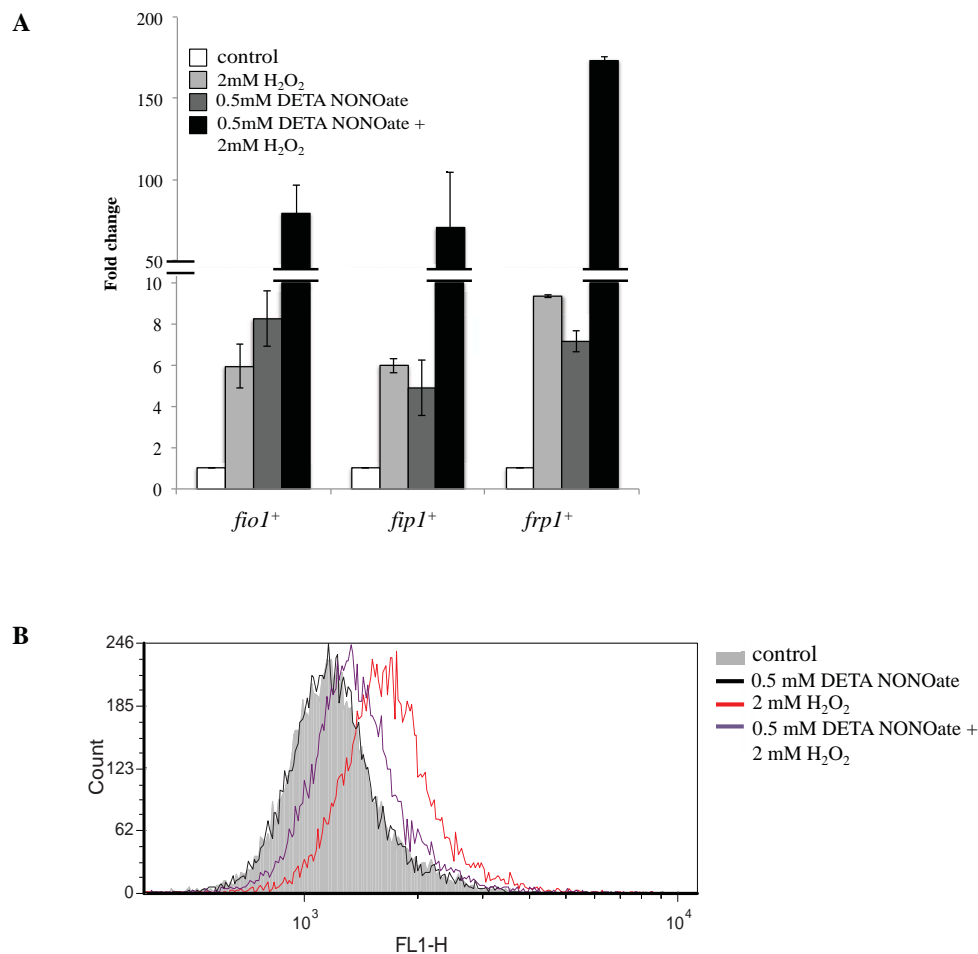
H_2O_2.

Figure 18. Effects of the DETA NONOate and H_2O_2 treatments on the expression of iron uptake genes and the intracellular ferrous (Fe^{2+}) level.
(A) The transcript levels of the genes involved in the reductive iron uptake system , ($fio1^+$, $fip1^+$, and $frp1^{+)}$. Transcript levels were examined by quantitative real-time PCR analysis using cDNA prepared from the cells grown in rich medium with the DETA NONOate and H_2O_2 treatments. The fold changes were normalized by the $act1^+$ transcript levels. Data are means from three independent experiments. (B) The intracellular Fe^{2+} levels measured using an Fe^{2+}-specific fluorescence probe RhoNox (final 5 μM) by flow cytometry.

3.2.3.2 DETA NONOate impairs the Fe^{3+} reduction by inhibiting the cysteine/cystine redox cycling under oxidative stress.

How does DETA NONOate negatively affect the reduction of Fe^{3+} under the H_2O_2 treatment? To address this, I focused on the intracellular level of cysteine (Cys), which is reported to effectively reduce Fe^{3+} to Fe^{2+}, due to its high affinity upon the Fe^{3+} ion (McAuliffe & Murray 1972) (Figure 19A). While the intracellular Cys level was not altered by the DETA NONOate treatment alone, it was slightly decreased once cells were exposed to H_2O_2. It is presumed that Cys was oxidized to reduce Fe^{3+} to replenish the Fe^{2+} pool after consumed by Fenton reactions, and oxidized Cys, cystine, is partly reduced again to balance

47

redox reactions (cysteine/cysteine cycling). In contrast, the DETA NONOate-pretreated cells dramatically decreased the Cys level under the H_2O_2 treatment, while cystine was increased. This is likely to correspond to inhibition of the cysteine/cysteine redox cycling by NO signaling (Figure 19B).
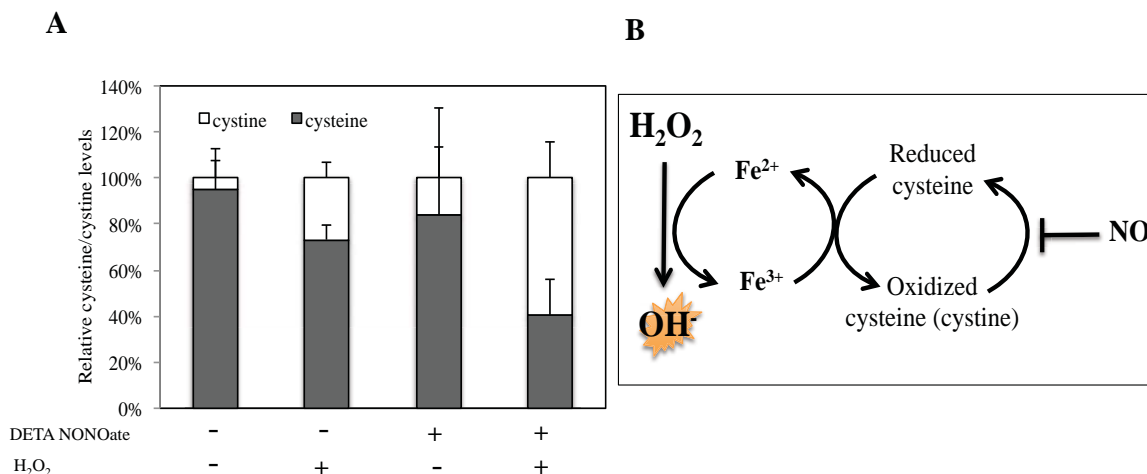
A

B

Figure 19. DETA NONOate alters cysteine (Cys) homeostasis under oxidative stress.
(A) Effects of DETA NONOate and/or H_2O_2 on the intracellular levels of Cys. Intracellular Cys represented by the specific peak area of Cys-bimaine was measured by using LC/MS. Data are means from three independent experiments. (B) Scheme depicting the potential action of NO in inhibiting iron-mediated Fenton reaction through the cysteine/cystine redox cycle.

3.2.3.3 NO-dependent Trx1 attenuation potentially inhibits iron-dependent Fenton reactions.

Next, I examined the potential mechanism that may alter the cysteine/cystine cycling in an NO-dependent manner. It is reported that in *E. coli* and *S. cerevisiae*, the thiol redox system is constituted primarily to the activity of thioredoxin (Trx) (Toledano *et al* ., 2007). In addition, Trx is notably involved in the reduction of cystine *in vitro* (Gusarov & Nudler 2005). *S. pombe* has two Trx isoforms, cytosolic Trx1 and mitochondrial Trx2. Thus, I first examined the expression of *trx1$^+$* and *trx2$^+$* genes under the DETA NONOate and/or H_2O_2 treatments (Figure 20A). The H_2O_2 treatment significantly increased the mRNA level of *trx1$^+$* whereas the DETA NONOate treatment alone had no significant effect. Interestingly, the DETA NONOate pretreatment significantly suppressed the transcript level of *trx1$^+$* under the H_2O_2 treatment. The transcript level of *trx2$^+$* remained constant under all treatments tested. These data indicate that NO may specifically interfere the activity of Trx1 at least at the transcriptional level to limit the cysteine/cystine redox cycle.

To elucidate whether Trx1 is associated with the NO-mediated cellular protective

mechanism, I investigated the effects of the lack of $trx1^+$ on the suppression of the Fe^{2+} level increase (Figure 18B) and the recovery of the cell survival rate (Figure 17A) under the H_2O_2 treatment in the DETA NONOate-pretreated cells. As expected, in $\Delta trx1$ cells under oxidative stress, the intracellular Fe^{2+} ion was not decreased by the DETA NONOate treatment (Figure 20B). Moreover, the DETA NONOate treatment did not rescue the cell viability of $\Delta trx1$ cells under the oxidative stress condition (Figure 20C). Taken together, it is suggested that NO limits iron-dependent Fenton reactions potentially through the attenuation of Trx1-mediated cysteine/cystine redox cycling (Figure 20D).
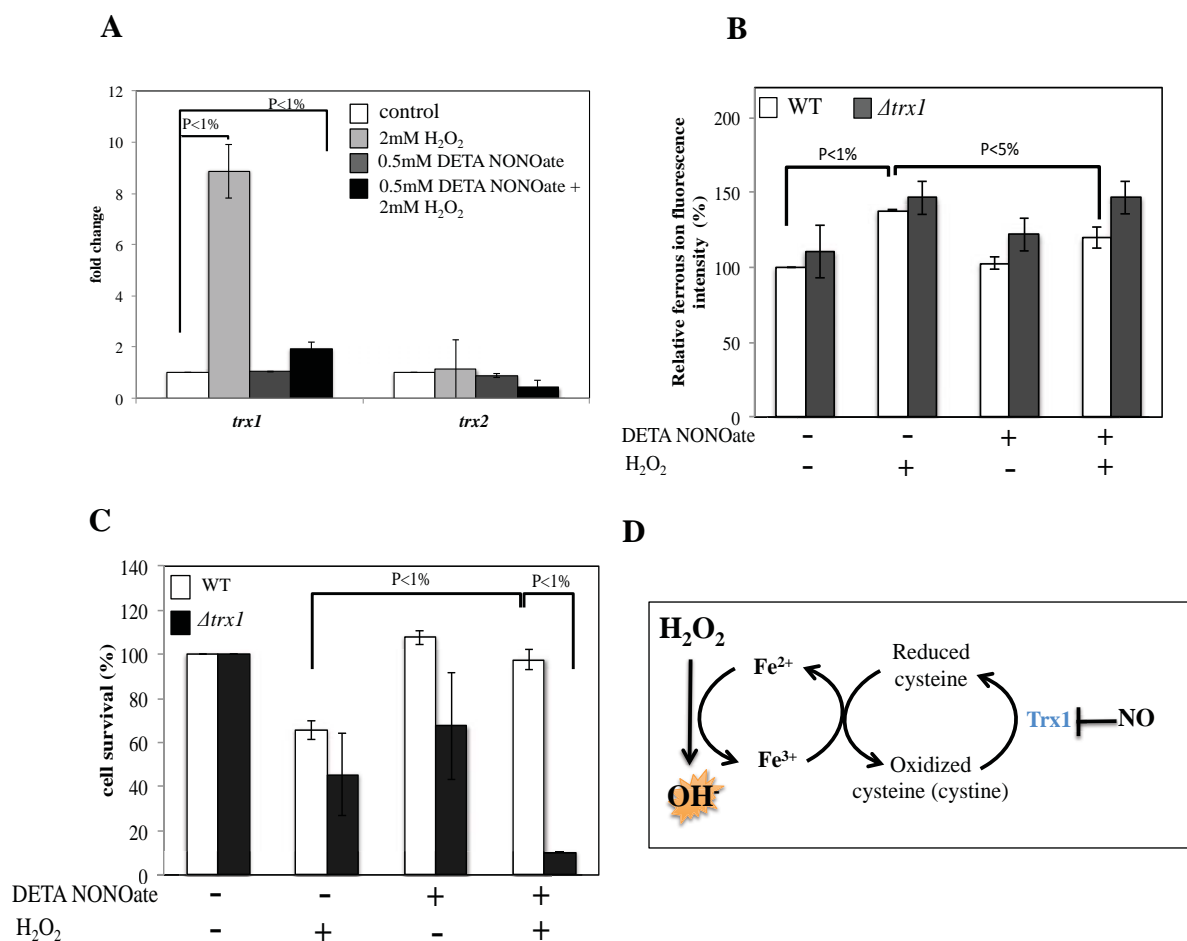

Figure 20. DETA NONOate alters the intracellular Fe^{2+} level and the cell viability through Trx1 activity.
(A) Effects of DETA NONOate and/or H_2O_2 on the transcription levels of thioredoxin (Trx) family proteins, including cytosolic and mitchondrial Trx encoded by $trx1^+$ and $trx2^+$, respectively. Data are means from three independent experiments. (B) Effects of DETA NONOate and/or H_2O_2 on the intracellular levels of Fe^{2+} ion of both the wild type and $trx1$-deleted ($\Delta trx1$) strains. Fe^{2+} was detected with a specific fluorescence probe RhoNox. Fluorescent intensity was measured through flow cytometry analysis, and means from three independent experiments are shown. (C) Cell viability of the wild type and $\Delta trx1$ strains under DETA NONOate and/or H_2O_2 treatments. Data are means from three independent experiments. (D) Proposed mechanism of NO-dependent Fenton reaction inhibition through the activity of Trx1. NO interferes the activity of cystoplasmic thioredoxin Trx1, leading to the inhibition of the sequential reductions of oxidized cysteine (cystine) to reduced cysteine (Cys) as well as ferric (Fe^{3+}) to ferrous (Fe^{2+}) ions, which in turn limits Fenton reactions.

49

3.2.4 DETA NONOate treatment promotes the H_2O_2 scavenging activity.

Given that DETA NONOate essentially inhibits Fenton reactions under H_2O_2 exposure, it is expected that high concentrations of H_2O_2 remain within the cell by the DETA NONOate treatment. If such conditions occur, additional mechanisms are necessary to overcome the toxicity of the high level of H_2O_2 itself. Amongst the up-regulated gene data set obtained from the DNA microarray analysis, I found that two H_2O_2 scavenging system-related genes, namely $gst2^+$ (encoding glutathione-S-transferase (GST)) and $srx1^+$ (encoding sulfiredoxin) were up-regulated by the DETA NONOate treatment. They were the top two DETA NONOate-induced genes belonging to the GO term cellular response upon oxidative stress with 9- and 6-fold increases, respectively (Table S8). Therefore, I further tested the involvement of those NO-induced H_2O_2-scavenging activities in combating H_2O_2.

3.2.4.1. Glutathione-S-transferase (GST) gene-mediated H_2O_2 scavenging mechanism

Despite the contribution to detoxifying xenobiotic compounds, GST is also known as an antioxidant enzyme (Kim *et al*., 2004). Amongst three isoforms of GSTs, Gst2 and Gst3 are highly capable of performing the H_2O_2-scavenging activity through their respective glutathione peroxidase catalytic function (Veal *et al*., 2002). Glutathione peroxidase catalyzes the reduction of H_2O_2 to water by converting the reduced form of glutathione (GSH) to its oxidized forms (GSSG) (Yamada *et al*., 1999). I found that in addition to $gst2^+$, the expression of $gst3^+$ was also induced, although slightly, by the DETA NONOate treatment (Table S8). Based on the experimental results, in wild-type cells under oxidative stress conditions, the GSH/GSSG ratio was significantly decreased by the DETA NONOate pretreatment (Table 3). This data suggested that DETA NONOate enhanced the consumption of GSH via the GSH peroxidase activity, in order to detoxify H_2O_2. However, Gst2 did not mainly contribute in the DETA NONOate-dependent H_2O_2 scavenging activity, since the GSH/GSSG ratio of *Δgst2* was altered similarly to the wild-type treated with DETA NONOate. In contrast, in *Δgst3*, the DETA NONOate treatment did not significantly reduce the GSH/GSSG ratio. Moreover, DETA NONOate did not recover the cell viability of the *Δgst3* strain under oxidative stress (Figure 21). These data suggest the potential NO-dependent H_2O_2 scavenging activity mainly through Gst3.

Table 3. GSH/GSSG ratio of the wild type and glutathione-S-transferase (GST) gene-deleted strains under the DETA NONOate treatment.

	GSH/GSSG ratio		
Strains	2mM H_2O_2	0.5 mM DETA NONOate + 2mM H_2O_2	Change in GSH/GSSG ratio (%)
WT	1.62 ± 0.47	0.19 ± 0.02	88.27
$\Delta gst2$	1.16 ± 0.01	0.13 ± 0.03	88.79
$\Delta gst3$	0.49 ± 0.02	0.36 ± 0.04	26.53
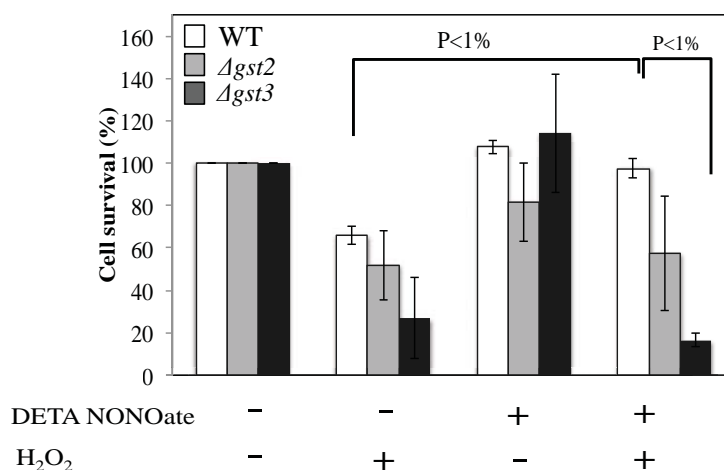
Figure 21. Effects of DETA NONOate and/or H_2O_2 on the cell viability of the wild type, $\Delta gst2$, and $\Delta gst3$ strains.
Cells were grown to the mid-log phase in rich medium, and 0.5 mM DETA NONOate was then applied to the cell cultures for 2 h, followed by 2 mM H_2O_2 treatment for the next 2 h. Single treatment with 0.5 mM DETA NONOate or 2 mM H_2O_2 and mock treatment were also performed as controls. Cultures were subjected to spread-plating in YES agar plates to enumerate viable yeast colonies.

3.2.4.2. Surfiredoxin gene-mediated H_2O_2 scavenging mechanism

To clarify the NO-dependent surfiredoxin Srx1 activity, I investigated the presence of hyperoxidized peroxiredoxin (sulfinic Tpx1, Tpx1-SO_2H), the substrate of the Srx1 enzymatic activity. The level of hyperoxidized Tpx1 is assessed by immunoblotting using anti-mammalian Prx-$SO_{2/3}$. This antibody can recognize hyperoxidized Tpx1, since Tpx1 is highly homolog to mammalian Prx1, including its peroxidatic cysteine residue. Although this antibody detects both sulfinic (-SO_2H) and sulfonic (-SO_3H) Tpx1, but it is generally assumed that only sulfinic Tpx1 are formed in cellular context (Abbas *et al*., 2013). Importantly, this antibody recognizes sulfinic Tpx1 as both monomeric and dimeric forms. The dimeric form of Tpx1-SO_2H represents an effective H_2O_2 scavenging activity of Tpx1. It is due to, during exposure to H_2O_2, dimeric form of Tpx1-SOH is more susceptible for sequential oxidation, yielding dimeric form of Tpx1-SO_2H. The dimeric form of Tpx1-SO_2H is then gradually transformed into monomeric form (Figure 22). Both dimeric and monomeric forms of sulfinic

Tpx1 are substrate for Srx1 catalytic function (Jara *et al*., 2007). Srx1 catalyzes the reduction of Tpx1-SO$_2$H yielding sulfenic Tpx1 (Tpx1-SOH) (Vivancos *et al*., 2005). The resulted Tpx1-SOH elicits the H$_2$O$_2$-scavenging activity by direct binding to H$_2$O$_2$ and returning to Tpx1-SO$_2$H., As the mRNA transcript levels of *srx1$^+$* gene was significantly induced by DETA NONOate, thus it is hypothesized that, the Tpx1-Srx1 system might act as a potent H$_2$O$_2$-scavenging mechanism induced by the DETA NONOate treatment.
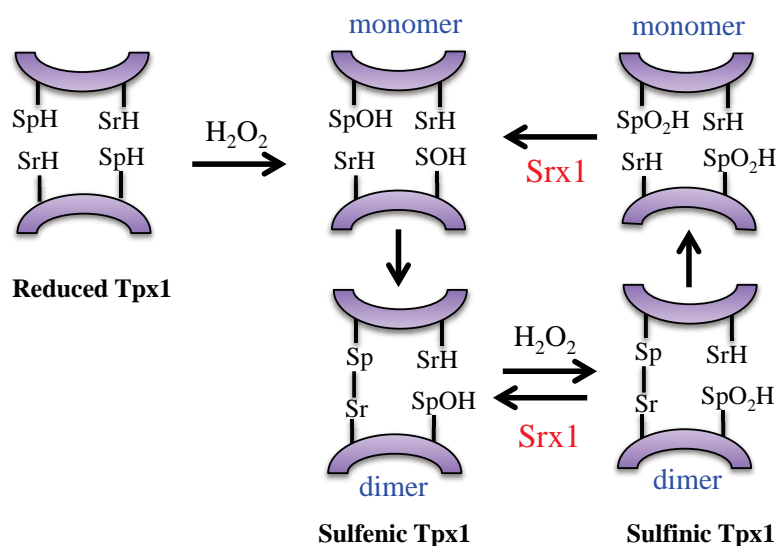
Figure 22. Tpx1-Srx1-catalyzed redox reactions.
H$_2$O$_2$ directly binds to the peroxidatic cysteine residue (S$_p$) of reduced Tpx1, resulting in sulfenic Tpx1 (Tpx1-SOH) with the SOH moiety. The monomeric Tpx1-SOH may turn to dimeric form by one disulfide bond formation of Cys-Sp to Cys-Sr (resolving Cys residue) of joint Tpx1 subunit. Such dimeric form is susceptible for sequential oxidation, resulting dimeric form of sulfinic Tpx1 (Tpx1-SO$_2$H). The dimeric form of Tpx1-SO$_2$H is gradually changed to monomeric forms. Srx1 is involved in catalyzing the reduction of both dimeric and monomeric form of Tpx1-SO$_2$H to Tpx1-SOH.

In WT cells, protein band correspond to Tpx1SO$_2$H was observed following 20 minutes exposure to H$_2$O$_2$. Interestingly, the monomeric form of Tpx1SO$_2$H was not detected. In Δ*srx1* cells, in addition to the dimeric form, monomeric sulfinic Tpx1 was observed. Thus it is likely that in WT cells, Srx1 effectively reduces dimeric sulfinic to sulfenic Tpx1 that maintains an effective Tpx1-dependent H$_2$O$_2$-scavenging activity. However, lack of *srx1$^+$* gene limits the reduction of dimeric sulfinic to sulfenic Tpx1 leading to the accumulation of sulfinic Tpx1 in monomeric forms (Figure 23A). Furthermore, the reduction of monomeric sulfinic Tpx1 is unlikely to occur, since the particular reaction is facilitated by Srx1 as well.

Further, I checked the effect of DETA NONOate upon cells viability of Δ*srx1* strain under oxidative stress. It was found that DETA NONOate had no positive effect upon Δ*srx1* cells survival rate under oxidative stress (Figure 23B). Thus, it is suggested that Srx1-Tpx1

system facilitates an effective H_2O_2 scavenging activity that constitutes to the NO-dependent oxidative stress tolerance.

Both $srx1^+$ and $gst3^+$ genes are known to be up-regulated by the Spc1 MAPK pathway. Hence, loss of $spc1^+$ caused a severe damage in the cell viability under the H_2O_2 stress (Figure 23B), as previously reported (Vivancos *et al.*, 2005, Veal *et al.*, 2002). Furthermore, DETA NONOate did not elicit its protective roles in enhancing oxidative stress tolerance in *Δspc1* cells. Thus, the DETA NONOate-dependent H_2O_2-scavenging activity is likely regulated via the activation of effector kinase of the MAPK cascade, Spc1.
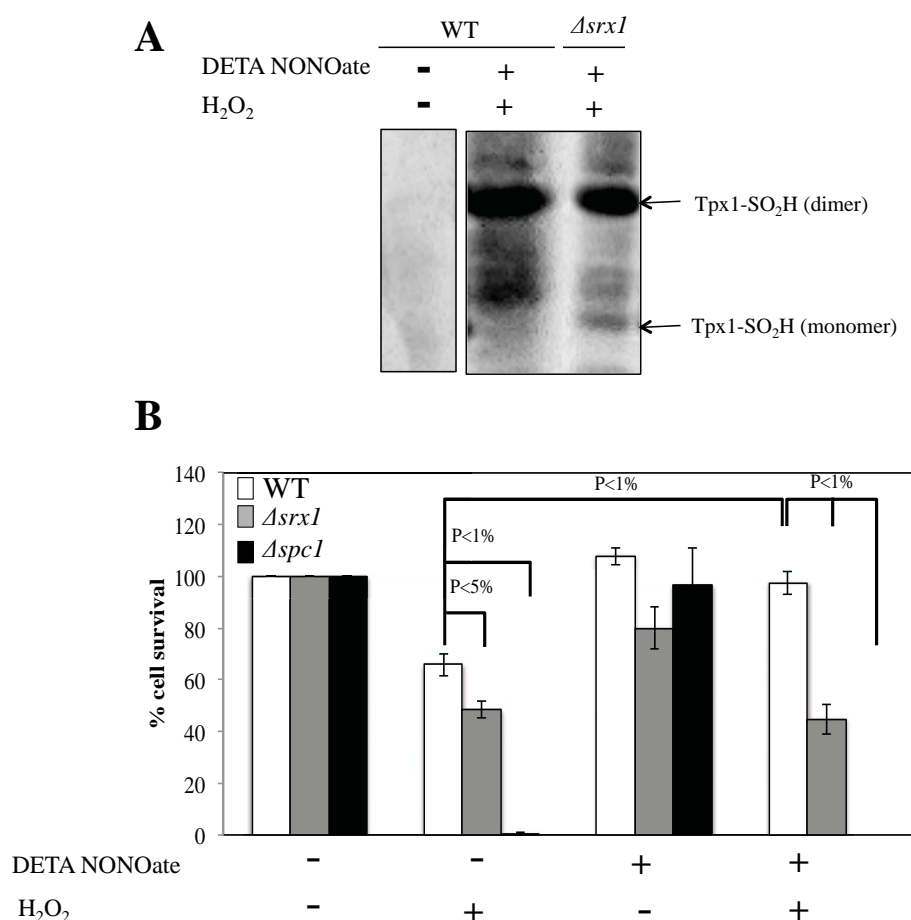

Figure 23. Role of sulfiredoxin (Srx1) in regulating hyperoxidized peroxiredoxin (Tpx1-SO₂H) levels and the cell viability in the cells lacking the $srx1^+$ or $spc1^+$ gene.
(A) Effects of Srx1 on the hyperoxidized peroxiredoxin Tpx1 (Tpx1-SO$_{2/3}$) level. Wild-type and *Δsrx1* cells were grown in YES medium to the mid-log phase (OD600= 0.8). 0.5 mM DETA NONOate was then added for 2 h prior to 2 mM H_2O_2 treatment for 20 min. Crude extracts were isolated and subjected to non-reducing SDS-PAGE and western blotting analysis. Hyperoxidized Tpx1, in both sulfinic and sulfenic forms, were detected by the anti-Prx-SO$_{2/3}$ antibody. GAPDH was used as a loading control. (B) Cell viability of the wild-type, *Δsrx1*, and *Δspc1* strains under the DETA NONOate and/or H_2O_2 treatments. Cells were grown to the mid-log phase in rich medium, and 0.5 mM DETA NONOate was then applied to the cell cultures for 2 h, followed by 2 mM H_2O_2 treatment for the next 2 h. Single treatment with 0.5 mM DETA NONOate or 2 mM H_2O_2 and mock treatment were also performed as controls. Cultures were subjected to spread-plating in YES agar plates to enumerate viable yeast colonies

4. Discussion

4.1 A Fine-tuned NO signaling is present in the fission yeast *S. pombe*

In this study, I first revealed that the fission yeast *S. pombe* exhibited dynamic alteration in both intracellular NO and RSNO levels (Figure 7). The NO concentration observed during the log phase is considered the physiological level relevant to proper cell growth. In order to maintain NO homeostasis, a putative NOD encoded by *SPAC869.02c* likely plays predominant roles (Figure 11 and 12B). Moreover, the Arg-dependent NOS activity is likely the constitutive NO source throughout the growth, and substantially prominent during the log phase (Figure 13A). NO was mostly localized in the vacuole (Figure 16B) that potentially serves as the NO-synthesis site specifically in the log phase. Supporting this hypothesis, the exponentially growing *S. pombe* cells store a high amount of basic amino acid Arg for nearly 21% of the total soluble amino acids in the vacuole (Chardwiriyapreecha *et al.,* 2010). Thereof, the abundance of Arg in the vacuole may potentially promote the stoichiometry of NOS reactions. It is definitely challenging to reveal the functions of this NOS-derived NO at the physiological level, since significant reduction of NO by the NOS inhibitor L-NAME did not cause any significant alteration upon the cell viability (Figure 13C). Hence, a comprehensive transcriptomic analysis under the L-NAME treatment should be carried out to clarify NOS-derived NO-sensitive genes. Except for the growth conditions, Kig and Temizkan (2009) proposed the roles of NOS-derived NO in regulating mating and sporulation of *S. pombe*, both of them are inhibited by the L-NAME treatment.

Considering that the low level of NO, simultaneously with the high level of RSNO, was observed in the stationary phase (Figure 7), I suggest that such dynamics is pertinent to the physiology of this phase. Given that stationary-phase cells exhibit the high MRC activity, it is likely that the ROS, especially superoxide (O_2^-), released from MRC mostly via complex I (Grivennikova & Vinogradov *et al.,* 2006) or II (Mc Lennan & Esposti 2000) may consume NO to further form peroxynitrite (ONOO-). As this is a potent nitrosylation agent (Patel *et al*., 1999), the RSNO level may be augmented. Since GSH is the most abundance thiol-containing compound and a potential S-nitrosylation target, the enhancement of the RSNO level is parallel to the increased GSNO level. Accordingly, the expression of a potential GSNOR Fmd2 was promoted once cells entered the stationary phase (Figure 12A and B) or were exposed to ROS-inducing reagents, such as H_2O_2 and menadione (superoxide generator) (Figure 15D). While nitrosylation of GSH is relevant to the detoxification of the ONOO-

radical, resultant GSNO itself may also severely affect cellular redox homeostasis. Therefore, conversion of GSNO to GSSG and ammonia via GSNOR Fmd2 is required. Furthermore, sequential GSH reductase (GR) reaction may complete the GSH cycling, by reducing GSSG to two GSH molecules in an NAD(P)H dependent manner. Consistently, the activity of GR is markedly increased in the stationary phase by about 454% compared to the GR activity in log-phase cells (Lee *et al.,* 1995, Lee et al., 1997). The menadione or H_2O_2 treatment of the log-phase cells escalated NO signaling, mimicking the stationary-phase conditions, except that ROS was introduced exogenously (Figure 15D). Unlike the menadione treatment that markedly induced Fmd2 expression, the H_2O_2 treatment slightly increased Fmd2 expression. Supporting our results, while the menadione treatment significantly increases the GR activity by nearly 172%, the H_2O_2 treatment only promotes the GR activity by 23% (Lee *et al.,* 1995). Evoking a significant alteration upon redox homeostasis by menadione, potentially, due to sequential generation of ONOO- and GSNO, as a result of a crosstalk between NO and O_2^-.

In addition to the NOS-like activity, mitochondria, particularly cytochrome *bc1* (complex III), likely contribute to NO generation during the stationary phase (Figure 15C). Supporting this conclusion, mitochondrial localization of NO was observed in this particular growth phase (Figure 16A). In mammalian cells, intriguingly, the production of NO by mitochondria has been reported to be hypoxia-specific (Castello *et al.,* 2006, Castello *et al.,* 2008, Nohl *et al.,* 2000). Hence, I speculate that the extensive consumption of oxygen through MRC during the stationary phase may consequently induce hypoxic environments in the individual mitochondria. This is supported by the factual data that the mRNA transcript of the hypoxia-inducible cytochrome c gene, $cyc1^+$, a homolog of *CYC7* of *S. cerevisiae*, was significantly induced when cells entered the stationary phase, although the transcript level of $sre1^+$, an endoplasmic reticulum membrane-bound transcription factor that responds to changes in oxygen-dependent sterol synthesis, as well as its target gene $hem13^+$, was not increased (Supplementary Figure S1). Thus, it is suggested that low-oxygen environment is locally occurred in the vicinity of mitochondria, but not in the entire cell. Generation of NO from complex III may potentially compete with oxygen for Cco reactions (Benamar et al., 2008), eventually leading to inhibition of further consumption of oxygen to alleviate local hypoxic environments. Such O_2 homeostasis might be important to maintain effective energy production via MRC as well as preventing from cellular hypoxia. Thus, it is worth noting that NO generated via MRC has a pivotal role in the negative control of the MRC activity for oxigen homeostasis.

4.2 NO protects *S. pombe* cells against H_2O_2-induced oxidative stress

NO has been reported to act either as an effector or a regulator molecule of complex cellular network causing various physiological events. Interestingly, NO plays dichotomous effects; whereas at low concentrations, NO behaves as a signaling molecule associated with "good" cellular events, such as protection against environmental stresses (Sasano *et al*., 2010; Nishimura *et al*., 2013) and cellular physiological functions (Wood *et al*., 2011; Phoa & Epe 2001), at much higher levels, however, NO causes deleterious or "bad" effects for the cell due to its toxicity. In particular, NO toxicity has been claimed to be engaged in pathological events, apoptosis, cell death, and cancer cells metastasis (Almeida *et al*., 2007; Silva *et al*., 2011, Choudari *et al*., 2013). In my study, it was observed that an exogenous NO (0.5 mM DETA NONOate) treatment upon *S. pombe* results in significant enhancement of the iron uptake system and reduction of the cellular respiratory activity at the transcriptional levels (Table 2), both leading to protection from oxidative stress. Similar results were observed in the transcriptomic profiling of pathogenic fungi *Histoplasma capsulatum* (Nittler *et al*., 2005) and *C. albicans* (Hromatka *et al*., 2005) in response to 1 mM DTPA NONOate, another NONOate-type of NO donor. A very recent data showed, however, that a higher DETA NONOate concentration (3 mM) leads to distinct responses upon *S. pombe*, as it causes reduced expression of macromolecule metabolic process and meiosis-related genes (Biswas & Ghosh 2014). Hence, regardless of the type of NO donor, the mode of actions affecting specific cellular response is likely dependent on the concentrations of NO.

Low levels of NO have been reported to elicit cytoprotective effects against environmental stresses. In mammals, iNOS-dependent NO generation, has been reported to be remarkably involved in cell survival against pathogen infections (Tuckova *et al*., 2000, Zamora *et al*., 2000, Chakravortty & Hensel 2003). Others and our laboratory have also elucidated the significance importance of NO signaling against stresses in the budding yeast *S. cerevisiae*, as NO induces tolerance responses toward multiple baking-associated stresses (Sasano *et al*., 2012), hydrostatic pressure (Domitrovic 2003), heat shock (Nishimura *et al*., 2013), as well as oxidative stress (Nasuno *et al*., 2014). This study revealed, for the first time, the protective effect of NO against the H_2O_2-induced oxidative stress in the fission yeast *S. pombe* (Figure 17A). Most strikingly, NO appears to orchestrate at least three mechanisms: (i) inhibition of MRC, (ii) inhibition of Fenton reactions via impairment of the Trx1-cysteine system, and (iii) induction of the Spc1-dependent H_2O_2 scavenging activity of Gst3 and the Tpx1-Srx1 systems (Figure 24).
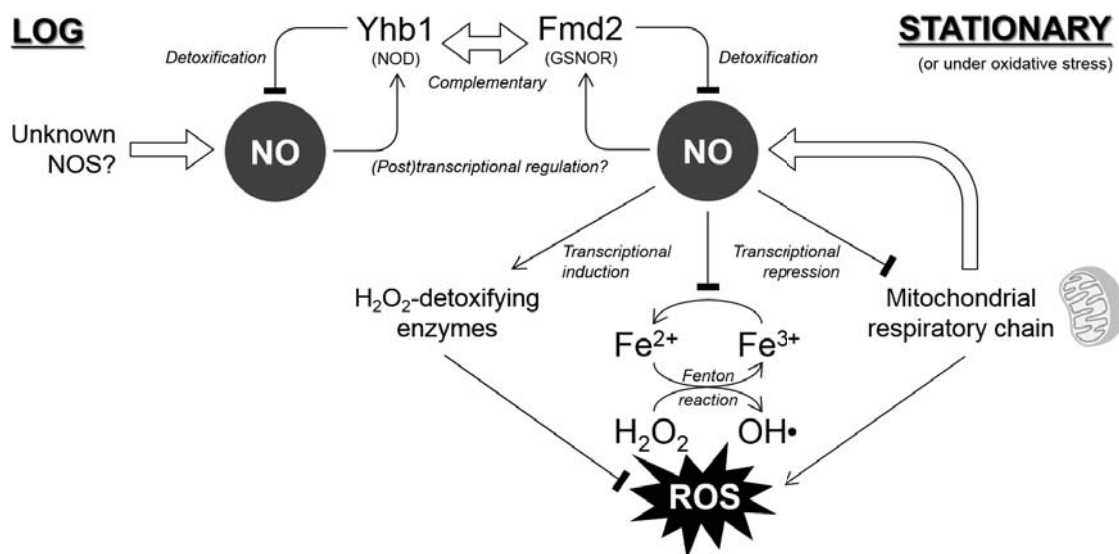
Figure 24. A proposed model for NO homeostasis and NO-mediated oxidative stress responses in *S. pombe*.
NO can be synthesized from both NO synthase (NOS) and mitochondria (complex III) via NIR activity. Each of the synthetic mechanism may promote specific regulatory systems to control intracellular NO levels in its appropriate levels avoiding NO-defective effects. Nitric oxide dioxygenase and GSNO-reductase are responsible to control NO levels produced via NOS and NIR pathway, respectively. NO-dependent mitochondria production may further trigger at least three antioxidant mechanisms: (i) inhibition of the conversion of Fe^{3+} into Fe^{2+} that inhibits Fenton reaction, (ii) upregulation of the genes encoding H_2O_2-detoxifying enzymes, and (iii) downregulation of the MRC genes.

It is not surprising that NO induces a regulatory role upon iron homeostasis. It has been reported that NO signaling is used as an early response of plant roots to iron deprivation to increase the iron availability (Graziano & Lamattina 2007). In mammals, NO has been determined to enhance iron uptake both at the mRNA transcript level (Kim & Ponka 1999) and the protein level (Oria *et al.*, 1995) of transferrin, in a dose-dependent manner via activation of iron regulatory protein 1 (IRP1) (Kim & Ponka 2002). In *S. pombe*, iron uptake system is negatively regulated by the iron sensing transcription factor Fep1. This transcriptional repressor senses and transduces iron concentration changes into the iron transport machinery by a direct iron-dependent interaction with the 5'-(A/T)GATAA-3' element found in the promoter region of the iron uptake genes (Pelletier *et al.*, 2002). In response to low levels of intracellular iron (Fe^{2+}), iron uptake gene expression is induced as the activity of Fep1 is attenuated through its dissociation from the promoter regions of the iron transport genes (Labbe *et al*, 2013). However, how the NO signaling alone can inactivate Fep1 under no significant change in the Fe^{2+} level (Figure 18B) is still unknown. From the DNA microarray result, I found that the transcript level of the *fep1*+ gene was reduced to one

third by the NO-donor treatment (Supplementary figure S2). Although the transcriptional control of the $fep1^+$ gene has not been elucidated yet, NO signaling might directly down-regulate $fep1^+$ to enhance iron uptake in preparation for the oxidative stress response. In addition to the Fenton reactions, it has been reported that NO can bind directly to Fe^{2+} to form inactive nitrosyl-iron complex, thus eliciting an alternative role of NO as an iron scavenger (Nara *et al.*, 1999). This might be also correlated to the enhanced transcription of the iron uptake genes in the NO-donor treated cells (Figure 18A).

Based on my results, the extreme induction of the iron uptake genes in the NO donor-treated cells upon exposure to a high H_2O_2 level (Figure 18A) is associated with the attenuation of the reduction of Fe^{2+} via Trx1 (Figure 20B). The repression of the $trx1^+$ transcript level by NO (Figure 20A) was found to initially compromise the iron homeostasis via inhibiting OH--derived Fenton reactions. The transcription of the $trx1^+$ gene is regulated by Pap1, which is a basic leucine zipper (bZIP)-type transcription factor (Song & Roe 2008). Since NO treatment did not alter the transcriptional levels of $pap1^+$ gene, it is likely that NO attenuates the activity of Pap1 post-translationally. Supporting this idea, mammalian c-Jun, a homolog of *S. pombe* Pap1, is susceptible for nitrosation, leading to ineffective DNA binding (Nikitovic *et al.*, 1998). However, the nitrosation site of c-Jun at Cys272 is not conserved in Pap1. Since the Pap1 activity is also regulated by its nuclear localization (Toone *et al.*, 1998), NO may interrupt Pap1 trafficking through modulation of a Ran GTP/GDP exchange factor Dcd1, essential for nuclear export of Pap1 (Toone *et al.*, 1998). To reveal this, effects of the NO donor pretreatment on the subcellular localization of Pap1 in the H_2O_2-treated cells should be investigated as the first step. Such NO-dependent Ran GTPase modulation is reported to occurr through S-nitrosation as described (Ckless *et al.*, 2004). Park & Imlay (2003) suggested that Fenton reactions are primarily driven by thiol amino acid Cys. Consistent with this finding, under the oxidative stress, I observed that in the DETA NONOate pretreated cells the intracellular level of Cys was markedly found in a lower level than that without the DETA NONOate pretreatment (Figure 19A). Although this study does not show a direct effect of the Trx1 activity toward the cysteine level, the attenuation of the $trx1^+$ gene by NO limits the reduction of Fe^{3+}, resulting in an insufficient amount of Fe^{2+} to maintain Fenton reactions (Figure 20B and D).

The MRC complex has been reported as a direct target of NO-based post-translational modifications. It is primarily because MRC may produce ROS that reacts with NO with high affinity, resulting in formation of nitrosation agents (Beltran *et al.*, 2000, Brown *et al.*, 2001). In this study, however, the DETA NONOate treatment down-regulates the MRC-related genes

at their transcriptional levels (Table 2). The details of the underlying mechanism of how NO represses the transcription of the MRC-related genes are yet unknown. Since the genes encoding MRC complexes exist both in mitochondrial and nucleus genome, thus NO may potentially alter the coordination of the transcription machinery important for the expression of the nuclear DNA- and mitochondrial DNA-encoding genes (Kelly *et al.*, 2004). Alternatively, NO may interact with RNA polymerase or specific nuclear/mitochondrial transcription factors to reduce transcription of the MRC-associated genes. Supporting the idea of NO-dependent RNA polymerase inhibition, a recent study shows that in *Salmonella*, an RNA polymerase regulator DksA serves as a sensor for nitrosative conditions, and its nitrosation of redox-active cysteine residues is associated with the fine tuning of the translational machinery level in accordance with nutritional shortages upon exposure to stresses (Henard *et al.*, 2014). Although no evidence is available about the direct effects of NO on *S. pombe* mitochondrial RNA polymerase (i.e. Rpo41) or the mitochondrial transcription factor (i.e Mtf1), both of which are essential for mitochondrial DNA transcription (Jiang *et al.*, 2011), it was reported that, in mammals, nitrosylation of **c**AMP **r**esponse **e**lement-**b**inding (CREB) protein acts as an upstream mechanism to mediate the transcription of mitochondrial DNA including MRC-related genes (Aquilano *et al.*, 2014). Moreover, NO production via iNOS has been reported to regulate the nuclear respiratory factor 1 (NRF1)-targeted genes, such as Complex II of the MRC complex (Vercauteren *et al.*, 2006, Suliman *et al.*, 2011, Au & Scheffler 1998). In *S. pombe*, there are numbers of mitochondrial transcription activators specifically modulating the biogenesis of MRC complexes. Among them, Cbp3 and Cbp6 are important for the transcription of complex III, while Mss51 is important for complex IV transcription (Kuhl *et al.*, 2013). Nitrosation of such factors and its physiological roles in regulating the MRC activity should be further analyzed.

In *S. pombe*, the H_2O_2-stress responsive pathway underlies in two independent but connected pathways, the Spc1-MAPK and Pap1 pathways, each of which is triggered by different H_2O_2 concentrations (Vivancos *et al.*, 2006). As an effector kinase, Spc1 stabilizes and phosphorylates a transcriptional regulator Atf1 to promote the expression of stress-responsive genes (Wilkinson *et al.*, 1996). This study revealed the potential contribution of Spc1 in NO-dependent antioxidants responses (Figure 23B), as both *srx1*[+] and *gst3*[+] are reported to be regulated via the Spc1/Atf1 pathway. In the DNA microarray data, however, there was only slight augmentation of representative Atf1-dependent mRNA transcripts, such as *ste11*[+] (encoding a transcription factor responsible for the expression of various meiotic genes in response to nitrogen starvation) and *pyp2* (encoding a phosphatase that mediates

Spc1 dephosphorylation to resume cell division) in response to 0.5 mM DETA NONOate. Therefore, it is still controversial whether NO signaling activates the common Spc1/Atf1 pathway or a specific Spc1-mediated pathway. Although the underlying mechanism to activate the Spc1 MAPK pathway by NO is unknown, this study demonstrates, for the first time, a potential role of NO signaling in regulating the Spc1-MAPK pathway. The induction of Atf1-targeted genes by NO might occur through augmentation of the reactive phosphorylation of the MAPK cascade or direct modification of Atf1 perhaps through nitrosation. Interestingly, mammalian p38, a homolog of *S. pombe* Spc1, has been reported as a direct target of NO for nitrosation at the Cys211 residue, which is also conserved in Spc1 Nitrosation of p38 promotes its phosphorylation by the upstream MAPKK (MKK3/6), leading to its activation (Browning *et al.*, 2000, Qi *et al.*, 2013). Nitrosation of denoted phosphatase has also been reported to improve the phosphorylation of MAPK (Pi *et al.*, 2009). Elucidation of how NO activates Spc1 and oxidative stress-specific downstream targets will provide novel insight of NO signaling toward the Spc1-MAPK cascade highly conserved among eukaryotic cellular systems.

5. Conclusions

This study provides the first evidence that the fine-tuned nitric oxide (NO) signaling is present in the fission yeast *Schizosaccharomyces pombe*. The individual NO synthetic mechanisms and the designated NO-detoxification enzymes at distinct growth phases implies dynamic changes of NO signaling, which are potentially associated with growth phase-specific physiological events. While NO is generated from arginine by an unidentified NO synthase (NOS) during the log phase, NO signaling in the stationary phase is specifically associated with Complex III of the mitochondrial respiratory chain (MRC). Intracellular NO and its derivatives S-nitrosothiols (RSNOs) are detoxified cooperatively via SPAC869.02c and Fmd2 corresponding to NO dioxygenase (NOD) and S-nitrosoglutathione reducatse (GSNOR), respectively.

A novel physiological role of NO signaling, enhancement of the oxidative stress tolerance, in *S. pombe* cells was also revealed in this study. To elucidate this mechanism, a DNA microarray analysis of the *S. pombe* cells treated with an NO donor, DETA NONOate, was performed. The treatment essentially triggers at least three concomitant anti-oxidative mechanisms at the transcriptional levels, each of which evokes a cytoprotective effect against oxidants: (i) repression of the cellular respiration-induced ROS generation, (ii) inhibition of the thioredoxin activity leading to impairment of Fe^{2+}-mediated Fenton reactions, and (iii) activation of the potent H_2O_2 scavengers through the sulfiredoxin-peroxiredoxin and glutathione peroxidase activities. Taken together, this study gives a new insight of diverse stress responses mediated by the multifunctional signaling molecule, NO.

6. Future Perspectives

Based on this study, it is found that *S. pombe* harbors a constitutive NO production via the NOS activity potentially associated with proper cellular functions. Therefore, it is likely that the functions of NOS in *S. pombe* might mimic those of the constitutive eNOS or nNOS system in mammalian cells. It is, thus, noteworthy to confirm the yet un-identified NOS of *S. pombe*. Accordingly, a Western blot analysis against mammalian eNOS or nNOS may serve as preliminary approach.

Furthermore, it is worth clarifying NOS-dependent NO synthesis in correlation to the pathophysiological property of numbers of neurodegenerative as well as metabolic-related diseases in fission yeast. The approach is highly supported by the fact that *S. pombe* proteins (at least 172 proteins) have similarity with members of human disease proteins, most of which are highly involved in cancer, metabolic, and neurological disease (Wood *et al*., 2002). In particular, *S. pombe* may function as a reliable model for pathophysiological studies of eNOS- and nNOS-related diseases such as cystic fibrosis or amyotrophic lateral sclerosis disorder, respectively, since, Abcc7 (ABC transporter) and Sod1 (superoxide dismustase) of *S. pombe* are homolog to the corresponding protein in mammals, related to those diseases (Graseman *et al*., 2003, Lee *et al*., 2009).

The fact that NO is able to regulate numbers of transcriptional regulator emerges the multifunctional role of NO as signaling molecule. Thus, the regulatory role of NO toward transcriptional regulator activity needs further clarification, mainly, regarding its molecular mechanism. Since cytotoxic stresses are mainly regulated by Spc1-MAPK cascade, thus, it is worth confirming the possibility of 0.5 mM DETA NONOate treatment leads cell tolerance responses against nutrient limitations or heat shock stresses. More importantly, as MAPK signaling cascade is evolutionary conserved, thus, NO can be expected as a potential modulator of the particular cascade in higher eukaryote. Thus revealing the molecular mechanism of NO-induced Spc1 activity may give conceptual perspective about the broader function of NO as signaling molecule in organisms.

7. Acknowledgements

8. References

Abello, N., Kerstjens, H. A., Postma, D. S., and Bischoff, R. (2009). Protein tyrosine nitration: selectivity, physicochemical and biological consequences, denitration, and proteomics methods for the identification of tyrosine-nitrated proteins. J. Proteome Res 8, 3222-3238.

Abbas, K., Riquier, S., & Drapier, J. C. (2007). Peroxiredoxins and Sulfiredoxin at the Crossroads of the NO and H_2O_2 Signaling Pathways. Met Enzymol 527, 113-128.

Ahluwalia, A., Foster, P., Scotland, R. S., Mc Lean, P. G., Mathur, A., Perretti, M., Moncada, S., and Hobbs, A. J. (2004). Antiinflammatory activity of soluble guanylate cyclase: cGMP-dependent down-regulation of P-selectin expression and leukocyte recruitment. PNAS 101, 1386-1391.

Almeida, B., Buttner, S., Olheimer, S., Silva, A., Mesquita, A., Sampaio-Marques, B., Osorio, N.S., Kollau, A., Mayer, B., Leao, C., Larajinha, J., Rodrigues, F., Madeo, F., and Ludovico,P. (2007). NO-mediated apoptosis in yeast. J Cell Sci 120, 3279-3288.

Andrew, P. J., and Mayer, B. (1999). Enzymatic function of nitric oxide synthases. Cardiovascular Res 43, 521-531.

Arnelle, D. R., and Stamler , J. S. (1995). NO^+, $NO^.$, and NO^- donation by s-nitrosothiols: implications for regulation of physiological functions by s-nitrosylation and acceleration of disulfide formation. Arch Biochem Biophys 318, 279-285.
Aquilano, K., Baldelli, S., & Cirolo, M. R. (2014). uclear recruitment of neuronal nitric-oxide synthase by α-syntrophin is crucial for the induction of mitochondrial biogenesis. J Biol Chem 289, 365-378.

Au, H. C., & Scheffler, I. E. (1998). romoter analysis of the human succinate dehydrogenase iron-protein gene. Both nuclear respiratory factors NRF-1 and NRF-2 are required. Eur J Biochem 251, 164-174.

Bartlett, R., and Nurse, P. (1990). Yeast as a model system for understanding the control of DNA replication in eukaryotes. BioEssays 12, 457-463.

Basu, S., Azarova, N. A., Font, M. D., King , S. B., Hogg, N., Gladwin, M. T., Shiva, S., and Kim-Saphiro, D. B. (2008). Nitrite reductase activity of cytochrome c. J Biol Chem 283, 32590-32597.

Becker, M., Muller, S., Nellen, W., Jurkowski, T. P., Jeltsch, A., and Ehrenhofer-Murray, A. E. (2012). Pmt1, a Dnmt2 homolog in *Schizosaccharomyces pombe*, mediates tRNA methylation in response to nutrient signaling. Nucleic Acids Res 40, 11648-11658.

Bellemare, D. R., Sanschagrin, M., Beaudoin, J., and Labbe, S. (2001). A novel copper-regulated promoter system for expression of heterologous proteins in *Schizosaccharomyces pombe*. Gene 273, 191-198.

Beltran, B., Mathur, A., Duchen , M. R., Erusalimsky, J. D., & Moncada, S. (2000). The effect of nitric oxide on cell respiration: A key to understanding its role in cell survival or death. PNAS 97, 14602-14607.

Benamar, A., Rolletschek, H., Borisjuk, L., Avelange-Macherel, M. H., Curien, G., Mostefei, H. A., et al. (2008). Nitrite-nitric oxide control of mitochondrial respiration at the frontier of anoxia. Biochim Biophys Acta 1777, 1268-1275.

Betterridge, D. J. (2000). What is oxidative stress? Metabolism 49, 3-8.

Biswas, P., and Ghosh, S. (2014). Global transcriptomic profiling of *Schizosaccharomyces pombe* in response to nitrosative stress. Gene, doi: 10.1016/j.gene.2014.12.067

Bonamore, A., and Boffi, A. (2008). Flavohemoglobin: structure and reactivity. IUMMB Life 60, 19-28.

Bredt, D. S., and Snyder, S. H. (1990). Isolation of nitric oxide synthetase, a calmodulin-requiring enzyme. PNAS 87, 682-685.
Brown, G. C. (2001). Regulation of mitochondrial respiration by nitric oxide inhibition of

cytochrome c oxidase. Biochim Biophy Acta 1504, 46-57.

Browning, D. D., McShane, M. P., Marty, C., & Ye, R. D. (2000). Nitric Oxide Activation of p38 Mitogen-activated Protein Kinase in 293T Fibroblasts Requires cGMP-dependent Protein Kinase. J Biol Chem 275, 2811-2816.

Calvo, I. A., Ayte, J., and Hidalgo, E. (2013). Reversible thiol oxidation in the H_2O_2-dependent activation of the transcription factor Pap1. J Cell Sci 126, 2279-2284.

Carbon, S., Ireland, A., Mungall, C. J., Shu, S., Marshall, B., and Lewis , S. (2009). AmiGO: online access to ontology and annotation data. Bioinformatics 25, 288-289.

Chakravortty, D., & Hensel, M. (2003). Inducible nitric oxide synthase and control of intracellular bacterial pathogens. Microbes Infect 5, 621-627.

Chen, D., Wilkinson, C. R., Watt, S., Penkett, C. J., Toone , W. M., Jones, N., and Bahler, J. (2008). Multiple pathways differentially regulate global oxidative stress responses in fission yeast. Mol Biol Cell 19, 308-317.

Castello, P. R., David, P. S., McClure, T., Crook, Z., and Poyton , R. O. (2006). Mitochondria cytochrome oxidase produces nitric oxide under hypoxic conditions: implications for oxygen sensing and hypoxic signaling in eukaryotes. Cell Metab 3, 277-287.

Castello, P. R., Woo, D. K., Ball, K., Wojcik, J., Liu, L., and Poyton , R. O. (2008). Oxygen-regulated isoforms of cytochrome c oxidase have differential effects on its nitric oxide production and on hypoxic signaling. PNAS 105, 8203-8208.

Chardwiriyapreecha, S., Mukaiyama, H., Sekito, T., Iwaki, T., Takegawa, K., and Kakinuma, Y. (2010). Avt5p is required for vacuolar uptake of amino acids in the fission yeast *Schizosaccharomyces pombe*. FEBS Lett 584, 2339-2345.

Chiang, K. T., Shinyashiki, M., Switzer , C. H., Valentine, J. S., Gralla, E. B., Thiele, D. J., and Fukuto, J.M (2000). Effects of nitric oxide on the copper-responsive transcription factor ace1 in *Saccharomyces cerevisiae*: cytotoxic and cytoprotective actions of nitric oxide. Arch Biochem Biophysics 377, 269-303.

Chiranand, W., McLeod, I., Zhou, H., Lynn, J. J., Vega, L. A., Myers, H., Yates, J.R., Lorenz, M.C., and Gustin, M.C. (2008). CTA4 transcription factor mediates induction of nitrosative stress response in *Candida albicans*. Eukaryot Cell 7, 268-278.

Choudhari, S. K., Chaudary, M., Badge, S., Gadbail, A. R., and Joshi, V. (2013). Nitric oxide and cancer: a review. World J Surg Oncol 11, doi: 10.1186/1477-7819-11-118.

Ckless, K., Reynaert, N. L., Taatjes, D. J., Lounsbury, K. M., van der Vliet, A., & Janssen, H. Y. (2004). In situ detection and visualization of S-nitrosylated proteins following chemical derivatization: identification of Ran GTPase as a target for S-nitrosylation. Nitric oxide 11, 216-227.

Coelho, M., Dereli, A., Haese, A., Malinovska, L., DeSantis, M. E., Shorter, J., Alberti, S., Gross, T., and Tolic- Nørrelykke, I.M. (2013). Fission yeast does not age under favorable conditions, but does so after stress. Curr Biol 23, 1844-1852.

Dijkers, P. F., and O'Farrel, P. H. (2009). Dissection of a hypoxia-induced, nitric oxide-mediated signaling cascade. Mol Biol Cell 20, 4083-4090.

Domitrovic, T., Palhano, F. L., Barja-Fidalgo, C., DeFreitas, M., Orlando, M. T., and Fernandes, P. M. (2003). Role of nitric oxide in the response of *Saccharomyces cerevisiae* cells to heat shock and high hydrostatic pressure. FEMS Yeast Res 3, 341-346.

Dym, O., and Eisenberg, D. (2001). Sequence-structure analysis of FAD-containing proteins. Protein Sci 10, 1712-1728.

Eckstein, H., and Schlobohm, H. (1997). A particulate guanylate cyclase (EC 4.6.1.2) from growing yeast cells (*Saccharomyces cerevisiae*). Z Naturforsch C 52, 373-379.

Engelman, R., Weisman-Shomer, P., Ziv, T., Xu, J., Arner, E. S., and Benhar. M. (2013). Multilevel regulation of 2-Cys peroxiredoxin reaction cycle by *S*-nitrosylation. J Biol Chem 288, 11312-11324.

Elder, R. T., Yu, M., Chen, M., Yanagida, M., and Zhao, Y. (2001). HIV-1 Vpr induces cell cycle G2 arrest in fission yeast (*Schizosaccharomyces pombe*) through a pathway involving regulatory and catalytic subunits of PP2A and acting on both Wee1 and Cdc25. Virology , 287, 359-370.

Engelman, R., Weisman-Shomer, P., Ziv, T., Xu, J., Arner, E. S., and Benhar. M. (2013). Multilevel regulation of 2-Cys peroxiredoxin reaction cycle by *S*-nitrosylation. J Biol Chem 288, 11312-11324.

Ford, P. C., Fernandez, B. O., and Lim, M. D. (2005). Mechanisms of reductive nitrosylation in iron and copper models relevant to biological systems. Chem Rev 105, 2439-2455.

Fujita, Y., Tohda, H., Giga-Hama, Y., and Takegawa, K. (2006). Heat shock-inducible expression vectors for use in *Schizosaccharomyces pombe*. FEMS Yeast Res 6, 883-887.

Fukuto, J. M., Carrington, S. J., Tantillo, D. J., Harrison, J. G., Ignarro, L.J., Freeman, B. A., Chen, A., and Wink, D.A. (2012). Small molecule signaling agents: the integrated chemistry and biochemistry of nitrogen oxides, oxides of carbon, dioxygen, hydrogen sulfide, and their derived species. Chem Res Toxicol 25, 769-793.

Furchgott, R. F., and Zawadzki, J. V. (1980). The obligatory role of endothelial cells in the relaxation of arterial smooth muscle by acetylcholine. Nature 288, 373-376.

Gaits, F., Degols, G., Shiozaki, K., and Russell, P. (1998). Phosphorylation and association with the transcription factor Atf1 regulate localization of Spc1/Sty1 stress-activated kinase in fission yeast. Genes Dev 12, 1464-1473.

Gardner, P. R. (2005). Nitric oxide dioxygenase function and mechanism of flavohemoglobin, hemoglobin, myoglobin and their associated reductases. J Inorg Biochem 99, 247-266.

Gardner, P. R., Gardner, A. M., Martin, L. A., and Salzman, A. L. (1998). Nitric oxide dioxygenase: An enzymic function for flavohemoglobin. PNAS 95, 10378-10383.

Giga-Hama, Y., Tohda, H., Takegawa, K., and Kumagai , H. (2007). *Schizosaccharomyces pombe* minimum genome factory. Biotechnol Appl Biochem, 46, 147-155.

Gladwin, M. T., and Kim-Saphiro, D. B. (2008). The functional nitrite reductase activity of the heme-globins. Blood 112, 2636-2647.

Go, Y. M., and Jones, D. P. (2011). Cysteine/cystine redox signaling in cardiovascular disease. Free Radic Biol Med 50, 495-509.

Grasemann, H., Storm, G. K., Buscher, R., Knauer, N., Silverman, E. S., Palmer, L. J., et al. (2003). Endothelial nitric oxide synthase variants in cystic fibrosis lung disease. Am J Respir Crit Care Med 167, 390-394.

Gray, J. V., Petsko, G. A., Johnston, G. C., Ringe, D., Singer, R. A., and Werner-Washburne, M. (2004). "Sleeping beauty": quiescence in *Saccharomyces cerevisiae*. Microbiol Mol Biol Rev 68, 187-206.

Graziano, M., & Lamattina, L. (2007). Nitric oxide accumulation is required for molecular and physiological responses to iron deficiency in tomato roots. Plant J 52, 949-960.

Grivennikova , V. G., and Vinogradov, A. D. (2006). Generation of superoxide by the mitochondrial Complex I. Biochim Biophys Acta 1757, 553-561.

Gusarov, I., and Nudler, E. (2005). NO-mediated cytoprotection: instant adaptation to oxidative stress in bacteria. PNAS 102, 13855-13860.

Haines, R. L., Codlin, S., and Mole, S. E. (2009). The fission yeast model for the lysosomal storage disorder Batten disease predicts disease severity caused by mutations in CLN3. Dis Model Mech 2, 84-92.

Heinrich, T. A., da Silva, R. S., Miranda, K. M., Switzer, C. H., Wink, D. A., and Fukuto, J. M. (2013). Biological nitric oxide signalling: chemistry and terminology. Br J Pharmacol 167, 1417-1429.

Henard, C. A., Tapscott, T., Crawford, M. A., Husain, M., Doulias, P. T., Porwolik, S., et al.

(2014). The 4-cysteine zinc-finger motif of the RNA polymerase regulator DksA serves as a thiol switch for sensing oxidative and nitrosative stress. Mol Microbiol 91, 790-804.

Hendgen-Cotta, U. B., Rassaf, K. T., and Kelm, M. (2010). A highlight of myoglobin diversity: the nitrite reductase activity during myocardial ischemia–reperfusion. Nitric oxide 22, 75-82.

Hromatka, B. S., Noble, M. S., and Johnson, D. A. (2005). Transcriptional response of candida albicans to nitric oxide and the role of the *yhb1* gene in nitrosative stress and virulence. Mol Biol Cell 16, 4814-4826.

Huang, Z., Shiva, S., Kim-Saphiro, D. B., Patel, R. P., Ringwood, L. A., Irby, C. E., Huang, K.T., Ho, C., Schechter, A.N., and Gladwin, M.T.(2005). Enzymatic function of hemoglobin as a nitrite reductase that produces NO under allosteric control. J Clin Invest 115, 2099-2107.

Hughes, M. N. (2008). Chemistry of nitric oxide and related species. Methods Enzymol 436, 3-19.

Hwang, K., Carapito, C., Bohmer, S., Leize, E., Dorsselaer, A., and Bernhardt, R. (2006). Proteome analysis of *Schizosaccharomyces pombe* by two-dimensional gel electrophoresis and mass spectrometry. Proteomics 6, 4115-4129.

Hybertson, B. M., Gao, B., Bose, S. K., and McCord, J. M. (2011). Oxidative stress in health and disease: The therapeutic potential of Nrf2 activation. Mol Aspects Med 32, 234-246.

Idiris, A., Tohda, K., Sasaki, M., Okada, K., Kumagai, H., Giga-Hama, Y., and Takegawa. K. (2010). Enhanced protein secretion from multiprotease-deficient fission yeast by modification of its vacuolar protein sorting pathway. Appl Microbiol Biotechnol , 85, 667-677.

Ignarro, L. J., Buga, G. M., Wood, K. S., Byrns, R. E., and Chaudhuri, G. (1987). Endothelium-derived relaxing factor produced and released from artery and vein is nitric oxide. PNAS 84, 9265-9269.

Ikeda, K., Morigasaki, S., Tatebe, H., Tamanoi, F., and Shiozaki, K. (2008). Fission yeast TOR complex 2 activates the AGC-family Gad8 kinase essential for stress resistance and cell cycle control. Cell Cycle 7, 358-364.

Janke, C., Magiera, M. M., Rathfelder, N., Taxis, C., Reber, S., Moreno-Borchart, A., Doenges, S., Schowb, E., Schiebel, E., Knop, M. (2004). Versatile toolbox for PCR-based tagging of yeast genes: new fluorescent proteins, more markers and promoter substitution cassettes. Yeast 21, 947-962.

Jara, M., Vivancos, A. P., Calvo, I. A., Moldon, A., Sanso, M., and Hidalgo, E. (2007). The peroxiredoxin Tpx1 is essential as a H_2O_2 scavenger during aerobic growth in fission yeast. Mol Biol Cell 18, 2288-2295.

Jensen, D. E., Belka, G. K., and Du Bois, G. C. (1998). *S*-nitrosoglutathione is a substrate for rat alcohol dehydrogenase class III isoenzyme. Biochem J 331, 659-668.

Kanadia, R. N., Kuo, W. N., Mcnabb, M., and Botchway, A. (1998). Constitutive nitric oxide synthase in *Saccharomyces cerevisiae*. Biochem Mol Biol Int , 45, 1081-1087.

Kang, M. H., Jung, H. J., Hyun, D. H., Park, E. H., and Lim, C. J. (2011). Protective roles and Pap1-dependent regulation of the *Schizosaccharomyces pombe spy1* gene under nitrosative and nutritional stresses. Mol Biol Rep 38, 1129-1136.

Kanke, M., Nishimura, K., Kanemaki, M., Kakimoto, M., Takahasi, T. S., Nakagawa, T., and Masukata. H. (2011). Auxin-inducible protein depletion system in fission yeast. BMC Cell Biol 12, doi:10.1186/1471-2121-12-8.

Kawano, Y., Ohtsu, I., Tamakoshi, A., Shiroyama, M., Tsuruoka, A., Saiki, K., Takumi. K., Nonaka, G., Nakanishi, T., Hishiki, T., Suematsu, M., and Takahi, H. (2014). Involvement of the *yciW* gene in l-cysteine and l-methionine metabolism in *Escherichia coli*. J Biosci Bioeng, doi: 10.1016/j.jbiosc.2014.08.012.

Kelly, D. P., & Scarpulla, R. C. (2004). Transcriptional regulatory circuits controlling mitochondrial biogenesis and function. Genes Dev 18, 357-368.

Kim, J. S., Bang, M. A., Lee, S., Chae, H. Z., and Kim, K. (2010). Distinct functional roles of peroxiredoxin isozymes and glutathione peroxidase from fission yeast, *Schizosaccharomyces*

pombe. BMB Rep 43, 170-175.

Kim, S., & Ponka, P. (2002). Nitric oxide-mediated modulation of iron regulatory proteins: implication for cellular iron homeostasis. Blood Cells Mol Dis 29, 400-410.

Kubienova, L., Kopency, D., Tylichova, M., Briozzo, P., Skopalova, J., Sebela, M., Navratil, M., Tache, R., Luhova, L., Barroso, J.B., and Petrlvalsky, M. (2013). Structural and functional characterization of a plant S-nitrosoglutathione reductase from *Solanum lycopersicum*. Biochemie 95, 889-902.

Kuhl, I., Fox, T. D., & Bonnefoy, N. (2012). *Schizosaccharomyces pombe* homologs of the *Saccharomyces cerevisiae* mitochondrial proteins Cbp6 and Mss51 function at a post-translational step of respiratory complex biogenesis. Mitochondrion 12, 381-390.

Kumar, R., and Singh, J. (2004). Expression and secretion of a prokaryotic protein streptokinase without glycosylation and degradation in *Schizosaccharomyces pombe*. Yeast 16, 1343-1358.

Kato, T., Zhou, X., and Ma, Y. (2013). Possible Involvement of nitric oxide and reactive oxygen species in glucose deprivation-induced activation of transcription factor Rst2. PLoS One, doi: 10.1371/journal.pone.0078012

Kig, C., and Temizkan, G. (2009). Nitric oxide as signaling molecule in the fission yeast *Schizosaccharomyces pombe*. Protoplasma 238, 59-66.

Kim, H. J., Jung, H. Y., and Lim, C. J. (2008). The *pap1*(+) gene of fission yeast is transcriptionally regulated by nitrosative and nutritional stress. FEMS Microbiol Lett 280, 176-181.

Kuo, W. N., Kanadia, R. N., and Mcnabb. (1998). Soluble guanylate cyclase in *Saccharomyces cerevisiae*. Biochem Mol Biol Int 45, 125-131.

Labbe, S., Khan, M. G., and Jacques, J. F. (2013). Iron uptake and regulation in *Schizosaccharomyces pombe*. Curr Opin Microbiol 16, 669-676.

Labbe, S., Pelletier, B., & Mercier, A. (2007). Iron homeostasis in the fission yeast *Schizosaccharomyces pombe*. Biometals 20, 523-537.

Lampiao, F., Stirjdom, H., and Plessis, S. S. (2006). Direct nitric oxide measurement in human spermatozoa: flow cytometric analysis using the fluorescent probe, diaminofluorescein. Int J Androl 29, 564-567.

Larsen, F. J., Weitzberg, E., Lundberg, J. O., and Ekblom, B. (2007). Effects of dietary nitrate on oxygen cost during exercise. Acta Physiol 191, 59-66.

Lawrence, C. L., Maekawa, H., Worthington, J. L., Reiter, W., Wilkinson, C. R., and Jones , N. (2007). Regulation of *Schizosaccharomyces pombe* Atf1 protein levels by Sty1-mediated phosphorylation and heterodimerization with Pcr1. J Biol Chem 282, 5160-5170.
Lee, J., Dawes, I. W., & Roe, J. H. (1995). Adaptive response of *Schizosaccharomyces pombe* to hydrogen peroxide and menadione. Microbiol 141, 3127-3132.

Lee, J., Dawes, I. A., and Roe, J. H. (1997). Isolation, expression, and regulation of the *pgr1*[+] gene encoding glutathione reductase absolutely required for the growth of *Schizosaccharomyces pombe*. BMB rep 272, 23042-23049.

Lee, J., Ryu, H., & Kowall, N. W. (2009). Differential regulation of neuronal and inducible nitric oxide synthase (NOS) in the spinal cord of mutant SOD1 (G93A) ALS mice. Biochem Biophys Res Commun 387, 202-206.

Li, H., Meininger, C. J., Hawker, J. R., Haynes, T. E., Kepka-Lenhart, D., Mistry, S. K., Moris, S.M., and Wu, G (2001). Regulatory role of arginase I and II in nitric oxide, polyamine, and proline syntheses in endothelial cells. Am J Physiol Endocrinol Metab 280, 75-82.
Luo, Y., Han, Z., Chin, S. M., and Linn, S. (1994). Three chemically distinct types of oxidants formed by iron-mediated Fenton reactions in the presence of DNA. PNAS , 91, 12438-12442.

Lyngso, C., Kjaerulff, S., Muller, S., Bratt, T., Mortesesn, U. H., and Dal Degan, F. (2010). A versatile selection system for folding competent proteins using genetic complementation in a

eukaryotic host. Protein Sci 19, 579-592.

Lewinska, A., and Bartosz, G. (2006). Yeast flavohemoglobin protects against nitrosative stress and controls ferric reductase activity. Redox Rep 11, 231-239.

Li, B., Craig , S., Castello, P. R., Kato, M., Easlon , E., and Li, X. (2011). Identification of potential calorie restriction-mimicking yeast mutants with increased mitochondrial respiratory chain and nitric oxide levels. J Aging Res, doi: 10.4061/2011/673185.

Lincoln, T. M., Wu, X., Sellak, H., Dey, N., and Choi, S. (2006). Regulation of vascular smooth muscle cell phenotype by cyclic GMP and cyclic GMP-dependent protein kinase. Front Biosci 11, 356-367.

Liu, L., Hausladen, A., Zeng , M., Que, L., Heitman , J., and Stamler , J. S. (2001). A metabolic enzyme for S-nitrosothiol conserved from bacteria to human. Nature 410, 490-494.

Lopez-Mirabal, H. R., and Winther, J. R. (2008). Redox characteristics of the eukaryotic cytosol. Mol Cell Res 1783, 629-640.

Majumdar, U., Biswas, P., Subhra Sarkar, T., Maiti, D., and Ghosh, S. (2012). Regulation of cell cycle and stress responses under nitrosative stress in *Schizosaccharomyces pombe*. Free Radic Biol Med 52, 2186-2200.

Martinez-Ruiz, A., and Lamas, J. (2004). S-nitrosylation: a potential new paradigm in signal transduction. Cardiovasc Res 62, 43-52.

Mc Lennan, H. R., and Esposti, M. D. (2000). The contribution of mitochondrial respiratory complexes to the production of reactive oxygen species. J Bioenerg Biomemb 32, 153-162.

McAuliffe, C. A., and Murray, S. G. (1972). Metal complexes of sulphur-containing amino acids. Inorg Chim Acta Rev 6, 103-121.

Mc Murry, J. L., Chrestensen, C. A., Scott, I. M., Lee, E. W., Rahn, A. M., Johansen, A. M., Forsberg, B. J., Harris, K.D., and Salerno, J.C. (2011). Rate, affinity and calcium dependence of nitric oxide synthase isoform binding to the primary physiological regulator calmodulin. FEBS 278, 4943-4954.

Mojardin, L., Botet, J., Quintales, L., Moreno, S., and Salas, M. (2013). New Insights into the RNA-based mechanism of action of the anticancer drug 5-fluorouracil in eukaryotic cells. PLOS One, doi: 10.1371/journal.pone.0078172.

Moreno, M. B., Duran, A., and Ribas, J. C. (2000). A family of multifunctional thiamine-repressible expression vectors for fission yeast. Yeast 16, 861-872.

Morigasaki, S., Ikner, A., Tatebe, H., and Shiozaki, K. (2013). Response regulator-mediated MAPKKK heteromer promotes stress signaling to the Spc1 MAPK in fission yeast. Mol Biol Cell 24, 1083-1092.
Morris, S. M. (2009). Recent advances in arginine metabolism: roles and regulation of the arginases. Br J Pharmacol 157, 922-930.

Morita, T., and Takegawa, K. (2004). A simple and efficient procedure for transformation of *Schizosaccharomyces pombe*. Yeast 21, 613-617.

Mukaide, T., Hattori, Y., Misawa, N., Funahashi, S., Jiang , L., Hirayama, T., Nagasawa, H., and Toyokuni, S. (2014). Histological detection of catalytic ferrous iron with the selective turn-on fluorescent probe RhoNox-1 in a Fenton reaction-based rat renal carcinogenesis model. Free Radic Res 48, 990-995.

Mukaiyama, H., Tohda, H., and Takegawa, K. (2010). Overexpression of protein disulfide isomerases enhances secretion of recombinant human transferrin in Schizosaccharomyces pombe. Appl Microbiol Biotechnol 86, 1135-1143.

Murad, F., Mittal, C. K., Arnold, W. P., Katsuki, S., and Kimura , H. (1978). Guanylate cyclase: activation by azide, nitro compounds, nitric oxide, and hydroxyl radical and inhibition by hemoglobin and myoglobin. Adv Cyclic Nucleotide Res 9, 145-158.

Murphy, M. P. (2009). How mitochondria produce reactive oxygen species. Biochem J 417, 1-13.

Nakase, Y., Nakase, M., Kashiwazaki, J., Murai, T., Otsubo, Y., Mabuchi, I., *et al*. (2013). The fission yeast β-arrestin-like protein Any1 is involved in TSC-Rheb signaling and the regulation of amino acid transporters. J Cell Sci, doi: 10.1242/jcs.128355.

Nakamura, J., Purvis , E. R., and Swenberg, j. A. (2003). Micromolar concentrations of hydrogen peroxide induce oxidative DNA lesions more efficiently than millimolar concentrations in mammalian cells. Nucleic Acid Res 31, 1790-1795.

Nara, K., Konno, D., Uchida, J., Kiuchi, Y., & Oguchi , K. (1999). Protective effect of nitric oxide against iron-induced neuronal damage. J Neural Transm 106, 835-848.

Nasuno, R., Aitoku, M., Manago, Y., Nishimura, A., Sasano, Y., and Takagi, H. (2014). Nitric oxide-mediated antioxidative mechanism in yeast through the activation of the transcription factor Mac1. PLOS One, doi: 10.1371/journal.pone.0113788.

Niki, E., Yoshida, Y., Saito, Y., and Noguchi, N. (2005). Lipid peroxidation: mechanisms, inhibition, and biological effects. Biochem Biophys Res Comm 338, 668-676.
Nikitovic, D., Holmgren, A., & Spyrou, G. (1998). Inhibition of AP-1 DNA binding by nitric oxide involving conserved cysteine residues in Jun and Fos. Biochem Biophys Res Commun 242, 109-112.

Nishimura, A., Kawahara, N., and Takagi, H. (2013). The flavoprotein Tah18-dependent NO synthesis confers high-temperature stress tolerance on yeast cells. Biochem Biophys Res Commun 430, 137-143.

Nittler, M. P., Hocking-Murray, D., Foo, C. K., & Sil, A. (2005). Identification of *Histoplasma capsulatum* transcripts induced in response to reactive nitrogen species. Mol Biol Cell 16, 4792-4813.

Noguchi, A., Takada, M., Nakayama, K., and Ishikawa, T. (2008). cGMP-independent anti-apoptotic effect of nitric oxide on thapsigargin-induced apoptosis in the pancreatic beta-cell line INS-1. Life Sci 83, 865-870.

Nohl, H., Staniek, K., Sobhian, B., Bahrami, S., Redl, H., and Kozlov, A. V. (2000). Mitochondria recycle nitrite back to the bioregulator nitric monoxide. Acta Biochim Pol 47, 913-921.

Novak, B., and Tyson, J. J. (1997). Modeling the control of DNA replication in fission yeast. PNAS 94, 9147-9152.

Ogasawara, Y., Funakoshi, M., and Ishii, K. (2009). Determination of reduced nicotinamide adenine dinucleotide phosphate concentration using high-performance liquid chromatography with fluorescence detection: ratio of the reduced form as a biomarker of oxidative stress. Biol Pharm Bull 32, 1819-1823.

Oria, R., Sanchez, L., Houston, T., Hentze, T., Liew, F. Y., & Brock, J. H. (1995). Effect of nitric oxide on expression of transferrin receptor and ferritin and on cellular iron metabolism in K562 human erythroleukemia cells. Blood 85, 2962-2966.

Park, S., & Imlay, J. A. (2003). High levels of intracellular cysteine promote oxidative DNA damage by driving the fenton reaction. J Bacteriol , 185, 1942-1950.

Patel, R. P., Hogg, N., Spencer, N. Y., Kalyanaraman, B., Matalon, S., & Darley-Usmar, V. M. (1999). Biochemical characterization of human S-nitrosohemoglobin. Effects on oxygen binding and transnitrosation. J Biol Chem 274, 15487-15492.

Pelletier, B., Beaudoin, J., Mukai, Y., & Labbe, S. (2002). Fep1, an Iron Sensor Regulating Iron Transporter Gene Expression in *Schizosaccharomyces pombe*. J Biol Chem 277, 22950-22958.

Phoa, N., and Epe, B. (2002). Influence of nitric oxide on the generation and repair of oxidative DNA damage in mammalian cells. Carcinogenesis 23, 469-475.
Pi, X., Wu, Y., Ferguson III, J. E., Portbury, A. L., & Patterson, C. (2009). SDF-1α stimulates JNK3 activity via eNOS-dependent nitrosylation of MKP7 to enhance endothelial migration. PNAS 106, 5675-5680.

Qi, S. H., Hao, L. Y., Yue, J., Zong, Y. Y., & Zhang, G. Y. (2013). Exogenous nitric oxide negatively regulates the S-nitrosylation p38 mitogen-activated protein kinase activation during cerebral ischaemia and reperfusion. Neuropathol Appl Neurobiol , 39, 284-297.

Quinn, J., Findlay, V., Dawson, K., Millar, B. A., Jones , N., Morgan , B. A., and Toone, W.M. (2002). Distinct regulatory proteins control the graded transcriptional response to increasing H_2O_2 levels in fission yeast *Schizosaccharomyces pombe*. Mol Biol Cell , 13, 805-816.

Radi, R. (2004). Nitric oxide, oxidants, and protein tyrosine nitration. PNAS , 101, 4003-4008.

Rinnerthaler, M., Buttner, S., Laun, P., Heeren, G., Felder, T. K., Klinger, H., *et al.* (2012). Yno1p/Aim14p, a NADPH-oxidase ortholog, controls extramitochondrial reactive oxygen species generation, apoptosis, and actin cable formation in yeast. PNAS 109, 8653-8663.

Roma, G. W., Crowley, L. J., Davis, C. A., and Barber, M. J. (2005). Mutagenesis of Glycine 179 modulates both catalytic efficiency and reduced pyridine nucleotide specificity in cytochrome b5 reductase. Biochem 44, 13467-13476.
Rosenfeld, E., Beauvoit, B., Rigoulet, M., & Salmon, J. M. (2002). Non-respiratory oxygen consumption pathways in anaerobically-grown *Saccharomyces cerevisiae*: evidence and partial characterization. Yeast 19, 1299-1321.

Sahoo, R., Dutta, T., Das, A., Sinha Ray, S., Sengupta , R., and Ghosh , S. (2006). Effect of nitrosative stress on *Schizosaccharomyces pombe*: inactivation of glutathione reductase by peroxynitrite. Free Radic Biol Med 40, 625-631.

Sarver, A., and deRisi, J. (2005). Fzf1p regulates an inducible response to nitrosative stress in *Saccharomyces cerevisiae*. Mol Biol Cell 16, 4781-4791.

Sasano, Y., Haitani, Y., Hashida, K., Ohtsu, I., Shima, J., and Takagi, H. (2012). Enhancement of the proline and nitric oxide synthetic pathway improves fermentation ability under multiple baking-associated stress conditions in industrial baker's yeast. Microb Cell Fact 11, doi:10.1186/1475-2859-11-40

Schafer, F. Q., and Buettner, G. R. (2001). Redox environment of the cell as viewed through the redox state of the glutathione disulfide/glutathione couple. Free Radic Biol Med 30, 1191-1212.

Schmidt, M. W., Houseman, A., Ivanov, A. R., and Wolf, D. A. (2007). Comparative proteomic and transcriptomic profiling of the fission yeast *Schizosaccharomyces pombe*. Mol Syst Biol 3, doi: 10.1038/msb4100117.

Sengupta, R., and Holmgren, A. (2013). Thioredoxin and thioredoxin reductase in relation to reversible S-nitrosylation. Antioxid Redox Signal 18, 259-269.

Shieh, Shieh, J. C., Wilkinson , M. G., and Millar, J. B. (1998). The Win1 Mitotic Regulator Is a Component of the Fission Yeast Stress-activated Sty1 MAPK Pathway. Mol Biol Cell 9, 311-322.

Shinyashiki, M., Chiang, K. T., Switzer, C. H., Gralla, E. B., Valentine, J. S., Thiele, D. J., and Fukuto, J.M. (2000). The interaction of nitric oxide (NO) with the yeast transcription factor Ace1: A model system for NO-protein thiol interactions with implications to metal metabolism. PNAS 97, 2491-2496.

Shiozaki, K., & Russell, P. (1995). Cell-cycle control linked to extracellular environment by MAP kinase pathway in fission yeast. Nature 378, 739-743.

Shiozaki, K., Russell, P., and Degols, G. (1996). Activation and regulation of the Spc1 stress-activated protein kinase in *Schizosaccharomyces pombe*. Mol Cell Biol , 16, 2870-2877.

Shiozaki, K., Shiozaki, M., and Russell, P. (1998). Heat stress activates fission yeast Spc1/StyI MAPK by a MEKK-independent mechanism. Mol Biol Cell 9, 1339-1349.

Shiozaki, K., Shiozaki, M., and Russell, P. (1997). Mcs4 mitotic catastrophe suppressor regulates the fission yeast cell cycle through the Wik1-Wis1-Spc1 kinase cascade. Mol Biol Cell 8, 409-419.

Silva, A., Almeida, B., Sampaio-Marques, B., Reis, M. I., Ohlmeier, S., Rodrigues, F., Vale, A., and Ludovico, P. (2011). Glyceraldehyde-3-phosphate dehydrogenase (GAPDH) is a specific substrate of yeast metacaspase. Biochim Biophys Acta 1813, 2044-2049.

Singh, S. P., Wishnok, J. S., Keshive, M., Deen, W. M., and Tannenbaum, S. R. (1996). The chemistry of the S-nitrosoglutathione/glutathione system. PNAS 93, 14428-14433.

Strijdom, H., Muller, C., and Lochner, A. (2004). Direct intracellular nitric oxide detection in isolated adult cardiomyocytes: flow cytometric analysis using the fluorescent probe, diaminofluorescein. J Mol Cell Cardiol 37, 897-902.

Stuehr, D. J. (1999). Mammalian nitric oxide synthases. Biochim Biophys Acta 411, 217-230.
Suliman, H. B., Babiker, A., Withers, C. M., Sweeney, T. E., Carraway, M. S., Tatro, L. G., et al. (2011). Nitric Oxide Synthase-2 regulates mitochondrial Hsp60 chaperone function during bacterial peritonitis in mice. Free Radic Biol Med 48, 736-746.

Song, J. Y., & Roe, J. H. (2008). The role and regulation of Trxl, a cytosolic thioredoxin in Schizosaccharomyces pombe. J Microbiol 46, 408-414.

Sullivan, J. C., and Pollock, J. S. (2006). Coupled and uncoupled NOS: separate but equal? Uncoupled NOS in endothelial cells is a critical pathway for intracellular signaling. Circ Res 98, 717-719.

Sun, L., Li, M., Suo, F., Liu, X., Shen, E., Yang, B., Dong, M., He, W., and Du, L. (2013). Global analysis of fission yeast mating genes reveals new autophagy factors. PLOS Gene, doi: 10.1371/journal.pgen.1003715.

Tamm, T. (2011). A Thiamine-regulatable epitope-tagged protein expression system in fission yeast. Methods Mol Biol 824, 417-432.
Toledano, M. B., Dalaunay-Moisan, A., Outten, C. E., and Igbaria, A. (2013). Functions. Antioxid Redox Signal 18, 1699-1711.

Toone, W. M., Kuge, S., Samuels, M., Morgan, B. A., Toda, T., & Jones, N. (1998). Regulation of the fission yeast transcription factor Pap1 by oxidative stress: requirement for the nuclear export factor Crm1 (Exportin) and the stress-activated MAP kinase Sty1/Spc1. Genes Dev 12, 1453-1463.

Totzeck, M., Hendgen-Cotta, U. B., Luedike, P., Berenbrink, M., Klare, J. P., Steinhoff, H. J., Semmler, D., Shiva, S., Williams, D., Gladwin, M.T., Schrader, J., Klemm, M., Cossins, A.R., and Rassaf, T. (2012). Nitrite regulates hypoxic vasodilation via myoglobin-dependent nitric oxide generation. Circulation 126, 325-334.

Tuckova, L., Flegelova, Z., Tiaskalova-Hogenova, H., & Zidek , K. (2000). Activation of macrophages by food antigens: enhancing effect of gluten on nitric oxide and cytokine production. J Leuko Biol 67, 312-318.

Turko, I. V., and Murad, F. (2002). Protein nitration in cardiovascular disease. Pharmacol Rev 89, 444-448.

Ullman, B. D., Myers, H., Chiranand, W., Lazzel, A. L., Zhao, Q., Vega, L. A., Lopez-Ribot, J. L., Gardner, P.R., and Gustin, M.C. (2004). Inducible defense mechanism against nitric oxide in *Candida albicans*. Eukaryot Cell 3, 715-723.

Veal, E. A., Day, A. M., and Morgan, B. A. (2007). Hydrogen peroxide sensing and signaling. Moll Cell 26, 1-14.
Vercauteren, K., Pasko, R. A., Gleyzer, N., Marino, V. M., & Scarpulla, R. C. (2006). PGC-1-related coactivator: immediate early expression and characterization of a CREB/NRF-1 binding domain associated with cytochrome c promoter occupancy and respiratory growth. Mol Cell Biol 26, 7409-7419.

Vivancos, A. P., Castillo, E. A., Biteau, B., Nicot, C., Ayte, J., and Toledano, M. B. (2005). A cysteine-sulfinic acid in peroxiredoxin regulates H_2O_2 sensing by the antioxidant Pap1 pathway. PNAS 102, 8875-8880.

Vivancos, A. P., Jara, M., Zuin, A., Sanso, M., and Hidalgo, E. (2006). Oxidative stress in *Schizosaccharomyces pombe*: different H_2O_2 levels, different response pathways. Mol Genet Genomics , 276, 495-502.

Wade, R. S., and Castro, C. E. (1990). Redox reactivity of iron(III) porphyrins and heme proteins with nitric oxide. Nitrosyl transfer to carbon, oxygen, nitrogen and sulfu. Chem Res Toxicol 3, 289-291.

Walter, U., and Gambaryan, S. (2009). cGMP and cGMP-dependent protein kinase in platelets

and blood cells. Handb Exp Pharmacol 191, 533-548.

Webb, A., Bond, R., Mc Lean, P., Uppal, R., Benjamin, N., and Ahluwalia, A. (2004). Reduction of nitrite to nitric oxide during ischemia protects against myocardial ischemia–reperfusion damage. PNAS 101, 13683-13688.

Wilkinson, M. G., Samuels, M., Takeda, T., Toone, W. M., Shieh, J. C., Toda, T., Millar, J.B., and Jones, N. (1996). The Atf1 transcription factor is a target for the Sty1 stress-activated MAP kinase pathway in fission yeast. Genes Dev 10, 2289-2301.

Wood, K. C., Batchelor, A. M., Bartus, K., Harris, K. L., Grathwaite, G., Vernon, J., *et al.* (2011). Picomolar nitric oxide signals from central neurons recorded using ultrasensitive detector cells. J Biol Chem 286, 43172-43181.

Wood, V., Gwilliam, R., Rajandream, M. A., Lyne, M., Lyne, R., Stewart, A., *et al.* (2002). The genome sequence of *Schizosaccharomyces pombe*. Nature , 415, 871-880.

Wright, A. M., Wu, G., and Hayton, T. W. (2010). Structural characterization of a copper nitrosyl complex with a $\{CuNO\}^{10}$ configuration. J Am Chem Soc 132, 14336-14337.

Wu, C., Parrott, A. M., Liu, T., Jain, M. R., Yang, Y., Sadoshima, J., and Li, H. (2011). Distinction of thioredoxin transnitrosylation and denitrosylation target proteins by the ICAT quantitative approach. J Proteomics 74, 2498-2509.

Yamada, K., Nakagawa, C. W., and Mutoh, N. (1999). *Schizosaccharomyces pombe* homologue of glutathione peroxidase, which does not contain selenocysteine, is induced by several stresses and works as an antioxidant. Yeast 15, 1125-1132.

Zamora, R., Vovodotz, Y., and Biliar, T. R. (2000). Inducible nitric oxide synthase and inflammatory diseases. Mol Med 6, 347-373.

9. Supplemetary Informations

Table S1. List of real time PCR (RT PCR) oligonucleotide primers used in this study

Oligonucelotide	Sequence
Fmd1-forward	TGCGGTGTCACAACTGGAT
Fmd1-reverse	ACAGCTACCGTTGAACCAGA
Fmd2-forward	ACTGCTGTAAGCTTCCTGATGA
Fmd2-reverse	AGGGATGTACATAAAACGTCCGA
Fmd3-forward	GGACGCATTCGCACTACTCA
Fmd3-reverse	ATTACAGGAGAAGCGGCTGG
SPAC869.02c-forward	GGGACATTGTCTGTTGACGA
SPAC869.02c-reverse	TCTAAAAATGCCGGGGTAGC
Fio1-forward	AGAGTTGAATCCTCTCTATAGCTG
Fio1-reverse	CAAGGGTGAAAAAGTCAAACCAT
Fip1-forward	ATGAAAGTATCGCCAATCGC
Fip1-reverse	AAGGGAAGGAGAAACATGGAAT
Frp1-forward	GCATGTGGCCTCTATGTAACT
Frp1-reverse	TCGTGAGACGAAATGAGCAA
Trx1-forward	TGCTACTTGGTGTGGACCTT
Trx1-reverse	GTGGCATCAGAGTAAGTGTTGG
Trx2-forward	CGGCGCTGATGTGAAAACTT
Trx2-reverse	ACGAATGGGGACACCAATATCC
Cyc1-forward	GTCCCAATTTGCACGGTGT
Cyc1-reverse	CTTATCGCGATTGGCTTCGG
Sre1-forward	TCTCCATTCACAGGTACTGTTCTC
Sre1-reverse	CGTGCAAAAGATAGAATAAACCGAG
Hem13-forward	TTTGGTGGTTTGGTGGTGGA
Hem13-reverse	TGCAATTTGTGGAAATGCTTGC

Table S2. The significantly up-regulated genes in response to DETA NONOate, in correspond to the ontology category biological process

Ontology	Gene ontology term	Up-regulated genes		
		Gene title	Log2ratio*	Gene symbol
Biological process	iron assimilation (GO:0033212)	Siderophore-iron transporter Str2	1.13	*str2*
		Ferrichrome synthetase Sib1	1.99	*sib1*
		Siderophore-iron transporter Str1	2.13	*str1*
		Ornithine N5 monooxygenase (predicted)	2.36	*sib2*
		Iron transport multicopper oxidase Fio1	3.42	*fio1*
		Iron permease Fip1	3.42	*fip1*
		Ferric-chelate reductase Frp1	5.52	*frp1*
		Siderophore-iron transporter Str3	7.05	*str3*

*log2ratio represents the fold change (log value) between DETA NONOate treatment to control (without DETA NONOate)

Table S3. The significantly up-regulated genes in response to DETA NONOate, in correspond to the ontology category cellular component

Ontology	Gene ontology term	Up-regulated genes		
		Gene title	Log2ratio*	Gene symbol
Cellular component	plasma membrane (GO:0005886)	Copper transporter complex subunit Ctr4	1.01	*ctr4*
		OPT oligopeptide transporter family protein (predicted)	1.03	*SPCC1840.12*
		Alpha-1,6-mannanase (predicted)	1.04	*mug191*
		Sulfate transporter (predicted)	1.07	*SPBC3H7.02*
		Spermidine family transporter (predicted)	1.26	*SPCC569.05c*
		Brefeldin A efflux transporter Bfr1	1.58	*bfr1*
		GPI anchored protein (predicted) /// GPI-anchored protein /// GPI-anchored protein	1.60	*SPAC212.08c /// SPAC212.12 /// SPAC750.07c*
		Hexose transporter Ght3	2.20	*ght3*
		Iron transport multicopper oxidase Fio1	3.42	*fio1*
		Iron permease Fip1	3.42	*fip1*
		Ferric-chelate reductase Frp2 (predicted)	4.14	*frp2*
		Ferric-chelate reductase Frp1	5.52	*frp1*
		Sequence orphan	9.68	*SPAC1F8.02c*

*log2ratio represents the fold change (log value) between DETA NONOate treatment to control (without DETA NONOate)

Table S4. The significantly up-regulated genes in response to DETA NONOate, in correspond to the ontology category molecular function

Ontology	Gene ontology term	Up-regulated genes		
		Gene title	Log2ratio*	Gene symbol
Molecular function	oxidoreductase activity (GO:0016491)	uroporphyrin methyltransferase (predicted)	1.01	*SPCC1739.06c*
		C-14 sterol reductase Erg24 (predicted)	1.04	*erg24*
		1-acyldihydroxyacetone phosphate reductase (predicted)	1.06	*ayr1*
		enoyl-[acyl-carrier protein] reductase (predicted)	1.08	*etr1*
		phosphoprotein phosphatase (predicted)	1.10	*SPAC1039.02*
		coproporphyrinogen III oxidase (predicted)	1.11	*hem13*
		2 OG-Fe(II) oxygenase superfamily protein Ofd2	1.12	*ofd2*
		dehydrogenase (predicted)	1.17	*SPAC2E1P3.01*
		pyridoxal reductase (predicted)	1.21	*SPCC1281.04*
		NADH/NADPH dependent indole-3-acetaldehyde reductase AKR3C2	1.22	*SPAC19G12.09*
		NAD binding dehydrogenase family protein	1.24	*SPACUNK4.17*
		conserved fungal protein	1.38	*SPBC17D11.03c*
		nitric oxide dioxygenase (predicted)	1.42	*SPAC869.02c*
		dihydrodiol dehydrogenase (predicted)	1.45	*SPAC513.06c*
		fumerate reductase (predicted)	1.46	*osm1*
		sphingosine hydroxylase Sur2	1.65	*sur2*
		copper amine oxidase-like protein Cao2	1.74	*cao2*
		NADP-dependent oxidoreductase (predicted)	1.78	*SPAPB24D3.08c*
		hexitol dehydrogenase (predicted)	1.92	*tms1*
		short chain dehydrogenase (predicted)	1.93	*SPAC22A12.17c*
		L-lactate dehydrogenase (predicted)	2.04	*SPAC186.08c*
		ornithine N5 monooxygenase (predicted)	2.36	*sib2*
		succinate-semialdehyde dehydrogenase (predicted)	2.52	*SPAC139.05*
		sulfiredoxin	2.64	*srx1*
		3-hydroxyacyl-CoA dehydrogenase (predicted)	2.77	*SPAC4H3.08*
		aldo/keto reductase family protein	2.85	*SPBC215.11c*
		aldo/keto reductase family protein	2.91	*SPAC750.01*
		iron transport multicopper oxidase Fio1	3.42	*fio1*
		NADH-dependent flavin oxidoreductase (predicted)	3.72	*SPBC23G7.10c*
		ferric-chelate reductase Frp2 (predicted)	4.14	*frp2*
		short chain dehydrogenase	4.25	*SPCC663.08c*
		ferric-chelate reductase Frp1	5.52	*frp1*

*log2ratio represents the fold change (log value) between DETA NONOate treatment to control (without DETA NONOate)

Table S5. The significantly down-regulated genes in response to DETA NONOate, in correspond to the ontology category biological process

Ontology	Gene ontology term	Up-regulated genes		
		Gene title	Log2ratio*	Gene symbol
Biological process	cellular respiration (GO:0045333)	TIM22 inner membrane protein import complex anchor subunit Tim18	-3.63	*sdh4*
		succinate dehydrogenase cytochrome B subunit	-2.66	*sdh3*
		succinate dehydrogenase iron-sulfur subunit protein	-2.60	*sdh2*
		cytochrome c1 Cyt1 (predicted)	-2.47	*cyt1*
		cytochrome c (predicted)	-2.26	*cyc1*
		ubiquinol-cytochrome-c reductase complex subunit 5	-2.10	*rip1*
		succinate dehydrogenase Sdh1 (predicted)	-2.07	*sdh1*
		ubiquinol-cytochrome-c reductase complex subunit 9 (predicted)	-1.96	*qcr9*
		cytochrome c oxidase subunit V (predicted)	-1.72	*cox5*
		mitochondrial processing peptidase (MPP) complex beta subunit Qcr1 (predicted)	-1.65	*qcr1*
		ubiquinol-cytochrome-c reductase complex subunit 6 (predicted)	-1.56	*qcr7*
		aconitate hydratase/mitochondrial ribosomal protein subunit L49, fusion protein (predicted)	-1.54	*SPBP4H10.15*
		ubiquinol-cytochrome-c reductase complex subunit 8, hinge protein (predicted)	-1.54	*qcr6*
		citrate synthase Cit1	-1.46	*cit1*
		ubiquinol-cytochrome-c reductase complex subunit 7	-1.45	*qcr8*
		dihydrolipoyllysine-residue succinyltransferase	-1.38	*kgd2*
		cytochrome c oxidase subunit VIII (predicted)	-1.30	*cox8*
		aconitate hydratase (predicted)	-1.23	*SPAC24C9.06c*
		cytochrome c oxidase subunit VIb (predicted)	-1.08	*cox12*
		Reiske ISP-associated protein, ubiquinol-cytochrome-c reductase complex subunit Qcr10 (predicted)	-1.07	*qcr10*
		alpha-ketoglutarate dehydrogenase	-1.03	*SPBC3H7.03c*
		cytochrome c oxidase subunit VI (predicted)	-1.02	*cox6*

*log2ratio represents the fold change (log value) between DETA NONOate treatment to control (without DETA NONOate)

Table S6. The significantly down-regulated genes in response to DETA NONOate, in correspond to the ontology category cellular component

Ontology	Gene ontology term	Up-regulated genes		
		Gene title	Log2ratio*	Gene symbol
Cellular component	mitochondrial respiratory chain (GO:0005746)	TIM22 inner membrane protein import complex anchor subunit Tim18	-3.63	*sdh4*
		succinate dehydrogenase cytochrome B subunit	-2.66	*sdh3*
		succinate dehydrogenase iron-sulfur subunit protein	-2.60	*sdh2*
		cytochrome c1 Cyt1 (predicted)	-2.47	*cyt1*
		cytochrome c (predicted)	-2.26	*cyc1*
		succinate dehydrogenase Sdh1 (predicted)	-2.07	*sdh1*
		cytochrome c oxidase subunit V (predicted)	-1.72	*cox5*
		ubiquinol-cytochrome-c reductase complex subunit 8, hinge protein (predicted)	-1.54	*qcr6*
		cytochrome c oxidase subunit VIII (predicted)	-1.30	*cox8*
		cytochrome c oxidase subunit VIb (predicted)	-1.08	*cox12*
		cytochrome c oxidase subunit VI (predicted)	-1.02	*cox6*

*log2ratio represents the fold change (log value) between DETA NONOate treatment to control (without DETA NONOate)

Table S7. The significantly down-regulated genes in response to DETA NONOate, in correspond to the ontology category molecular function

Ontology	Gene ontology term	Up-regulated genes		
		Gene title	Log2ratio*	Gene symbol
Molecular function	iron-sulfur cluster binding (GO:0051536)	glutamate synthase Glt1 (predicted)	-4.72	*glt1*
		mitochondrial electron transfer flavoprotein-ubiquinone oxidoreductase (predicted)	-3.14	*SPAC20G8.04c*
		succinate dehydrogenase iron-sulfur subunit protein	-2.60	*sdh2*
		mitochondrial iron-sulfur protein Isa1	-2.21	*isa1*
		monothiol glutaredoxin Grx5	-2.08	*grx5*
		tRNA (uracil(54)-C(5))-methyltransferase	-1.61	*SPAC4G8.07c*
		aconitate hydratase/mitochondrial ribosomal protein subunit L49, fusion protein (predicted)	-1.54	*SPBP4H10.15*
		biotin synthase	-1.53	*bio2*
		homoaconitate hydratase Lys2	-1.47	*lys2*
		dihydroxy-acid dehydratase (predicted)	-1.45	*SPAC17G8.06c*
		3-isopropylmalate dehydratase Leu2 (predicted)	-1.36	*leu2*
		flavoprotein	-1.28	*aif1*
		mitochondrial lipoic acid synthetase Lip5 (predicted)	-1.22	*lip5*
		wybutosine biosynthesis protein Tyw1 (predicted)	-1.00	*SPCC1020.08*

*log2ratio represents the fold change (log value) between DETA NONOate treatment to control (without DETA NONOate)

Table S8. The significantly up-regulated genes relevant for oxidative stress responses

Gene Title	Log2 Ratio	Gene Symbol
glutathione S-transferase Gst2	3.22	*gst2*
sulfiredoxin	2.64	*srx1*
zf PARP type zinc finger protein	2.31	*SPAC13F5.07c*
F-box protein Pof14	2.11	*pof14*
sequence orphan	1.67	*SPAC23H3.15c*
ThiJ domain protein	1.01	*SPCC757.03c*
ThiJ domain protein	1.00	*SPAC5H10.02c*
methionine sulfoxide (predicted)	0.99	*SPBC216.04c*
glutathione peroxidase Gpx1	0.91	*gpx1*
glutathione S-transferase Gst3	0.85	*gst3*
1-alkyl-2-acetylglycerophosphocholine esterase	0.75	*plg7*
D-arabinono-1,4-lactone oxidase (predicted)	0.74	*alo1*
glutathione S-transferase (predicted)	0.67	*SPCC1281.07c*
transcription factor Hsr1	0.63	*hsr1*
glutathione-dependent formaldehyde dehydrogenase (predicted)	0.56	*FMD3*
gamma-glutamyltranspeptidase Ggt2	0.54	*ggt2*
alpha,alpha-trehalase Ntp1	0.48	*ntp1*
peptide methionine sulfoxide reductase (predicted)	0.48	*SPAC29E6.05c*
thioredoxin peroxidase (predicted)	0.43	*SPCC330.06c*
protein disulfide isomerase	0.37	*SPAC17H9.14c*
transcription factor, Atf-CREB family Atf1	0.37	*atf1*
RNA-binding protein Cip1	0.37	*cip1*
RNA-binding protein Csx1	0.36	*csx1*
mitochondrial glutathione reductase Pgr1	0.35	*pgr1*
cytosolic thioredoxin Trx1	0.33	*trx1*
thioredoxin peroxidase Tpx1	0.32	*tpx1*
Svf1 family protein Svf2	0.30	*SPBC36B7.02*
dual specificity protein kinase Lkh1	0.27	*lkh1*
glutathione S-transferase Gst1	0.24	*gst1*
sequence orphan	0.21	*SPAC18G6.09c*
RTA1-like protein	0.12	*tco1*
MAP kinase Sty1	0.10	*sty1*
transcription factor Pap1/Caf3	0.09	*pap1*
glutaredoxin Grx2	0.09	*grx2*
TLDc domain protein 1	0.09	*mug63*
RNA-binding protein Cip2	0.04	*cip2*
MAPK-activated protein kinase Cmk2	0.02	*cmk2*

*log2ratio represents the fold change (log value) between DETA NONOate treatment to control (without DETA NONOate)

Supplemetary Figure S1. The transcriptional levels of hypoxic-induced genes
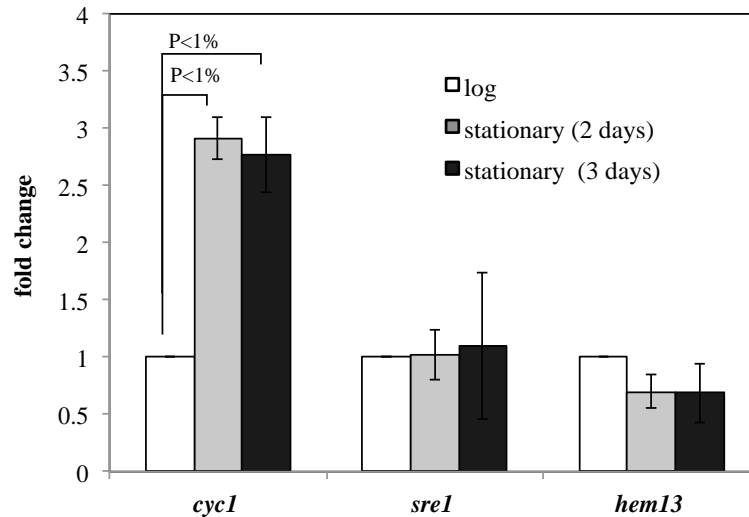

Figure S1. The mRNA transcriptional levels of hypoxic-induced gene throughout growth phases. Yeast cells were grown in rich medium, YES, to either log or stationary phase (2 and 3 days of incubation). The transcript levels of hypoxic-induced genes, including $cyc1^+$ (encoding hypoxia-specific mitochondrial cytochrome c), $sre1^+$ (an endoplasmic reticulum membrane-bound transcription factor that responds to changes in oxygen-dependent sterol synthesis), and $hem13^+$ (Sre1-target genes) were assessed by Real Time PCR with its respective specific oligonucleotide primers. The fold changes were normalized with respect to $act1^+$ transcript levels. Results are means of three independent experiments.

Supplemetary Figure S2. The transcriptional levels of $fep1^+$ gene
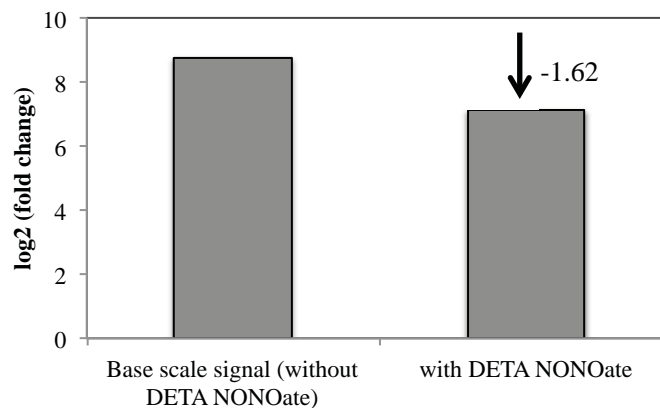

Figure S2. The mRNA transcriptional levels of iron sensing transcription factor $fep1^+$. Yeast cells were grown in rich medium, YES, to log phase then 0.5mM DETA NONOate was treated for 2 hours.Transcriptional response was analyzed through microarray analysis.